

NESTING STATISTICS IN THE $O(n)$ LOOP MODEL ON RANDOM PLANAR MAPS

GAËTAN BOROT, JÉRÉMIE BOUTTIER, AND BERTRAND DUPLANTIER

ABSTRACT. In the $O(n)$ loop model on random planar maps, we study the depth – in terms of the number of levels of nesting – of the loop configuration, by means of analytic combinatorics. We focus on the “refined” generating series of pointed disks or cylinders, which keep track of the number of loops separating the marked point from the boundary (for disks), or the two boundaries (for cylinders). For the general $O(n)$ loop model, we show that these generating series satisfy functional relations obtained by a modification of those satisfied by the unrefined generating series. In a more specific $O(n)$ model where loops cross only triangles and have a bending energy, we can explicitly compute the refined generating series. We analyze their non-generic critical behavior in the dense and dilute phases, and obtain the large deviations function of the nesting distribution, which is expected to be universal. By a continuous generalization of the KPZ relation in Liouville quantum gravity, *i.e.*, by taking into account the probability distribution of the Euclidean radius of a ball of given quantum area, our results are in full agreement with the multifractal spectra of extreme nesting of CLE_κ in the disk, as obtained by Miller, Watson and Wilson [71], and with its natural generalization to the Riemann sphere.

1. INTRODUCTION

The enumeration of maps, which are models for discretized surfaces, developed initially from the work of Tutte [90, 91, 92]. The discovery of matrix model techniques [19] and the development of bijective techniques based on coding by decorated trees [21, 79] led in the past 30 years to a wealth of results. An important motivation comes from the conjecture that the geometry of large random maps is universal, *i.e.*, there should exist ensembles of random metric spaces depending on a small set of data (like the central charge and a symmetry group attached to the problem) which describe the continuum

Date: May 10, 2016.

The authors wish to thank Philippe di Francesco, Clément Hongler, Jason Miller, Scott Sheffield and Wendelin Werner for insightful comments, as well as the organizers of the Journées Cartes at IHÉS. We also would like to thank the Isaac Newton Institute (INI) for Mathematical Sciences for its hospitality and support during the 2015 program “Random Geometry” supported by EPSRC Grant Number EP/K032208/1, where the third author joined the project, and where preliminary versions of this work were presented. B.D. also gratefully acknowledges the support of a Simons Foundation fellowship on the INI Random Geometry program, and thanks the Max Planck Institute for Mathematics, Bonn, for its hospitality. G.B. acknowledges financial support from the Simons Foundation and the Max-Planck Gesellschaft. J.B. acknowledges financial support from the Agence Nationale de la Recherche via the grants ANR-12-JS02-001-01 “Cartaplus” and ANR-14-CE25-0014 “GRAAL”, and the City of Paris through the project “Combinatoire à Paris”. B.D. acknowledges financial support from the Agence Nationale de la Recherche via the grant ANR-14-CE25-0014 “GRAAL”; he is also partially funded by the CNRS Projet international de coopération scientifique (PICS) “Conformal Liouville Quantum Gravity” n°PICS06769.

limit of random maps. Two-dimensional quantum gravity aims at the description of these random continuum objects and physical processes on them, and the universal theory which should underly it is Liouville quantum gravity possibly coupled to a conformal field theory [57, 47, 43]. Understanding rigorously the emergent fractal geometry of such limit objects is nowadays a major problem in mathematical physics. Another important problem is to establish the convergence of random maps towards such limit objects. Solving various problems of map enumeration is often instrumental in this program, as it provides useful probabilistic estimates.

As of now, the geometry of large random planar maps with faces of bounded degrees (*e.g.*, quadrangulations) is fairly well understood. In particular, their scaling limit is the Brownian map [65, 61, 66, 62], the complete proof of convergence in the Gromov-Hausdorff sense being obtained in [66, 62]. This universality class is often called in physics that of “pure gravity”. Recent progress generalized part of this understanding to planar maps containing faces whose degrees are drawn from a heavy tail distribution. In particular, the limiting object is the so-called α -stable map, which can be coded in terms of stable processes whose parameter α is related to the power law decay of the degree distribution [64].

The next class of interesting models concerns random maps equipped with a statistical physics model, like percolation [55], the Ising model [54, 16], or the Q -Potts model [22, 8, 93]. It is well-known, at least on fixed lattices [42, 5, 89, 76, 75], that the Q -state Potts model can be reformulated as a fully packed loop model with a fugacity \sqrt{Q} per loop, for random maps this equivalence is explained in detail in [10]. The $O(n)$ model also admits a famous representation in terms of loops [26, 75] with n the fugacity per loop. The interesting feature of the $O(n)$ model is that it gives rise to universality classes which depend continuously on n , as can be detected at the level of critical exponents [73, 74, 75, 31, 46, 58, 32, 59, 44]. The famous KPZ relations [57] (see also [23, 25]) relate, at least from the physics point of view, the critical exponents of these models on a fixed regular lattice, with their corresponding critical exponent on random planar maps, as was repeatedly checked for a series of models [57, 54, 31, 32, 58, 29].

It is widely believed that after a Riemann conformal map to a given planar domain, the proper conformal structure for the continuum limit of random planar maps weighted by the partition functions of various statistical models is described by the *Liouville theory of quantum gravity* (see, *e.g.*, the reviews [47, 43, 72] and [30, 63]). In the particular case of *pure* random planar maps, the universal metric structure of the Brownian map [62, 66, 63] has very recently been identified with that directly constructed from Liouville quantum gravity [67, 69, 68]. After this Riemann conformal mapping, the configuration of critical $O(n)$ loops is believed to be described in the continuous limit by the so-called *conformal loop ensemble* [84, 86], denoted by CLE_κ and depending on a continuous index $\kappa \in (8/3, 8)$, with the correspondence $n = 2 \cos \pi(1 - \frac{4}{\kappa})$ for $n \in (0, 2]$ [28, 51, 29]. In Liouville quantum gravity, the CLE_κ is in presence of an independent Gaussian free field (GFF), which both governs the random area measure and quantum conformal welding along SLE curves [37, 85, 38, 33, 30], and expectedly also the random metric associated with the random map in the continuous limit [63, 67, 69, 68]. In the framework of Liouville quantum gravity, the KPZ relations have now been mathematically proven for the GFF

[37], for multiplicative cascades [7] and in the framework of Gaussian multiplicative chaos [78, 35].

Yet, little is known on the *metric* properties of large random maps weighted by an $O(n)$ model, even from a physical point of view. In this work, we shall rigorously investigate the *nesting* properties of loops in those maps. From the point of view of 2d quantum gravity, it is a necessary, albeit perhaps modest, step towards a more complete understanding of the geometry of these large random maps. For instance, one should first determine the typical ‘depth’ (*i.e.*, the number of loops crossed) on a random map before trying to determine how deep geodesics are penetrating the nested loop configuration. While this last question seems at present to be out of reach, its answer is expected to be related to the value of the almost sure Hausdorff dimension of large random maps with an $O(n)$ model, a question which is still under active debate (see, *e.g.*, Refs. [27, 1]).

Our approach is based on analytic combinatorics, and mainly relies on the substitution approach developed in [12, 11]. For instance, we compute generating series of cylinders (planar maps with two boundary faces) weighted by s^P , where P is the number of loops separating the two boundaries. This type of results is new and has a combinatorial interest *per se*; we find that the new variable s appears in a remarkably simple way in the generating series. While the present article is restricted to the case of planar maps, the tools that we present will be applied to investigate in a subsequent work the topology of nesting in maps of arbitrary genus and number of boundaries [15].

We also relate the asymptotic of our findings for large number of loops and volume, to extreme nesting in CLE_κ in the plane. The large deviations functions, obtained here for nesting on random planar maps, are shown to be rigorously identical to some transforms in Liouville quantum gravity, of the Euclidean large deviations functions for CLE_κ as obtained in Ref. [71], via a somehow subtle resurgence and extension of the KPZ relation.

Notations. If F and G are non-zero and depend on some parameter $\varepsilon \rightarrow 0$, $F \asymp G$ means that $\ln F \sim \ln G$ when $\varepsilon \rightarrow 0$, while $F \sim G$ means there exists $C > 0$ such that $F \sim CG$ when $\varepsilon \rightarrow 0$. If F is a formal series in some parameter u , $[u^m] F$ is the coefficient of u^m in F .

2. GENERAL DEFINITIONS, REMINDERS AND MAIN RESULTS

2.1. The $O(n)$ loop model on random maps. We start by reminding the definition of the model, following the presentation of Refs. [12, 11].

2.1.1. Maps and loop configurations. A *map* is a finite connected graph (possibly with loops and multiple edges) drawn on a closed orientable compact surface, in such a way that the edges do not cross and that the connected components of the complement of the graph (called *faces*) are simply connected. Maps differing by an homeomorphism of their underlying surfaces are identified, so that there are countably many maps. The map is *planar* if the underlying surface is topologically a sphere. The *degree* of a vertex or a face is its number of incident edges (counted with multiplicity). To each map we may associate its *dual map* which, roughly speaking, is obtained by exchanging the roles of vertices and faces. For $m \geq 1$, a *map with m boundaries* is a map with m distinguished faces, labeled from 1 to m . By convention all the boundary faces are rooted, that is to say for each boundary face f we pick an oriented edge (called a *root*) having f on its right.

The *perimeter* of a boundary is the degree of the corresponding face. Non-boundary faces are called *inner faces*. A *triangulation with m boundaries* (resp. a *quadrangulation with m boundaries*) is a map with m boundaries such that each inner face has degree 3 (resp. 4).

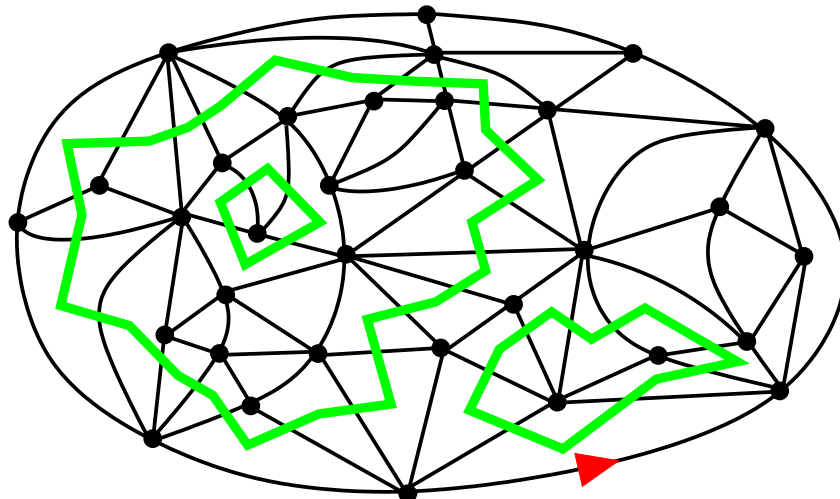


FIGURE 1. A planar triangulation with a boundary of perimeter 8 (with root in red, the distinguished face being the outer face), endowed with a loop configuration (drawn in green).

Given a map, a *loop* is an undirected simple closed path on the dual map (*i.e.*, it covers edges and vertices of the dual map, and hence visits faces and crosses edges of the original map). This is not to be confused with the graph-theoretical notion of loop (an edge incident twice to the same vertex), which plays no role here. A *loop configuration* is a collection of disjoint loops, and may be viewed alternatively as a collection of *crossed edges* such that every face of the map is incident to either 0 or 2 crossed edges. When considering maps with boundaries, we assume that the boundary faces are not visited by loops. Finally, a *configuration* of the $O(n)$ loop model on random maps is a map endowed with a loop configuration, see Figure 1 for an example.

Remark 2.1. In the original formulation in Refs. [46, 58, 59, 40], the loops cover vertices and edges the map itself. Our motivation for drawing them on the dual map is that it makes our combinatorial decompositions easier to visualize.

2.1.2. Statistical weights and partition functions. Colloquially speaking, the $O(n)$ loop model is a statistical ensemble of configurations in which n plays the role of a fugacity per loop. In addition to this “nonlocal” parameter, we need also some “local” parameters, controlling in particular the size of the maps and of the loops. Precise instances of the model can be defined in various ways.

The simplest instance is the $O(n)$ loop model on random triangulations [46, 58, 59, 40]: here we require the underlying map to be a triangulation, possibly with boundaries. There are two local parameters g and h , which are the weights per inner face (triangle) which is, respectively, not visited and visited by a loop. The Boltzmann weight attached to a

configuration C is thus $w(C) = n^{\mathcal{L}} g^{T_1} h^{T_2}$, with \mathcal{L} the number of loops of C , T_1 its number of unvisited triangles and T_2 its number of visited triangles.

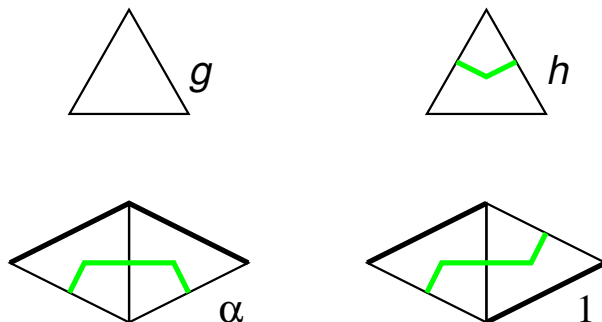


FIGURE 2. Top row: local weights for the $O(n)$ loop model on random triangulations. Bottom row: in the bending energy model, an extra weight α is attached to each segment of a loop between two successive turns in the same direction.

A slight generalization of this model is the *bending energy model* [11], where we incorporate in the Boltzmann weight $w(C)$ an extra factor α^B , where B is the number of pairs of successive loop turns in the same direction, see Figure 2. Another variant is the $O(n)$ loop model on random quadrangulations considered in [12] (and its “rigid” specialization). Finally, a fairly general model encompassing all the above, and amenable to a combinatorial decomposition, is described in [11, Section 2.2]. We now define the partition function. Fixing an integer $m \geq 1$, we consider the ensemble of allowed configurations where the underlying map is planar and has m boundaries of respective perimeters $\ell_1, \ell_2, \dots, \ell_m \geq 1$ (called perimeters). We will mainly be interested in $m = 1$ (disks) and $m = 2$ (cylinders). The corresponding partition function is then the sum of the Boltzmann weights $w(C)$ of all such configurations. We find convenient to add an auxiliary weight u per vertex, and define the partition function as

$$(2.1) \quad F_{\ell_1, \dots, \ell_m}^{(m)} = \delta_{m,1} \delta_{\ell_1,0} u + \sum_C u^{|V(C)|} w(C),$$

where the sum runs over all desired configurations C , and $|V(C)|$ denotes the number of vertices of the underlying map of C , also called *volume*. For $m = 1$, we introduce the shorthand notations

$$(2.2) \quad F_\ell \equiv F_\ell^{(1)}.$$

By convention, the partition function for $m = 1$ includes an extra term $\delta_{\ell_1,0} u$, which means that we consider the map consisting of a single vertex on a sphere to be a planar map with $m = 1$ boundary of perimeter $\ell_1 = 0$.

2.2. Phase diagram and critical points. When we choose the parameters to be real positive numbers such that the sum (2.1) converges, we say that the model is *well-defined* (it induces a probability distribution over the set of configurations). Under mild assumptions on the model (*e.g.*, the face degrees are bounded), this is the case for u small, and

there exists a critical value u_c above which the model ceases to be well-defined:

$$(2.3) \quad u_c = \sup\{u \geq 0 : \forall \ell \quad F_\ell < \infty\}.$$

If $u_c = 1$ (resp. $u_c > 1$, $u_c < 1$), we say that the model is at a *critical* (resp. *subcritical*, *supercritical*) point.

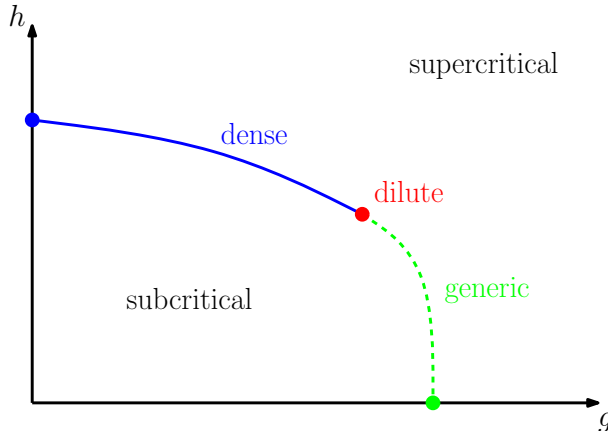


FIGURE 3. Qualitative phase diagram of $O(n)$ loop model on random maps: there is a line of critical points separating the subcritical and supercritical phase. Critical points may be in three different universality classes: generic, dilute and dense.

At a critical point, the partition function has a singularity at $u = 1$, and the nature (universality class) of this singularity is characterized by some critical exponents, to be discussed below. For $n \in (0, 2)$, three different universality classes of critical points may be obtained in the $O(n)$ loop model on random triangulations, which we call *generic*, *dilute* and *dense*. [58]

The generic universality class is that of “pure gravity”, also obtained in models of maps without loops. The location of these points in the (g, h) plane forms the phase diagram of the model, displayed qualitatively on Figure 3, and established in [11] – see also the earlier works [58, 46, 59, 40]. For the bending energy model, the phase diagram is similar for α not too large, but as α grows the line of nongeneric critical points shrinks and vanishes eventually [10, Section 5.5]. The same universality classes, and a similar phase diagram, is also obtained for the rigid $O(n)$ loop model on quadrangulations [12], and is expected for more general loop models, where g and h should be thought as a fugacity per empty and visited faces, respectively.

2.3. Critical exponents. We now discuss some exponents that characterize the different universality classes of critical points of the $O(n)$ loop model. Some of them are well-known while others are introduced here for the purposes of the study of nesting. In the case of the dilute and dense universality classes, the known exponents are rational functions of the parameter:

$$(2.4) \quad b = \frac{1}{\pi} \arccos\left(\frac{n}{2}\right),$$

which decreases from $\frac{1}{2}$ to 0 as n increases from 0 to 2. An entry \bullet indicates that the

exponent	subcrit.	generic	dilute	dense	$n = 0$	Perc.	Ising	3-Potts	KT
b			b	b	$\frac{1}{2}$	$\frac{1}{3}$	$\frac{1}{4}$	$\frac{1}{6}$	0
γ_{str}		$-\frac{1}{2}$	$-b$	$-\frac{b}{1-b}$	-1	$-\frac{1}{2}$	$-\frac{1}{3}$	$-\frac{1}{5}$	0
central charge		0	$1 - \frac{6b^2}{1+b}$	$1 - \frac{6b^2}{1-b}$	-2	0	$\frac{1}{2}$	$\frac{4}{5}$	1
c			1	$\frac{1}{1-b}$	2	$\frac{3}{2}$	$\frac{4}{3}$	$\frac{6}{5}$	1
a	$\frac{3}{2}$	$\frac{5}{2}$	$2 + b$	$2 - b$	$\frac{3}{2}$	$\frac{5}{3}$	$\frac{7}{4}$	$\frac{11}{6}$	2
d_H	2	4	•	•	•	4	•	•	•
d_H^{gasket}	2	4	$3 + 2b$	$3 - 2b$	2	$\frac{7}{3}$	$\frac{5}{2}$	$\frac{8}{3}$	3
ν	0	0	$\frac{1}{2} - b$	$\frac{1-2b}{2(1-b)}$	0	$\frac{1}{4}$	$\frac{1}{3}$	$\frac{4}{10}$	$\frac{1}{2}$
κ			$\frac{1-b}{4}$	$\frac{4}{1-b}$	8	6	$\frac{16}{3}$	$\frac{24}{5}$	4

FIGURE 4. Summary of critical exponents for the $O(n)$ model. (The last 5 columns are for the dense phase.) Pure gravity corresponds to $n = 0$ model in the dilute phase, critical percolation to the $n = 1$ model in the dense phase, the Ising model and its interfaces to both the $n = 1$ model in the dilute phase and the $n = \sqrt{2}$ model in the dense phase; the Kosterlitz-Thouless transition is that of the $n = 2$ model. More generally, the critical Q -Potts model and its FK cluster boundaries correspond to the $O(n = \sqrt{Q})$ model in the dense phase.

exponent is not unknown. At the time of writing, there is no consensus about the value of d_H^{gasket} in the physics literature, although the value 4 (independently of n), or a so-called Watabiki formula have been proposed (see *e.g.*, [18, 27, 1] and references therein). All other exponents can be derived rigorously in the $O(n)$ model on triangulations, as well as the model with bending energy, and are expected to be universal. We actually reprove these results – the only new statement concerns ν – for the dense and dilute phase of the model with bending energy with not too large α during the course of the article.

2.3.1. *Volume exponent.* The singularity of the partition function in the vicinity of a critical point is captured in the so-called *string susceptibility exponent* γ_{str} :

$$(2.5) \quad F_\ell|_{\text{sing}} \sim (1-u)^{1-\gamma_{\text{str}}}, \quad u \rightarrow 1,$$

where ℓ is fixed, and $F_\ell|_{\text{sing}}$ denotes the leading singular part in the asymptotic expansion of F_ℓ around $u = 1$. As u is coupled to the volume, the generating series of maps with fixed volume V behaves as:

$$[u^V] F_\ell \sim V^{\gamma_{\text{str}}-2}, \quad V \rightarrow \infty.$$

In the context of the $O(n)$ loop model, γ_{str} may take the *generic* value $-\frac{1}{2}$, already observed in models of maps without loops ($n = 0$); the *dilute* value $-b$; and the *dense* value $-\frac{b}{1-b}$. In all cases we consider, γ_{str} is comprised between -1 and 0 . The parameter $c \in (1, 2)$ defined by:

$$\gamma_{\text{str}} := -bc$$

will play an important role (note that it has nothing to do with the central charge).

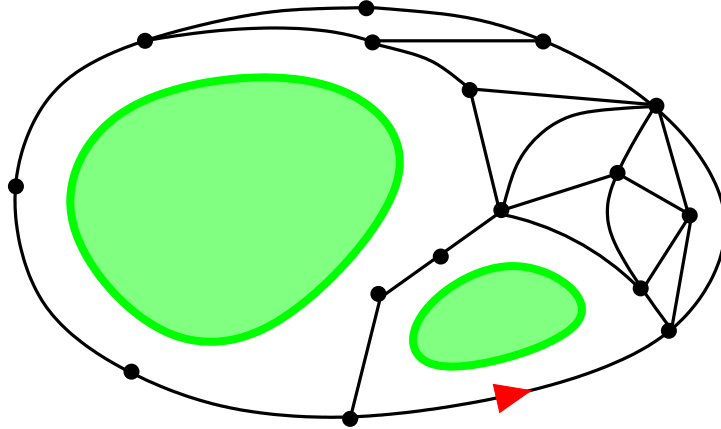


FIGURE 5. The gasket of the map depicted in Figure 1.

2.3.2. *Perimeter exponent.* A second exponent is obtained as we keep $u = 1$ fixed but take one boundary to be of large perimeter. Clearly, this requires F_ℓ to be finite for all ℓ , hence the model to be either subcritical or critical, since $\gamma_{\text{str}} \in (-1, 0)$. We have the asymptotic behavior:

$$(2.6) \quad F_\ell \sim \frac{\gamma_+^\ell}{\ell^a}, \quad \ell \rightarrow \infty,$$

where γ_+ is a non-universal constant, and a is a universal exponent comprised between $\frac{3}{2}$ and $\frac{5}{2}$, which can take more precisely four values for a given value of n : $\frac{3}{2}$ (subcritical point), $\frac{5}{2}$ (generic critical point), $2 + b$ (dilute critical point) and $2 - b$ (dense critical point).

2.3.3. *Gasket exponents.* Consider a disk \mathcal{D} with one boundary face and a loop configuration. If we (i) take the connected component, in the complement in \mathcal{D} of all faces carrying loops, which contain the boundary face, and (ii) fill in the holes of perimeter k by a face of degree k , we obtain a disk \mathcal{D}' (which does not contain a loop configuration), called the *gasket*. (Compare Figures 1 and 5.) In Corollary 6.6, we will combine known properties of the generating series of disks in the model with bending energy to show that the probability that a vertex chosen at random uniformly in a disk of volume V and finite perimeter belongs to the gasket behaves like:

$$\mathbb{P}[\bullet \in \text{gasket} \mid V] \sim V^{-\nu}, \quad V \rightarrow \infty,$$

with $\nu = c(\frac{1}{2} - b)$.

Relying on the work of Le Gall and Miermont [64], we showed in [12] that the almost sure fractal dimension of the gasket when $V \rightarrow \infty$, denoted d_H^{gasket} , is equal to $3 - 2b$ in the dense phase, $3 + 2b$ in the dilute phase. This contrasts with the well-known value $d_H = 4$ for the fractal dimension of disks at the generic critical point. We can only expect $d_H > d_H^{\text{gasket}}$. Ref. [27] relates it to the value of yet another critical exponent, which expresses how deep geodesics enter in the nested configuration of loops.

2.4. Main results on random maps. This paper is concerned with the statistical properties of nesting between loops. The situation is simpler in the planar case since every loop is contractible, and divides the underlying surface into two components. The nesting structure of large maps of arbitrary topology will be analyzed in a forthcoming work [15].

In the general $O(n)$ loop model, the generating series of disks and cylinders have been characterized in [12, 11, 14], and explicitly computed in the model with bending energy in [11], building on the previous works [40, 13]. This characterization is a linear functional relation which depends explicitly on n , accompanied by a non-linear consistency relation depending implicitly on n . We remind the steps leading to this characterization in Sections 3-4. In particular, we review in Section 3 the nested loop approach developed in [12], which allows enumerating maps with loop configurations in terms of generating series of usual maps. We then derive in Section 4 the functional relations for maps with loops as direct consequences of the well-known functional relations for generating series of usual maps. The key to our results is the derivation in Section 4.4 of an analog characterization for refined generating series of pointed disks (resp. cylinders), in which the loops which separates the origin (resp. the second boundary) and the (first) boundary face are counted with an extra weight s each. We find that the characterization of the generating series is only modified by replacing n with ns in the linear functional relation, while keeping n in the consistency relation. Subsequently, in the model with bending energy, we can compute explicitly the refined generating series, in Section 5. We analyze in Section 6 the behavior of those generating series at a non-generic critical point which pertains to the $O(n)$ model. In the process, we rederive the phase diagram of the model with bending energy, and we eventually find:

Theorem 2.2. *Fix (g, h, α) and $n \in (0, 2)$ such that the model with bending energy achieves a non-generic critical point for the vertex weight $u = 1$. In the ensemble of random pointed disks of volume V and perimeter L , the distribution of the number P of separating loops between the marked point and the boundary face behaves as:*

$$\mathbb{P}\left[P = \frac{c \ln V}{\pi} p \mid V, L = \ell\right] \sim (\ln V)^{-\frac{1}{2}} V^{-\frac{c}{\pi} J(p)},$$

$$\mathbb{P}\left[P = \frac{c \ln V}{2\pi} p \mid V, L = V^{\frac{c}{2}} \ell\right] \sim (\ln V)^{-\frac{1}{2}} V^{-\frac{c}{2\pi} J(p)},$$

where $\ell > 0$ is fixed, and $p \ll \ln V$, and:

$$J(p) = \ln \left(\frac{2}{n} \frac{p}{\sqrt{1+p^2}} \right) + \operatorname{arccot}(p) - \arccos(n/2).$$

We expect this result to be universal among all $O(n)$ loop models at non-generic critical points. The explicit, non-universal finite prefactors in those asymptotics are given in the more precise Theorem 6.8. We establish a similar result in Section 7 and Theorem 7.1 for the number of loops separating the boundaries in cylinders.

The large deviations function has the following properties (see Figure 6):

- $J(p) \geq 0$ for positive p , and achieves its minimum value 0 at p_{opt} given below.
- $J(p)$ is strictly convex, and $J''(p) = \frac{1}{p(p^2+1)}$.
- $J(p)$ has a slope $\ln(2/n)$ when $p \rightarrow \infty$.

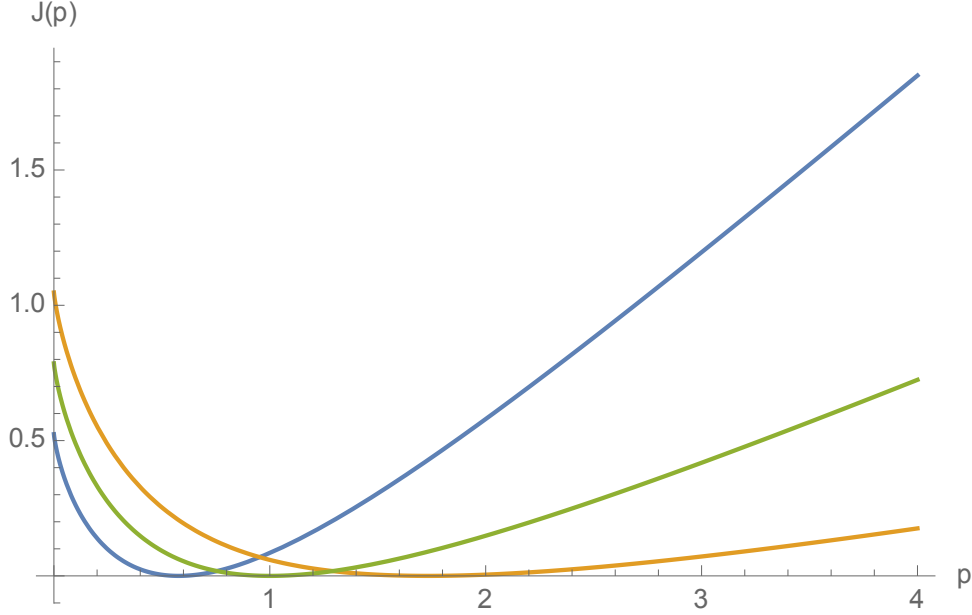


FIGURE 6. The function $J(p)$ for $n = 1$, $n = \sqrt{2}$ (Ising) and $n = \sqrt{3}$ (3-Potts).

- When $p \rightarrow 0$, we have $J(p) = \arcsin(n/2) + p \ln(2p/n) + O(p)$.

The Gaussian behavior of the large deviations function around its minimum p_{opt} implies:

Corollary 2.3. *In pointed disks as above, the depth behaves almost surely like $\frac{cp_{\text{opt}}}{j\pi} \ln V$, with Gaussian fluctuations of order $O(\sqrt{\ln V})$:*

$$\frac{P - \frac{cp_{\text{opt}}}{j\pi} \ln V}{\sqrt{\ln V}} \rightarrow \mathcal{N}(0, \sigma^2), \quad p_{\text{opt}} = \frac{n}{\sqrt{4 - n^2}}, \quad \sigma^2 = \frac{2^{3-j}nc}{\pi(4 - n^2)^{\frac{3}{2}}}.$$

with $j = 1$ if we keep L finite, or $j = 2$ if we scale $L = \ell V^{\frac{c}{2}}$ for a finite positive ℓ .

Establishing the critical behavior of the generating series and the phase diagram requires analyzing special functions related to the Jacobi theta functions and elliptic functions in the trigonometric limit. The lengthy computations with these special functions are postponed to the Appendix to ease the reading. In Section 8, we generalize these results to a model where loops are weighted by independent, identically distributed random variables. Lastly, Section 9, the content of which is briefly described below, uses a different perspective, and re-derives the above results on random maps from the Liouville quantum gravity approach. The latter is applied to similar earlier results obtained in Ref. [71] for a CLE_κ in the unit disk.

2.5. Comparison with CLE properties. It is strongly believed that, if the random disks were embedded conformally to the unit disk \mathbb{D} , the loop configuration would be described in the thermodynamic $V \rightarrow \infty$ limit by the *conformal loop ensemble* in presence of Liouville quantum gravity. On a regular planar lattice, the critical $O(n)$ -model on a regular planar lattice is expected to converge in the continuum limit to the universality

class of the $\text{SLE}_\kappa/\text{CLE}_\kappa$, for

$$(2.7) \quad n = 2 \cos [\pi(1 - 4/\kappa)] \quad n \in (0, 2] \quad \begin{cases} \kappa \in (8/3, 4], & \text{dilute phase} \\ \kappa \in [4, 8), & \text{dense phase} \end{cases}$$

and the same is expected to hold at a non-generic critical point in the dilute or dense phase on a random planar map. Although both conjectures are far from being rigorously established, we may try to relate the large deviations properties of nesting, as derived in the critical regime in the $O(n)$ loop model on a random planar map, to the corresponding nesting properties of CLE_κ , in order to support both conjectures altogether.

In [71] (see also [70]), Miller, Watson and Wilson were able to derive the almost sure multifractal dimension spectrum of *extreme nesting* in the conformal loop ensemble. Let Γ be a CLE_κ in \mathbb{D} . For each point $z \in \mathbb{D}$, let $\mathcal{N}_z(\varepsilon)$ be the number of loops of Γ which surround the ball $B(z, \varepsilon)$ centered at z and of radius $\varepsilon > 0$. For $\nu > 0$, define

$$\Phi_\nu = \Phi_\nu(\Gamma) := \left\{ z \in D : \lim_{\varepsilon \rightarrow 0} \frac{\mathcal{N}_z(\varepsilon)}{\ln(1/\varepsilon)} = \nu \right\}.$$

The almost-sure Hausdorff dimension of this set is given in terms of the distribution of conformal radii of outermost loops in CLE_κ . More precisely, let \mathcal{U} be the connected component containing the origin in the complement $\mathbb{D} \setminus \mathcal{L}$ of the largest loop \mathcal{L} of Γ surrounding the origin in \mathbb{D} . The cumulant generating function of $T = -\ln(\text{CR}(0, \mathcal{U}))$ was computed in [82], and is given by

$$(2.8) \quad \Lambda_\kappa(\lambda) := \ln \mathbb{E} [e^{\lambda T}] = \ln \left(\frac{-\cos(4\pi/\kappa)}{\cos \left(\pi \sqrt{\left(1 - \frac{4}{\kappa}\right)^2 + \frac{8\lambda}{\kappa}} \right)} \right),$$

for $\lambda \in (-\infty, 1 - \frac{2}{\kappa} - \frac{3\kappa}{32})$. The symmetric Legendre-Fenchel transform, $\Lambda_\kappa^* : \mathbb{R} \rightarrow \mathbb{R}^+$ of Λ_κ is defined by

$$(2.9) \quad \Lambda_\kappa^*(x) := \sup_{\lambda \in \mathbb{R}} (\lambda x - \Lambda_\kappa(\lambda)).$$

The authors of [71] then define

$$(2.10) \quad \gamma_\kappa(\nu) := \begin{cases} \nu \Lambda_\kappa^*(1/\nu), & \text{if } \nu > 0 \\ 1 - \frac{2}{\kappa} - \frac{3\kappa}{32} & \text{if } \nu = 0, \end{cases}$$

which is right continuous at 0. Then, for $\kappa \in (8/3, 8)$, the Hausdorff dimension of the set Φ_ν is almost surely [71, Theorem 1.1],

$$\dim_{\mathcal{H}} \Phi_\nu = \max(0, 2 - \gamma_\kappa(\nu)).$$

As a Lemma to this result, the authors of Ref. [71] estimate, for $\varepsilon \rightarrow 0$, the asymptotic nesting probability around point z ,

$$(2.11) \quad \mathbb{P}(\mathcal{N}_z(\varepsilon) \approx \nu \ln(1/\varepsilon) \mid \varepsilon) \asymp \varepsilon^{\gamma_\kappa(\nu)},$$

where the sign \approx stands for a growth of the form $(\nu + o(1)) \ln(1/\varepsilon)$, and where \asymp means an asymptotic equivalence of logarithms. In Section 9, we consider the unit disk in Liouville quantum gravity (LQG), *i.e.*, we equip it with a random measure, formally written here as $\mu_\gamma = e^{\gamma h} d^2 z$, where $\gamma \in [0, 2]$ and h is an instance of a GFF on \mathbb{D} , $d^2 z$

being Lebesgue measure. The random measure μ_γ is called Liouville quantum measure. We define accordingly $\delta := \int_{B(z,\varepsilon)} \mu_\gamma$ as the (random) quantum area of the ball $B(z,\varepsilon)$. In this setting, the KPZ formula, which relates a Euclidean conformal weight x to its LQG counterpart Δ [37], reads

$$(2.12) \quad x = U_\gamma(\Delta) := \frac{\gamma^2}{4} \Delta^2 + \left(1 - \frac{\gamma^2}{4}\right) \Delta.$$

Studying extreme nesting in LQG then consists in looking for the distribution of loops of a CLE_κ around the same ball $B(z,\varepsilon)$, the latter being now *conditioned* to have a given quantum measure δ , and to measure this nesting in terms of the logarithmic variable $\ln(1/\delta)$, instead of $\ln(1/\varepsilon)$. We thus look for the probability,

$$(2.13) \quad \mathbb{P}_\mathcal{Q}(\mathcal{N}_z \approx p \ln(1/\delta) \mid \delta), \quad p \in \mathbb{R}^+,$$

which is the analogue of the left-hand side of (2.11) in Liouville quantum gravity, and which we may call the *quantum nesting probability*.

By taking into account the distribution of the Euclidean radius ε for a given δ [36, 37], we obtain two main results, a first general one deriving via the KPZ relation the large deviations in nesting of a CLE_κ in LQG from those in the Euclidean disk \mathbb{D} , as derived in Ref. [71], and a second one identifying these Liouville quantum gravity results to those obtained here for the critical $O(n)$ model on a random map.

Theorem 2.4. *In Liouville quantum gravity, the cumulant generating function Λ_κ (2.8) with $\kappa \in (8/3, 8)$, is transformed into the quantum one,*

$$(2.14) \quad \Lambda_\kappa^\mathcal{Q} := \Lambda_\kappa \circ 2U_\gamma,$$

where Λ_κ is given by (2.8) and U_γ is the KPZ function (2.12), with $\gamma = \min\{\sqrt{\kappa}, 4/\sqrt{\kappa}\}$. The Legendre-Fenchel transform, $\Lambda_\kappa^{\mathcal{Q}*} : \mathbb{R} \rightarrow \mathbb{R}^+$ of $\Lambda_\kappa^\mathcal{Q}$ is defined by

$$\Lambda_\kappa^{\mathcal{Q}*}(x) := \sup_{\lambda \in \mathbb{R}} (\lambda x - \Lambda_\kappa^\mathcal{Q}(\lambda)).$$

The quantum nesting distribution (2.13) in the disk is then, when $\delta \rightarrow 0$,

$$\begin{aligned} \mathbb{P}_\mathcal{Q}(\mathcal{N}_z \approx p \ln(1/\delta) \mid \delta) &\asymp \delta^{\Theta(p)}, \\ \Theta(p) &= \begin{cases} p\Lambda_\kappa^{\mathcal{Q}*}(1/p), & \text{if } p > 0 \\ 3/4 - 2/\kappa & \text{if } p = 0 \text{ and } \kappa \in (8/3, 4] \\ 1/2 - \kappa/16 & \text{if } p = 0 \text{ and } \kappa \in [4, 8). \end{cases} \end{aligned}$$

Corollary 2.5. *The generating function associated with CLE_κ nesting in Liouville quantum gravity is explicitly given for $\kappa \in (\frac{8}{3}, 8)$ by*

$$\Lambda_\kappa^\mathcal{Q}(\lambda) = \Lambda_\kappa \circ 2U_\gamma(\lambda) = \ln \left(\frac{\cos[\pi(1 - 4/\kappa)]}{\cos[\pi(2c\lambda + |1 - 4/\kappa|)]} \right), \quad c = \min\{1, \kappa/4\},$$

$$\lambda \in \left[\frac{1}{2} - \frac{2}{\kappa}, \frac{3}{4} - \frac{2}{\kappa}\right] \text{ for } \kappa \in \left(\frac{8}{3}, 4\right]; \quad \lambda \in \left[\frac{1}{2} - \frac{\kappa}{8}, \frac{1}{2} - \frac{\kappa}{16}\right] \text{ for } \kappa \in [4, 8).$$

Remark 2.6. $\Theta(p)$ is right-continuous at $p = 0$.

Remark 2.7. Theorem 2.4 shows that the KPZ relation can directly act on an arbitrary continuum variable, here the conjugate variable in the cumulant generating function (2.8) for the CLE_κ log-conformal radius. This seems the first occurrence of such a role for the KPZ relation, which usually concerns scaling dimensions.

Remark 2.8. As the derivation in Sec. 9 will show, the map $\Lambda_\kappa \mapsto \Lambda_\kappa^\mathcal{Q}$ in (2.14) to go from Euclidean geometry to Liouville quantum gravity is fairly general: the composition of Λ by the KPZ function U_γ would hold for any large deviations problem, the large deviations function being the Legendre-Fenchel transform of a certain generating function Λ .

Theorem 2.9. *The quantum nesting probability of a CLE_κ in a proper simply connected domain $D \subsetneq \mathbb{C}$, for the number \mathcal{N}_z of loops surrounding a ball centered at z and conditioned to have a given Liouville quantum area δ , has the large deviations form,*

$$\mathbb{P}_\mathcal{Q}\left(\mathcal{N}_z \approx \frac{cp}{2\pi} \ln(1/\delta) \mid \delta\right) \asymp \delta^{\frac{c}{2\pi}J(p)}, \quad \delta \rightarrow 0,$$

where c and J are the same as in Theorem 2.2.

A complementary result concerns the case of the Riemann sphere.

Theorem 2.10. *On the Riemann sphere $\widehat{\mathbb{C}}$, the large deviations function $\widehat{\Theta}$ which governs the quantum nesting probability,*

$$\mathbb{P}_\mathcal{Q}^{\widehat{\mathbb{C}}}(\mathcal{N} \approx p \ln(1/\delta) \mid \delta) \asymp \delta^{\widehat{\Theta}(p)}, \quad \delta \rightarrow 0,$$

is related to the similar function Θ for the disk topology, as obtained in Theorem 2.4, by

$$\widehat{\Theta}(2p) = 2\Theta(p).$$

From Theorem 2.9, we get explicitly,

$$\mathbb{P}_\mathcal{Q}^{\widehat{\mathbb{C}}} \left(\mathcal{N} \approx \frac{cp}{\pi} \ln(1/\delta) \mid \delta \rightarrow 0 \right) \asymp \delta^{\frac{c}{\pi}J(p)},$$

where c and J are as in Theorem (2.2).

Remark 2.11. The reader will have noticed the perfect matching of the LQG results for CLE_κ in Theorems 2.4, 2.9 and 2.10 with the main Theorem 2.2 for the $O(n)$ model on a random planar map, with the proviso that the first ones are local versions (*i.e.*, in the $\delta \rightarrow 0$ limit), while the latter one gives a global version (*i.e.*, in the $V \rightarrow \infty$ limit).

3. FIRST COMBINATORIAL RESULTS ON PLANAR MAPS

3.1. Reminder on the nested loop approach. We remind that F_ℓ is the partition function for a loop model on a planar map with a boundary of perimeter ℓ . The nested loop approach describes it in terms of $\mathcal{F}_p = \mathcal{F}_p(g_1, g_2, \dots)$. By definition, this is the generating series of usual maps (*i.e.*, without a loop configuration) which are planar, have a rooted boundary of perimeter p , and counted with a Boltzmann weight g_k per inner face of degree k ($k \geq 1$). By convention, we assume that boundaries are rooted. We then have the fundamental relation [11]

$$(3.1) \quad F_\ell = \mathcal{F}_\ell(G_1, G_2, \dots),$$

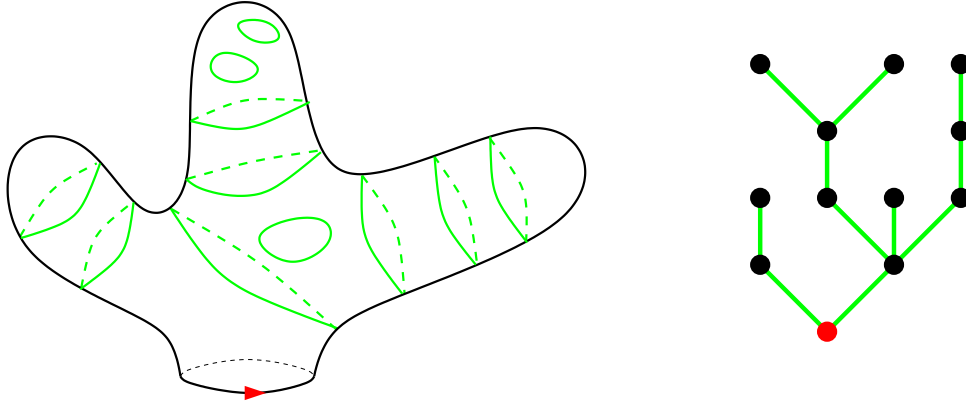


FIGURE 7. Left: schematic representation of a loop configuration on a planar map with one boundary. Right: the associated nesting tree (the red vertex corresponds to the gasket).

where the G_k 's satisfy the fixed point condition

$$(3.2) \quad G_k = g_k + \sum_{\ell' \geq 0} A_{k,\ell'} \mathcal{F}_{\ell'}(G_1, G_2, \dots) = g_k + \sum_{\ell' \geq 1} A_{k,\ell'} F_{\ell'},$$

where $A_{k,\ell}$ is the generating series of sequences of faces visited by a loop, which are glued together so as to form an annulus, in which the outer boundary is rooted and has perimeter k , and the inner boundary is unrooted and has perimeter ℓ . Compared to the notations of [11], we decide to include in $A_{k,\ell}$ the weight n for the loop crossing all faces of the annulus. We call G_k the renormalized face weights.

Throughout the text, unless it is precised in the paragraph headline that we are working with usual maps, the occurrence of \mathcal{F} will always refer to $\mathcal{F}(G_1, G_2, \dots)$.

3.2. The nesting graphs. Given a configuration C of the $O(n)$ loop model on a map, we may cut the underlying surface along every loop, which splits it into several connected components c_1, \dots, c_N . Let T be the graph on the vertex set $\{c_1, \dots, c_N\}$ where there is an edge between c_i and c_j if and only if they have a common boundary, *i.e.*, they touch each other along a loop (thus the edges of T correspond to the loops of C).

If the map is planar, T is a tree called the *nesting tree* of C , see Figure 7. Each loop crosses a sequence of faces which form an annulus. This annulus has an outer and inner boundary, and we can record their perimeter on the half-edges of T . As a result, T is a rooted tree whose half-edges carry nonnegative integers. If the map has a boundary face, we can root T on the vertex corresponding to the connected component containing the boundary face. Then, for any vertex $v \in T$, there is a notion of parent vertex (the one incident to v and closer to the root) and children vertices (all other incident vertices). We denote $\ell(v)$ the perimeter attached to the half-edge arriving to v from the parent vertex. In this way, we can convert T to a tree T' where each vertex v carries the non-negative integer $\ell(v)$.

The nesting tree is closely related to the gasket decomposition introduced in [12, 11]. Consider the canonical ensemble of disks in the $O(n)$ model such that vertices receive a Boltzmann weight u , and the probability law it induces on the tree T' . The probability

that a vertex v with perimeter ℓ has m children with perimeters $\{\ell_1, \dots, \ell_m\}$ is:

$$P_{\ell \rightarrow \ell_1, \dots, \ell_m} = \frac{1}{m!} \frac{\sum_{k_1, \dots, k_m \geq 0} [\prod_{i=1}^m A_{k_i, \ell_i} F_{\ell_i}] \partial_{g_{k_1}} \cdots \partial_{g_{k_m}} \mathcal{F}_\ell(g_1, g_2, \dots)}{F_\ell}.$$

We see that T' forms a Galton-Watson tree with infinitely many types. It would be interesting to study the convergence of this random tree. As the theory of Galton-Watson processes with infinitely many types is much less developed than the well understood case of finitely many types, this article will not explore this question.

If one decides to consider a map M with a given finite set of marked elements – *e.g.*, boundary faces or marked points –, one can define the *reduced nesting tree* $(T'_{\text{red}}, \mathbf{p})$ by:

- (i) For each mark in M , belonging to a connected component c_i , putting a mark on the corresponding vertex of Γ_0 ;
- (ii) erasing all vertices in Γ_0 which correspond to connected components which, in the complement of all loops and of the marked elements in M , are homeomorphic to disks ;
- (iii) replacing any maximal simple path of the form $v_0 - v_1 - \cdots - v_p$ with $p \geq 2$ where $(v_i)_{i=1}^p$ represent connected components homeomorphic to cylinders, by a single edge

$$v_0 \overset{p}{-} v_p$$

carrying a length p . By convention, edges which are not obtained in this way carry a length $p = 1$.

The outcome is a tree, in which vertices may carry the marks that belonged to the corresponding connected components, and whose edges carry positive integers \mathbf{p} . By construction, given a finite set of marked elements, one can only obtain finitely many inequivalent T'_{red} .

In a forthcoming article, we will analyze the probability that a given topology of nesting tree analyze $O(n)$ loop model, conditioned on the lengths of the arms, as well as the generalization to non-simply connected maps. In the present article, we focus on the case of two marks: either a marked point and a boundary face, or two boundary faces. Then, the reduced nesting graph is either the graph with a single vertex (containing the two marked elements) and no edge, or the graph with two vertices (each of them containing a marked element) connected by an arm of length $P \geq 0$. Our goal consists in determining the distribution of P , which is the number of loops separating the two marked elements in the map (the pruning consisted in forgetting all information about the loops which were not separating). Yet, the tools we shall develop are an important step in the study of the reduced nesting graph in maps of arbitrary topology and with more than 2 marked elements.

3.3. Maps with several boundaries. We denote $F_{\ell_1, \ell_2}^{(2)}$ the partition function for a loop model on a random planar map with 2 labeled boundaries of respective perimeters ℓ_1, ℓ_2 , and similarly $\mathcal{F}_{\ell_1, \ell_2}^{(2)} \equiv \mathcal{F}_{\ell_1, \ell_2}^{(2)}(g_1, g_2, \dots)$ for the partition function of usual maps. Such maps can be obtained from disks by marking an extra face and rooting it at an edge. At

the level of partition functions, this amounts to:

$$(3.3) \quad \mathcal{F}_{\ell_1, \ell_2}^{(2)} = \ell_2 \frac{\partial}{\partial g_{\ell_2}} \mathcal{F}_{\ell_1}, \quad F_{\ell_1, \ell_2}^{(2)} = \ell_2 \frac{\partial}{\partial g_{\ell_2}} F_{\ell_1}.$$

Differentiating the fixed point relation (3.1), we can relate $F_{\ell_1, \ell_2}^{(2)}$ to partition functions of usual maps:

$$(3.4) \quad F_{\ell_1, \ell_2}^{(2)} = \mathcal{F}_{\ell_1, \ell_2}^{(2)} + \sum_{\substack{k \geq 1 \\ \ell \geq 0}} \mathcal{F}_{\ell_1, k}^{(2)} R_{k, \ell} F_{\ell, \ell_2}^{(2)},$$

where we have introduced the generating series $R_{k, \ell} = A_{k, \ell}/k$, which now enumerate annuli whose outer and inner boundaries are both unrooted. In this equation, the evaluation of the generating series of usual maps at G_k given by (3.2) is implicit.

3.4. Separating loops and transfer matrix. We say that a loop in a map \mathcal{M} with 2 boundaries is separating if after its removal, each connected component contains one boundary. The combinatorial interpretation of (3.4) is transparent : the first term counts cylinders where no loop separates the two boundaries, while the second term counts cylinders with at least one separating loop (see Figure 8).

With this remark, we can address a refined enumeration problem. We denote $F_{\ell_1, \ell_2}^{(2)}[s]$ be the partition function of cylinders carrying a loop model, with an extra weight s per loop separating the two boundaries. Obviously, the configurations without separating loops are enumerated by $\mathcal{F}_{\ell_1, \ell_2}^{(2)}$. If a configuration has at least one separating loop, let us cut along the first separating loop, and remove it. It decomposes the cylinder into : a cylinder without separating loops, that is adjacent to the first boundary ; the annulus that carried the first separating loop ; a cylinder with one separating loop less, which is adjacent to the second boundary. We therefore obtain the identity :

$$(3.5) \quad F_{\ell_1, \ell_2}^{(2)}[s] = \mathcal{F}_{\ell_1, \ell_2}^{(2)} + s \sum_{\substack{k \geq 1 \\ \ell \geq 0}} \mathcal{F}_{\ell_1, k}^{(2)} R_{k, \ell} F_{\ell, \ell_2}^{(2)}[s].$$

We retrieve (3.4) when $s = 1$, *i.e.*, when separating and non-separating loops have the same weight. We remind for the last time that \mathcal{F} 's should be evaluated at the renormalized face weights G_k .

We can present these relations concisely with matrix notations. Let $\mathbf{F}_s^{(2)}$ (resp. \mathbf{R}) be the semi-infinite matrices with entries $F_{\ell_1, \ell_2}^{(2)}[s]$ (resp. R_{ℓ_1, ℓ_2}) with row and columns indices $\ell_1, \ell_2 \geq 0$. It allows the repackaging of (3.5) as:

$$(3.6) \quad \mathbf{F}_s^{(2)} = \mathcal{F}^{(2)} + s \mathcal{F}^{(2)} \mathbf{R} \mathbf{F}_s^{(2)}.$$

Therefore:

$$(3.7) \quad \mathbf{F}_s^{(2)} = \frac{1}{1 - s \mathcal{F}^{(2)} \mathbf{R}} \mathcal{F}^{(2)}.$$

Then, $\mathbf{\Gamma}_s = (1 - s \mathcal{F}^{(2)} \mathbf{R})^{-1}$ acts as a transfer matrix.

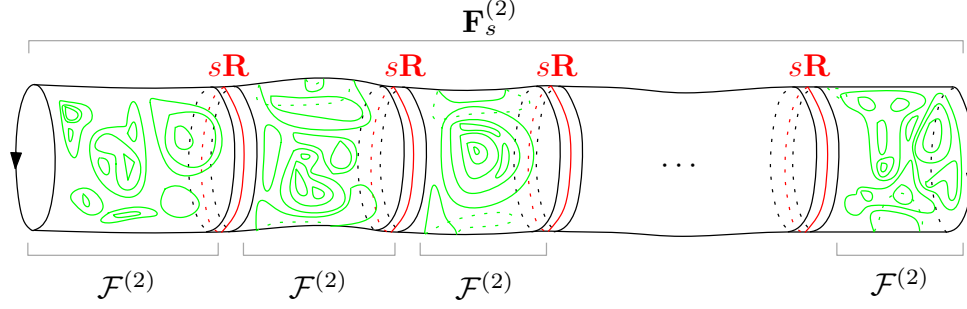


FIGURE 8. Illustration of (3.6).

3.5. Pointed maps. Remind that u denote the vertex weight. In general, a partition function Z^\bullet of pointed maps can easily be obtained from the corresponding partition function Z of maps :

$$(3.8) \quad Z^\bullet = u \frac{\partial}{\partial u} Z.$$

We refer to the marked point as the *origin* of the map. Let us apply this identity to disks with loops. We have to differentiate (3.1) and remember that the renormalized face weights depend implicitly on u :

$$(3.9) \quad F_\ell^\bullet = \mathcal{F}_\ell^\bullet + \sum_{\substack{k \geq 1 \\ \ell' \geq 1}} \mathcal{F}_{\ell,k}^{(2)} R_{k,\ell'} F_{\ell'}^\bullet.$$

Obviously, the first term enumerates disks where the boundary and the origin are not separated by a loop.

Let us introduce a refined partition function $F_\ell^\bullet[s]$ that includes a Boltzmann weight s per separating loop between the origin and the boundary. Cutting along the first – if any – separating loop starting from the boundary and repeating the argument of § 3.4, we find:

$$(3.10) \quad F_\ell^\bullet[s] = \mathcal{F}_\ell^\bullet + s \sum_{\substack{k \geq 1 \\ \ell' \geq 1}} \mathcal{F}_{\ell,k}^{(2)} R_{k,\ell'} F_{\ell'}^\bullet[s].$$

If we introduce the semi-infinite line vectors \mathbf{F}_s^\bullet (resp. \mathcal{F}_s^\bullet) whose entries are $\mathcal{F}_\ell^\bullet[s]$ (resp. $\mathcal{F}_\ell^\bullet[s]$) for $\ell \geq 0$, (3.10) can be written in matrix form:

$$(3.11) \quad \mathbf{F}_s^\bullet = \mathcal{F}^\bullet + s \mathcal{F}^{(2)} \mathbf{R} \mathbf{F}_s^\bullet.$$

The solution reads:

$$(3.12) \quad \mathbf{F}_s^\bullet = \frac{1}{1 - s \mathcal{F}^{(2)} \mathbf{R}} \mathcal{F}^\bullet = \Gamma_s \mathcal{F}^\bullet,$$

involving again the transfer matrix.

4. FUNCTIONAL RELATIONS

4.1. More notations: boundary perimeters. It is customary to introduce generating series for the perimeter of a boundary. Here, we will abandon the matrix notations of § 3.4, and rather introduce:

$$(4.1) \quad \mathbf{F}(x) = \sum_{\ell \geq 0} \frac{F_\ell}{x^{\ell+1}}, \quad \mathcal{F}(x) = \sum_{\ell \geq 0} \frac{\mathcal{F}_\ell}{x^{\ell+1}},$$

which enumerate disks with loops (resp. usual disks) with a weight $x^{-(\ell+1)}$ associated to a boundary of perimeter ℓ . Likewise, for the generating series of cylinders, we introduce:

$$(4.2) \quad \mathbf{F}^{(2)}(x_1, x_2) = \sum_{\ell_1, \ell_2 \geq 1} \frac{F_{\ell_1, \ell_2}^{(2)}}{x_1^{\ell_1+1} x_2^{\ell_2+1}},$$

$$(4.3) \quad \mathbf{F}_s^{(2)}(x_1, x_2) = \sum_{\ell_1, \ell_2 \geq 1} \frac{F_{\ell_1, \ell_2}^{(2)}[s]}{x_1^{\ell_1+1} x_2^{\ell_2+1}},$$

$$(4.4) \quad \mathcal{F}^{(2)}(x_1, x_2) = \sum_{\ell_1, \ell_2 \geq 1} \frac{\mathcal{F}_{\ell_1, \ell_2}^{(2)}}{x_1^{\ell_1+1} x_2^{\ell_2+1}},$$

etc. We will also find convenient to define introduce generating series of annuli¹:

$$(4.5) \quad \mathbf{R}(x, z) = \sum_{k+\ell \geq 1} R_{k, \ell} x^k z^\ell,$$

$$(4.6) \quad \mathbf{A}(x, z) = \sum_{\substack{k \geq 1 \\ \ell \geq 0}} A_{k, \ell} x^{k-1} z^\ell = \partial_x \mathbf{R}(x, z).$$

4.2. Reminder on usual maps. The properties of the generating series of usual disks $\mathcal{F}(x)$ have been extensively studied. We now review the results of [11]. We say that a sequence of nonnegative face weights $(g_k)_{k \geq 1}$ is admissible if for any $\ell \geq 0$, we have $\mathcal{F}_\ell^\bullet < \infty$; by extension, we say that a sequence of real-valued face weights $(g_k)_{k \geq 1}$ is admissible if $(|g_k|)_{k \geq 1}$ is admissible. Then, $\mathcal{F}(x)$ satisfies the one-cut lemma and a functional relation coming from Tutte's combinatorial decomposition of rooted maps:

Proposition 4.1. *If $(g_k)_{k \geq 1}$ is admissible, then the formal series $\mathcal{F}(x)$ is the Laurent series expansion at $x = \infty$ of a holomorphic function in a maximal domain of the form $\mathbb{C} \setminus \gamma$, where $\gamma = [\gamma_-, \gamma_+]$ is a segment of the real line depending on the vertex and face weights. Its endpoints are characterized so that $\gamma_\pm = \mathfrak{s} \pm 2\sqrt{\mathfrak{r}}$ and \mathfrak{r} and \mathfrak{s} are the unique formal series in the variables u and $(g_k)_{k \geq 1}$ such that:*

$$(4.7) \quad \oint_\gamma \frac{dz}{2i\pi} \frac{(z - \sum_{k \geq 1} g_k z^{k-1})}{\sigma(z)} = 0,$$

$$(4.8) \quad u + \oint_\gamma \frac{dz}{2i\pi} \frac{z(z - \sum_{k \geq 1} g_k z^{k-1})}{\sigma(z)} = 0.$$

¹Our definition for \mathbf{A} differs by a factor of $1/x$ from the corresponding A in [11].

where $\sigma(z) = \sqrt{z^2 - 2\mathfrak{s}z + \mathfrak{s}^2 - 4\mathfrak{r}}$. Besides, the endpoints satisfy $|\gamma_-| \leq \gamma_+$, with equality iff $g_k = 0$ for all odd k 's.

Remark 4.2. \mathfrak{r} and \mathfrak{s} have combinatorial interpretations, described in [17]. In particular, the generating series of pointed rooted maps is:

$$\mathfrak{s}^2 + 2\mathfrak{r} = \frac{3(\gamma_+^2 + \gamma_-^2) + 2\gamma_+\gamma_-}{8}.$$

We shall then use the same notation for the formal series and the holomorphic function.

Proposition 4.3. $\mathcal{F}(x)$ behaves like $u/x + O(1/x^2)$ when $x \rightarrow \infty$, like $O((x - \gamma_{\pm})^{1/2})$ when $x \rightarrow \gamma_{\pm}$, and its boundary values on the cut satisfy the functional relation:

$$(4.9) \quad \forall x \in \mathring{\gamma}, \quad \mathcal{F}(x + i0) + \mathcal{F}(x - i0) = x - \sum_{k \geq 1} g_k x^{k-1}.$$

If γ_- and γ_+ are given, there is a unique holomorphic function $\mathcal{F}(x)$ on $\mathbb{C} \setminus \gamma$ satisfying these properties.

Although (4.9) arises as a consequence of Tutte's equation and analytical continuation, it has itself not received a combinatorial interpretation yet.

With Proposition 4.1 in hand, the analysis of Tutte's equation for generating series of maps with several boundaries, and their analytical continuation, has been performed in a more general setting in [14, 9]. The outcome for usual cylinders (see also [14, 39]) is the following:

Proposition 4.4. If $(g_k)_{k \geq 1}$ is admissible, the formal series $\mathcal{F}^{(2)}(x, y)$ is the Laurent series expansion of a holomorphic function in $(\mathbb{C} \setminus \gamma)^2$ when $x, y \rightarrow \infty$, where γ is as in Proposition 4.1. We have the functional relation, for $x \in \mathring{\gamma}$ and $y \in \mathbb{C} \setminus \gamma$:

$$\mathcal{F}^{(2)}(x + i0, y) + \mathcal{F}^{(2)}(x - i0, y) = -\frac{1}{(x - y)^2}.$$

4.3. Reminder on maps with loops. The relation (3.1) between disks with loops and usual disks allows carrying those results to the loop model. We say that a sequence of face weights $(g_k)_{k \geq 1}$ and annuli weights $(A_{k,l})_{k,l \geq 0}$ is admissible if the sequence of renormalized face weights $(G_k)_{k \geq 1}$ given by (3.2) is admissible as it is meant for usual maps. From now on, we always assume admissibility (in the loop model sense).

So, $\mathbf{F}(x)$ satisfies the one-cut property (the analog of Proposition 4.1), and we still denote γ_{\pm} the endpoints of the cuts, which now depend on face weights $(g_k)_{k \geq 1}$ and annuli weights $(A_{k,l})_{k,l \geq 1}$. Admissibility also implies that the annuli generating series $\mathbf{A}(x, z)$, defined in (4.6), is holomorphic in a neighborhood of $\gamma \times \gamma$. And, its boundary values on the cut satisfy the functional relation:

Proposition 4.5. For any $x \in \mathring{\gamma}$,

$$(4.10) \quad \mathbf{F}(x + i0) + \mathbf{F}(x - i0) + \oint_{\gamma} \frac{dz}{2i\pi} \mathbf{A}(x, z) \mathbf{F}(z) = x - \sum_{k \geq 1} g_k x^{k-1}.$$

With Proposition 4.1 in hand, the analysis of Tutte's equation for the partition functions of maps having several boundaries in the loop model, and their analytical continuation,

has been performed in [14, 9]. The functional relation for $\mathbf{F}^{(2)}(x_1, x_2)$ can be deduced from Proposition 4.5 by marking a face (see § 3.3). The outcome is the following.

Proposition 4.6. *The formal series $\mathbf{F}^{(2)}(x, y)$ is the Laurent series expansion of a holomorphic function in $(\mathbb{C} \setminus \gamma)^2$ when $x, y \rightarrow \infty$, with γ as in Proposition 4.5. Besides, it satisfies the functional relation, for $x \in \mathring{\gamma}$ and $y \in \mathbb{C} \setminus \gamma$:*

$$(4.11) \quad \mathbf{F}^{(2)}(x + i0, y) + \mathbf{F}^{(2)}(x - i0, y) + \oint_{\gamma} \frac{dz}{2i\pi} \mathbf{A}(x, z) \mathbf{F}^{(2)}(z, y) = -\frac{1}{(x - y)^2}.$$

It is subjected to the growth condition $\mathbf{F}^{(2)}(x_1, x_2) \in O((x_i - \gamma_{\pm})^{-\frac{1}{2}})$ when $x_i \rightarrow \gamma_{\pm}$.

Likewise, differentiating (4.10) with respect to the vertex weight u , we deduce from Proposition 4.3 that the generating series of pointed rooted disks satisfies a linear, homogeneous equation. Indeed, we remark that the right-hand side in (4.10) does not depend on u :

Proposition 4.7. *For any $x \in \mathring{\gamma}$,*

$$(4.12) \quad \mathbf{F}^{\bullet}(x + i0) + \mathbf{F}^{\bullet}(x - i0) + \oint_{\gamma} \frac{dz}{2i\pi} \mathbf{A}(x, z) \mathbf{F}^{\bullet}(z) = 0.$$

It is subjected to the growth conditions $\mathbf{F}^{\bullet}(x) = u/x + O(1/x^2)$ when $x \rightarrow \infty$ and $\mathbf{F}^{\bullet}(x) \in O((x - \gamma_{\pm})^{-1/2})$ when $x \rightarrow \gamma_{\pm}$.

4.4. Separating loops. The functional relations for the refined generating series (cylinders or pointed disks) including a weight s per separating loop, are very similar to those of the unrefined case.

Proposition 4.8. *At least for $|s| < 1$ and $s = 1$, the formal series $\mathbf{F}_s^{(2)}(x, y)$ is the Laurent expansion of a holomorphic function in $(\mathbb{C} \setminus \gamma)^2$ when $x, y \rightarrow \infty$, and γ is the segment already appearing in Proposition 4.5 and is independent of s . For any $x \in \mathring{\gamma}$ and $y \in \mathbb{C} \setminus \gamma$, we have:*

$$(4.13) \quad \mathbf{F}_s^{(2)}(x + i0, y) + \mathbf{F}_s^{(2)}(x - i0, y) + s \oint_{\gamma} \frac{dz}{2i\pi} \mathbf{A}(x, z) \mathbf{F}_s^{(2)}(z, y) = -\frac{1}{(x - y)^2}.$$

Proposition 4.9. *At least for $|s| < 1$ and $s = 1$, the formal series $\mathbf{F}_s^{\bullet}(x)$ is the Laurent expansion of a holomorphic function in $(\mathbb{C} \setminus \gamma)$. It has the growth properties $\mathbf{F}_s^{\bullet}(x) = u/x + O(1/x^2)$ when $x \rightarrow \infty$, and $\mathbf{F}_s^{\bullet}(x) \in O((x - \gamma_{\pm})^{-1/2})$ when $x \rightarrow \gamma_{\pm}$. Besides, for any $x \in \mathring{\gamma}$, we have:*

$$(4.14) \quad \mathbf{F}_s^{\bullet}(x + i0) + \mathbf{F}_s^{\bullet}(x - i0) + s \oint_{\gamma} \frac{dz}{2i\pi} \mathbf{A}(x, z) \mathbf{F}_s^{\bullet}(z) = 0.$$

Proof. Let us denote $\mathbf{F}_{[q]}^{(2)}$, the generating series of cylinders with exactly q separating loops, and $\mathbf{F}_{[-1]}^{(2)} \equiv 0$ by convention. We first claim that for any $q \geq 0$, $\mathbf{F}_{[q]}^{(2)}(x, y)$ defines a holomorphic function in $(\mathbb{C} \setminus \gamma)^2$, and satisfies the functional relation: for any $x \in \mathring{\gamma}$ and $y \in \mathbb{C} \setminus \gamma$,

$$(4.15) \quad \mathbf{F}_{[q]}^{(2)}(x + i0, y) + \mathbf{F}_{[q]}^{(2)}(x - i0, y) = \oint_{\gamma} \frac{dz_1}{2i\pi} \mathcal{F}_0^{(2)}(x, z_1) \oint_{\gamma} \frac{dz_2}{2i\pi} \check{R}(z_1, z_2) \mathbf{F}_{[q-1]}^{(2)}(z_2, y).$$

The assumption of admissibility guarantees that $\mathbf{A}(\xi, \eta)$ is holomorphic in a neighborhood of $\gamma \times \gamma$, ensuring that the contour integrals in (4.15) are well-defined. Since $\mathbf{F}^{(2)}(x, y) = \mathbf{F}_{s=1}^{(2)}(x, y)$, by dominated convergence we deduce that $\mathbf{F}_s^{(2)}(x, y)$ is an analytic function of s – uniformly for $x, y \in \mathbb{C} \setminus \gamma$ – with radius of convergence at least 1. Then, we can sum over $q \geq 0$ the functional relation (4.15) multiplied by s^q : the result is the announced (4.13), valid in the whole domain of analyticity of $\mathbf{F}_s^{(2)}$ as a function of s .

The claim is established by induction on q . Since $\mathbf{F}_{[0]}^{(2)} = \mathcal{F}^{(2)}$, the claim follows by application of Proposition 4.4 for usual cylinders with renormalized face weights, *i.e.*, vanishing annuli weights in the functional relation (4.11). We however emphasize that the cut γ is determined by Proposition 4.5, thus depends on annuli weights via the renormalized face weights.

Assume the statement holds for some $q \geq 0$. We know from the combinatorial relation (3.6) that:

$$(4.16) \quad \mathbf{F}_{[q+1]}^{(2)} = \mathcal{F}^{(2)} \mathbf{R} \mathbf{F}_{[q]}^{(2)}$$

with the matrix notations of § 3.4. The analytic properties of $\mathcal{F}^{(2)}$ and of $\mathbf{F}_{[q]}^{(2)}$ – as known from the induction hypothesis – allows the rewriting:

$$(4.17) \quad \mathbf{F}_{[q+1]}^{(2)}(x, y) = \oint_{\gamma} \frac{dz_1}{2i\pi} \mathcal{F}^{(2)}(x, z_1) \oint_{\gamma} \frac{dz_2}{2i\pi} \check{R}(z_1, z_2) \mathbf{F}_{[q]}^{(2)}(z_2, y).$$

The expression on the right emphasizes that the left-hand side, though initially defined as a formal Laurent series in x and y , can actually be analytically continued to $(\mathbb{C} \setminus \gamma)^2$. Besides, for $x \in \dot{\gamma}$ and $y \in \mathbb{C} \setminus \gamma$, we can compute the combination:

$$\begin{aligned} & \mathbf{F}_{[q+1]}^{(2)}(x + i0, y) + \mathbf{F}_{[q+1]}^{(2)}(x - i0, y) \\ &= \oint_{\gamma} \frac{dz_1}{2i\pi} (\mathcal{F}^{(2)}(x + i0, z_1) + \mathcal{F}^{(2)}(x - i0, z_1)) \oint_{\gamma} \frac{dz_2}{2i\pi} \mathbf{R}(z_1, z_2) \mathbf{F}_{[q]}^{(2)}(z_2, y) \\ &= - \oint_{\gamma} \frac{dz_1}{2i\pi} \frac{1}{(x - z_1)^2} \oint_{\gamma} \frac{dz_2}{2i\pi} \mathbf{R}(z_1, z_2) \mathbf{F}_{[q]}^{(2)}(z_2, y) \\ &= - \oint_{\gamma} \frac{dz_2}{2i\pi} \partial_x \mathbf{R}(x, z_2) \mathbf{F}_{[q]}^{(2)}(z_2, y). \end{aligned}$$

Hence the statement is valid for $\mathbf{F}_{[q+1]}^{(2)}$ and we conclude by induction. We thus have established Proposition 4.8.

The proof of Proposition 4.9 is similar, except that we use $\mathbf{F}_{[0]}^{\bullet} = \mathcal{F}^{\bullet}$ for initialization, and later, the combinatorial relation (3.11) instead of (3.6). \square

4.5. Depth of a vertex. We now consider the depth P of a vertex chosen at random in a disk configuration of the loop model. P is by definition the number of loops that separate it from the boundary. This quantity gives an idea about how nested maps in the loop model are. Equivalently, P is the depth of the origin in an ensemble of pointed disk configurations. We can study this ensemble in the microcanonical approach – *i.e.*, fixing the volume equal to V and the perimeter equal to L – or in the canonical approach – randomizing the volume V with a weight u^V and the perimeter with a weight $x^{-(L+1)}$.

In the canonical approach, the Laplace transform of the depth distribution can be expressed in terms of the refined generating series of § 3.5:

$$(4.18) \quad \mathbb{E}[s^{D^\bullet}] = \frac{\mathbf{F}_s^\bullet(x)}{\mathbf{F}_1^\bullet(x)}.$$

In the microcanonical approach, the probability that, in an ensemble of pointed disks of volume V and perimeter L , the depth takes the value P reads:

$$\mathbb{P}[P \mid V, L] = \frac{[u^V \cdot x^{-(L+1)} \cdot s^P] \mathbf{F}_s^\bullet(x)}{[u^V \cdot x^{-(L+1)}] \mathbf{F}^\bullet(x)}.$$

5. COMPUTATIONS IN THE LOOP MODEL WITH BENDING ENERGY

We shall focus on the class of loop models with bending energy – see § 2.1.2 – studied in [11], for which the computations can be explicitly carried out. The annuli generating series in this model are:

$$(5.1) \quad \mathbf{R}(x, z) = n \ln \left(\frac{1}{1 - \alpha h(x + z) - (1 - \alpha^2) h^2 x z} \right), \quad \mathbf{A}(x, z) = n \left(\frac{\varsigma'(x)}{z - \varsigma(x)} + \frac{\varsigma''(x)}{2\varsigma'(x)} \right),$$

where:

$$(5.2) \quad \varsigma(x) = \frac{1 - \alpha h x}{\alpha h + (1 - \alpha^2) h^2 x}$$

is a rational involution. Note that, for $\alpha = 1$, we have $\varsigma(x) = 1 - hx$, so $\varsigma''(x) = 0$. In general:

$$\frac{\varsigma''(x)}{2\varsigma'(x)} = -\frac{1}{x + \frac{\alpha}{(1-\alpha^2)h}} = -\frac{1}{x - \varsigma(\infty)}.$$

If f is a holomorphic function in $\mathbb{C} \setminus \gamma$ such that $f(x) \sim c_f/x$ when $x \rightarrow \infty$, we can evaluate the contour integral:

$$(5.3) \quad \oint_{\gamma} \frac{dz}{2i\pi} \mathbf{A}(x, z) f(z) = -n\varsigma'(x) f(\varsigma(x)) + nc_f \frac{\varsigma''(x)}{2\varsigma'(x)}.$$

5.1. Preliminaries. Technically, the fact that $\mathbf{A}(x, z)$ is a rational function with a single pole allows for an explicit solution of the model, and the loop model with bending energy provides a combinatorial realization of such a situation. The key to the solution is the use of an elliptic parametrization $x = x(v)$. It depends on a parameter $\tau = iT$ which is completely determined by the data of γ_{\pm} and $\varsigma(\gamma_{\pm})$. The domain $\mathbb{C} \setminus (\gamma \cup \varsigma(\gamma))$ is mapped to the fundamental rectangle (Figure 9)

$$(5.4) \quad \{v \in \mathbb{C}, \quad 0 < \operatorname{Re} v < 1/2, \quad |\operatorname{Im} v| < T\},$$

with values at the corners:

$$(5.5) \quad \begin{aligned} x(\tau) &= x(-\tau) = \gamma_+, & x(\tau + 1/2) &= x(-\tau + 1/2) = \gamma_-, \\ x(0) &= \varsigma(\gamma_+), & x(1/2) &= \varsigma(\gamma_-). \end{aligned}$$

Besides, when x is in the physical sheet,

$$v(\varsigma(x)) = \tau - v(x).$$

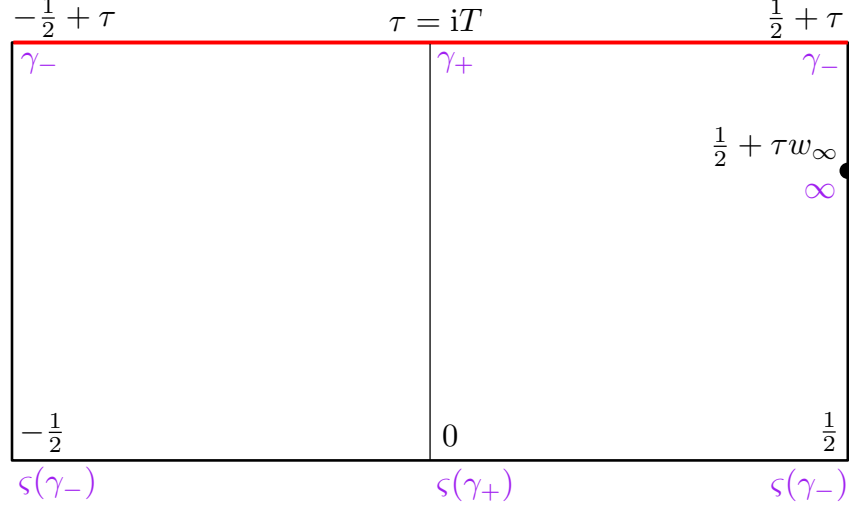


FIGURE 9. The fundamental rectangle in the v -plane. We indicate the image of special values of x in purple, and the image of the cut γ in red. The left (resp. right) panel is the image of $\text{Im } x > 0$ (resp. $\text{Im } x < 0$).

Since the involution ς is decreasing, $\varsigma(\gamma_-)$ belongs to the union of $(\varsigma_+(\gamma), +\infty) \sqcup (-\infty, \gamma_-)$, and therefore $x = \infty$ is mapped to $v_\infty = \frac{1}{2} + \tau w_\infty$ with $0 < w_\infty < 1/2$. When $\alpha = 1$, by symmetry we must have $w_\infty = 1/2$.

The function $v \mapsto x(v)$ is analytically continued for $v \in \mathbb{C}$ by the relations:

$$(5.6) \quad x(-v) = x(v+1) = x(v+2\tau) = x(v).$$

This parametrization allows the conversion [40, 11] of the functional equation:

$$(5.7) \quad \forall x \in \mathring{\gamma}, \quad f(x+i0) + f(x-i0) - n \varsigma'(x) f(\varsigma(x)) = 0$$

for an analytic function $f(x)$ in $\mathbb{C} \setminus \gamma$, into the functional equation:

$$(5.8) \quad \forall v \in \mathbb{C}, \quad \tilde{f}(v+2\tau) + \tilde{f}(v) - n \tilde{f}(v-\tau) = 0, \quad \tilde{f}(v) = \tilde{f}(v+1) = -\tilde{f}(-v),$$

for the analytic continuation of the function $\tilde{f}(v) = f(x(v))x'(v)$. The second condition in (5.8) enforces the continuity of $f(x)$ on $\mathbb{R} \setminus \gamma$. We set:

$$(5.9) \quad b = \frac{\arccos(n/2)}{\pi}.$$

The new parameter b ranges from 1 to 0 when n ranges from -2 to 2 , and $b = 1/2$ corresponds to $n = 0$. Solutions of the first equation of (5.8) with prescribed meromorphic singularities can be build from a fundamental solution Υ_b , defined uniquely by the properties:

$$(5.10) \quad \Upsilon_b(v+1) = \Upsilon_b(v), \quad \Upsilon_b(v+\tau) = e^{i\pi b} \Upsilon_b(v), \quad \Upsilon_b(v) \underset{v \rightarrow 0}{\sim} \frac{1}{v}.$$

Its expression and main properties are reminded in Appendix D.

Remark. We will encounter the linear equation with non-zero right-hand side given by a rational function $g(x)$:

$$(5.11) \quad f(x + i0) + f(x - i0) - n\zeta'(x)f(x) = g(x).$$

It is enough to find a particular solution in the class of rational function and subtract it to $f(x)$ to obtain a function $f^{\text{hom}}(x)$ satisfying (5.11) with vanishing right-hand side. This can be achieved for $n \neq \pm 2$ by:

$$(5.12) \quad f^{\text{hom}}(x) = f(x) - \frac{1}{4 - n^2} \left(2g(x) + n\zeta'(x)g(\zeta(x)) \right).$$

5.2. Disk and cylinder generating series. We now review the results of [11] for the generating series of disks $\mathbf{F}(x)$ for subcritical weights. Let $\mathbf{G}(v)$ be the analytic continuation of

$$(5.13) \quad x'(v)\mathbf{F}(x(v)) - \frac{\partial}{\partial v} \left(\frac{2\mathbf{V}(x(v)) + n\mathbf{V}(\zeta(x(v)))}{4 - n^2} - \frac{nu \ln [\zeta'(x(v))]}{2(2 + n)} \right),$$

where $\mathbf{V}(x) = \frac{x^2}{2} - \sum_{k \geq 1} \frac{g_k x^k}{k}$ collects the weights of empty faces. In the model we study, empty faces are triangles counted with weight g each, so $\mathbf{V}(x) = \frac{x^2}{2} - \frac{gx^3}{3}$. However, there is no difficulty in including Boltzmann weights for empty faces of higher degree as far as the solution of the linear equation is concerned, so we shall keep the notation $\mathbf{V}(x)$. Note that the last term in (5.13) is absent if $\alpha = 1$. Let us introduce $(\tilde{g}_k)_{k \geq 1}$ as the coefficients of expansion:

$$(5.14) \quad \frac{\partial}{\partial v} \left(-\frac{2\mathbf{V}(x(v))}{4 - n^2} + \frac{2 \ln x(v)}{2 + n} \right) = \sum_{k \geq 0} \frac{\tilde{g}_k}{(v - v_\infty)^{k+1}} + O(1), \quad v \rightarrow v_\infty$$

Their expressions for the model where all faces are triangles are recorded in Appendix C.

Proposition 5.1 (Disks). [11] *We have:*

$$\mathbf{G}(v) = \sum_{k \geq 0} \frac{1}{2} \frac{(-1)^k \tilde{g}_k}{k!} \frac{\partial^k}{\partial v_\infty^k} \left[\Upsilon_b(v + v_\infty) + \Upsilon_b(v - v_\infty) - \Upsilon_b(-v + v_\infty) - \Upsilon_b(-v - v_\infty) \right].$$

The endpoints γ_\pm are determined by the two conditions:

$$(5.15) \quad \mathbf{G}(\tau + \varepsilon) = 0, \quad \varepsilon = 0, \frac{1}{2},$$

which follow from the finiteness of the generating series $\mathbf{F}(x)$ at $x = \gamma_\pm$.

If $\alpha = 1$, the 4 terms expression can be reduced to 2 terms using $\tau - v_\infty = v_\infty \bmod \mathbb{Z}$ and the pseudo-periodicity of the special function Υ_b . We do not reprove Theorem 5.1, as the scheme is similar to the next proposition that we prove.

Remarkably, the generating series of pointed disks and of cylinders have very simple expressions.

Proposition 5.2 (Pointed disks). *Define $\mathbf{G}^\bullet(v)$ as the analytic continuation of:*

$$(5.16) \quad x'(v)\mathbf{F}^\bullet(x(v)) + \frac{\partial}{\partial v} \left(\frac{nu \ln [\zeta'(x(v))]}{2(2 + n)} \right).$$

(for $\alpha = 1$ the last term is absent). We have:

$$(5.17) \quad \mathbf{G}^\bullet(v) = \frac{u}{2+n} \left[-\Upsilon_b(v+v_\infty) - \Upsilon_b(v-v_\infty) + \Upsilon_b(-v+v_\infty) + \Upsilon_b(-v-v_\infty) \right].$$

Proof. In the functional equation of Proposition 4.7, we can evaluate the contour integral using (5.3) and $\mathbf{F}^\bullet(x) \sim 1/x$ when $x \rightarrow \infty$. Thus:

$$(5.18) \quad \forall x \in \mathring{\gamma}, \quad \mathbf{F}^\bullet(x+i0) + \mathbf{F}^\bullet(x-i0) - n\zeta'(x)\mathbf{F}^\bullet(\zeta(x)) = -\frac{nu}{x-\zeta(\infty)}.$$

We can find a rational function of x which is a particular solution to (5.18), and subtract it to $\mathbf{F}^\bullet(x)$ to obtain a solution of the linear equation with vanishing right-hand side. This is the origin of the second term in (5.16). The construction reviewed in § 5.1 then implies that $\mathbf{G}^\bullet(v)$ satisfies the functional relation:

$$(5.19) \quad \mathbf{G}^\bullet(v+2\tau) + \mathbf{G}^\bullet(v) - n\mathbf{G}^\bullet(v+\tau) = 0, \quad \mathbf{G}^\bullet(v) = \mathbf{G}^\bullet(v+1) = -\mathbf{G}^\bullet(-v).$$

$\mathbf{G}^\bullet(v)$ inherits the singularities of (5.16). If $\alpha \neq 1$, we have a simple poles in the fundamental domain at:

$$(5.20) \quad \operatorname{Res}_{v \rightarrow v_\infty} dv \mathbf{G}^\bullet(v) = \frac{-2u}{2+n}, \quad \operatorname{Res}_{v \rightarrow (\tau-v_\infty)} dv \mathbf{G}^\bullet(v) = \frac{-nu}{2+n}.$$

(5.17) provides the unique solution to this problem. When $\alpha = 1$, we have $\zeta(\infty) = \infty$, and $v_\infty = \frac{1+\tau}{2}$, therefore $v_\infty = \tau - v_\infty$. Then, we have a unique simple pole in the fundamental domain:

$$\operatorname{Res}_{v \rightarrow v_\infty} dv \mathbf{G}^\bullet(v) = -u.$$

In this case, we find:

$$\mathbf{G}^\bullet(v) = \frac{u}{1+e^{-i\pi b}} \left[-\Upsilon_b(v-v_\infty) + \Upsilon_b(-v-v_\infty) \right].$$

Using the properties of Υ_b under translation, this is still equal to the right-hand side of (5.17). In other words, formula (5.17) is well-behaved when $v_\infty \rightarrow (\tau - v_\infty)$. \square

Proposition 5.3 (Cylinders). [13] Define $\mathbf{G}^{(2)}(v_1, v_2)$ as the analytic continuation of:

$$(5.21) \quad x'(v_1)x'(v_2)\mathbf{F}^{(2)}(x(v_1), x(v_2)) + \frac{\partial}{\partial v_1} \frac{\partial}{\partial v_2} \left(\frac{2 \ln [x(v_1) - x(v_2)] + n \ln [\zeta(x(v_1)) - x(v_2)]}{4 - n^2} \right).$$

We have:

$$(5.22) \quad \mathbf{G}^{(2)}(v_1, v_2) = \frac{1}{4-n^2} \left[\Upsilon'_b(v_1+v_2) - \Upsilon'_b(v_1-v_2) - \Upsilon'_b(-v_1+v_2) + \Upsilon'_b(-v_1-v_2) \right].$$

Proof. This result is proved in [13] for $\alpha = 1$, but its proof actually holds when ζ is any rational involution. The fact that ζ is an involution implies that $\mathbf{G}^{(2)}(v_1, v_2)$ is a symmetric function of v_1 and v_2 , as:

$$\frac{dx_1 dx_2}{(x_1 - x_2)^2} = \frac{d\zeta(x_1) d\zeta(x_2)}{(\zeta(x_1) - \zeta(x_2))^2}.$$

It must satisfy:

$$(5.23) \quad \mathbf{G}^{(2)}(v_1, v_2) + \mathbf{G}^{(2)}(v_1 + 2\tau, v_2) - n\mathbf{G}^{(2)}(v_1 + \tau, v_2) = 0,$$

$$(5.24) \quad \mathbf{G}^{(2)}(v_1, v_2) = \mathbf{G}^{(2)}(v_1 + 1, v_2) = -\mathbf{G}^{(2)}(-v_1, v_2).$$

It has a double pole at $v_1 = v_2$ so that $\mathbf{G}^{(2)}(v_1, v_2) = \frac{2}{4-n^2} \frac{1}{(v_1-v_2)^2} + O(1)$, double poles at $v_1 = v_2 + (\mathbb{Z} \oplus \tau\mathbb{Z})$ ensuing from (5.23)-(5.24), and no other singularities. Equation (5.22) provides the unique solution to this problem. \square

5.3. Refinement: separating loops. We have explained in § 4.4 that the functional equation satisfied by refined generating series, with a weight s per separating loop, only differs from the unrefined case by keeping the same cut γ , but replacing $n \rightarrow ns$ in the linear functional equations. Thus defining:

$$(5.25) \quad b(s) = \frac{\arccos(ns/2)}{\pi},$$

we immediately find:

Corollary 5.4 (Refined pointed disks). *Let $\mathbf{G}_s^\bullet(v)$ be the analytic continuation of:*

$$(5.26) \quad x'(v)\mathbf{F}_s^\bullet(x(v)) + \frac{\partial}{\partial v} \left(\frac{ns \ln[\zeta'(x(v))]}{2(2+ns)} \right).$$

We have:

$$(5.27) \quad \mathbf{G}_s^\bullet(v) = \frac{2}{2+ns} \left(-\Upsilon_{b(s)}(v+v_\infty) - \Upsilon_{b(s)}(v-v_\infty) + \Upsilon_{b(s)}(-v+v_\infty) + \Upsilon_{b(s)}(-v-v_\infty) \right).$$

\square

Corollary 5.5 (Refined cylinders). *Let $\mathbf{G}_s^{(2)}(v_1, v_2)$ be the analytic continuation of:*

$$x'(v_1)x'(v_2)\mathbf{F}_s^{(2)}(x(v_1), x(v_2)) + \frac{\partial}{\partial v_1} \frac{\partial}{\partial v_2} \left(\frac{2 \ln [x(v_1) - x(v_2)] + ns \ln [\zeta(x(v_1)) - x(v_2)]}{4 - n^2 s^2} \right).$$

We have:

$$(5.28) \quad \mathbf{G}_s^{(2)}(v_1, v_2) = \frac{1}{4 - n^2 s^2} \left[\Upsilon'_{b(s)}(v_1 + v_2) - \Upsilon'_{b(s)}(v_1 - v_2) - \Upsilon'_{b(s)}(-v_1 + v_2) + \Upsilon'_{b(s)}(-v_1 - v_2) \right].$$

\square

6. DEPTH OF A VERTEX IN DISKS

We now study the asymptotic behavior of the distribution of the depth P of the origin of a pointed disk, in loop model with bending energy.

6.1. Phase diagram and the volume exponent. The phase diagram of the model with bending energy is Theorem 6.1 below, and was established in [11]. We review its derivation, and push further the computations of [11] to derive (Corollary 6.5 below) the well-known exponent γ_{str} appearing in the asymptotic number of pointed rooted disks of fixed, large volume V . We remind that the model depends on the weight g per empty triangle, h per triangle crossed by a loop, and the bending energy α , and the weight u per vertex is set to 1 unless mentioned otherwise. A non-generic critical point occurs when γ_+ approaches the fixed point of the involution:

$$\gamma_+^* = \varsigma(\gamma_+^*) = \frac{1}{h(\alpha + 1)}.$$

In this limit, the two cuts γ and $\varsigma(\gamma)$ merge at γ_+^* , and one can justify on the basis of combinatorial arguments [11, Section 6] that $\gamma_- \rightarrow \gamma_-^*$ with:

$$|\gamma_-^*| < |\gamma_+^*| \quad \text{and} \quad \varsigma(\gamma_-^*) \neq \gamma_-^*.$$

In terms of the parametrization $x(v)$, it amounts to letting $T \rightarrow 0$, and this is conveniently measured in terms of the parameter:

$$q = e^{-\frac{\pi}{T}} \rightarrow 0.$$

To analyse the non-generic critical regime, we first need to derive the asymptotic behavior of the parametrization $x(v)$ and the special function $\Upsilon_b(v)$. This is performed respectively in Appendix B and D. The phase diagram and the volume exponent can then be obtained after a tedious algebra, which is summarized in Appendix E. The results of this analysis are:

Theorem 6.1. [11] *Assume $\alpha = 1$, and introduce the parameter:*

$$\rho = 1 - 2h\gamma_-^* = 1 - \frac{\gamma_-^*}{\gamma_+^*}.$$

There is a non-generic critical line, parametrized by $\rho \in (\rho_{\min}, \rho_{\max}]$:

$$\begin{aligned} \frac{g}{h} &= \frac{4(\rho b \sqrt{2+n} - \sqrt{2-n})}{-\rho^2(1-b^2)\sqrt{2-n} + 4\rho b \sqrt{2+n} - 2\sqrt{2-n}} \\ h^2 &= \frac{\rho^2 b}{24\sqrt{4-n^2}} \frac{\rho^2 b(1-b^2)\sqrt{2+n} - 4\rho\sqrt{2-n} + 6b\sqrt{2+n}}{-\rho^2(1-b^2)\sqrt{2-n} + 4\rho b \sqrt{2+n} - 2\sqrt{2-n}}. \end{aligned}$$

It realizes the dense phase of the model. The endpoint

$$\rho_{\max} = \frac{1}{b} \sqrt{\frac{2-n}{2+n}}$$

corresponds to the fully packed model $g = 0$, with the critical value $h = \frac{1}{2\sqrt{2}\sqrt{2+n}}$. The endpoint

$$\rho_{\min} = \frac{\sqrt{6+n} - \sqrt{2-n}}{(1-b)\sqrt{2+n}}$$

is a non-generic critical point realizing the dilute phase, and it has coordinates:

$$\begin{aligned}\frac{g}{h} &= 1 + \sqrt{\frac{2-n}{6+n}}, \\ h^2 &= \frac{b(2-b)}{3(1-b^2)(2+n)} \left(1 - \frac{1}{4\sqrt{(2-n)(6+n)}}\right).\end{aligned}$$

The fact that the non-generic critical line ends at $\rho_{\max} < 2$ is in agreement with $|\gamma_-^*| < |\gamma_-^*|$.

Theorem 6.2. *There exists $\alpha_c(n) > 1$ such that, in the model with bending energy $\alpha < \alpha_c(n)$, the qualitative conclusions of the previous theorem still hold, with more a complicated parametrization of the critical line given in Appendix E. For $\alpha = \alpha_c(n)$, only a non-generic critical point in the dilute phase exists, and for $\alpha > \alpha_c(n)$, non-generic critical points do not exist.*

Theorem 6.3. *Assume (g, h) are chosen such that the model has a non-generic critical point for vertex weight $u = 1$. When $u < 1$ tends to 1, we have:*

$$q \sim \left(\frac{1-u}{\Delta}\right)^c.$$

with the universal exponent:

$$c = \begin{cases} \frac{1}{1-b} & \text{dense} \\ 1 & \text{dilute} \end{cases}.$$

The non-universal constant reads, for $\alpha = 1$:

$$\Delta = \begin{cases} \frac{6(n+2)}{b} \frac{\rho^2(1-b)^2\sqrt{2+n}+2\rho(1-b)\sqrt{2-n}-2\sqrt{2+n}}{\rho^2b(1-b^2)\sqrt{2+n}-4\rho(1-b^2)\sqrt{2-n}+6b\sqrt{2+n}} & \text{dense} \\ \frac{24}{b(1-b)(2-b)} & \text{dilute} \end{cases}.$$

For $\alpha \neq 1$, its expression is much more involved, but all the ingredients to obtain it are in Appendix E.

We can deduce the asymptotic growth of the number of planar maps with respect to the volume. The details of the proof are given in Appendix F.

Corollary 6.4. *Assume (g, h) are chosen such that the model has a non-generic critical point for vertex weight $u = 1$. The number of rooted maps of volume $V \rightarrow \infty$ with a marked point in the gasket behaves as:*

$$[u^V \cdot x^{-4}] \mathbf{F}^{\bullet \text{ in gasket}}(x) \sim \frac{A_{\text{gasket}}}{\Delta^{\frac{c}{2}} [-\Gamma(-\frac{c}{2})]} V^{1+\frac{c}{2}}.$$

The constant prefactor is non-universal:

$$A_{\text{gasket}} = \frac{4((1-2\alpha)\cos(\pi w_\infty^*) + 2 - 2\alpha)}{(1-\alpha^2)^2 h^2 (\cos(\pi w_\infty^*) + 1)},$$

and for $\alpha = 1$ it simplifies to:

$$A_{\text{gasket}} = \frac{\rho(\frac{\rho}{4} - 1)}{h^2}.$$

Corollary 6.5. *Assume (g, h) are chosen such that the model has a non-generic critical point for vertex weight $u = 1$. The number of pointed rooted planar maps of volume $V \rightarrow \infty$ behaves like:*

$$[u^V \cdot x^{-4}] \mathbf{F}^\bullet(x) \sim \frac{A}{\Delta^{bc}[-\Gamma(-bc)] V^{1+bc}}.$$

Therefore:

$$\gamma_{\text{str}} = -bc.$$

For $\alpha = 1$, the constant reads:

$$A = \frac{\rho(\rho^2(1-b^2)\sqrt{2-n} - 6\rho b\sqrt{2+n} + 6\sqrt{2-n})}{2h^3}.$$

and for $\alpha \neq 1$, it is given in Appendix F.

We can deduce the behavior when $V \rightarrow \infty$ of the probability that in a pointed rooted disk of volume V , the origin belongs to the gasket:

Corollary 6.6. *Assume (g, h) are chosen such that the model has a non-generic critical point for vertex weight $u = 1$. When $V \rightarrow \infty$:*

$$\mathbb{P}[\bullet \text{ in gasket} \mid V, L = 3] \sim \frac{A_{\text{gasket}}}{A} \frac{\Gamma(-bc)}{\Gamma(-\frac{c}{2})} \frac{1}{\Delta^{c(\frac{1}{2}-b)} V^{c(\frac{1}{2}-b)}}.$$

6.2. Singular behavior of refined generating series. We would like to the asymptotic behavior of the weighted count of:

- (i) pointed disks with fixed volume V and fixed depth P , in such a way that $V, P \rightarrow \infty$.
- (ii) cylinders with fixed volume V , with two boundaries separated by P loops, in such a way that $V, P \rightarrow \infty$.

This information can be extracted from the canonical ensemble where a map with a boundary of perimeter L_i is weighted by $x^{-(L_i+1)}$, each separating loop is counted with a weight s , and each vertex with a weight u . The generating series of interest are respectively $\mathbf{F}_s^\bullet(x)$ for (i), and $\mathbf{F}_s^{(2)}(x_1, x_2)$ for (ii). To retrieve the generating series of maps with fixed, large V and D , we must obtain scaling asymptotics for these generating series when $u \rightarrow 1$ and $s \rightarrow 2/n$ or $-2/n$. In the $b(s)$ -plane, this corresponds to $b(s) \rightarrow 0$ or 1 . We shall see that the singularity at $s \rightarrow -2/n$ is actually subdominant.

As for fixing boundary perimeters, two regimes can be addressed. Either we want L_i to diverge, in which case we should derive the previous asymptotics when x approached the singularity $\gamma_+ \rightarrow \gamma_+^*$, since the other endpoint $|\gamma_-| < |\gamma_+^*|$ is subdominant. Or, we want to keep L_i finite. In that case, we can work in the canonical ensemble by choosing x away from $[\gamma_-, \gamma_+]$. We will actually consider the canonical ensemble with a control parameter w_i such that $x_i = x(\frac{1}{2} + \tau w_i)$, and derive asymptotics for w_i in some compact region containing $[0, 1)$. The asymptotic count of maps with fixed, finite boundary perimeter L_i can then be retrieved by a contour integration around $w_i = w_\infty^*$.

In a nutshell, we will set $x = x(v_i)$ with $v_i = \varepsilon_i + \tau w_i$ and $\varepsilon_i = 0$ to study a i -th boundary of large perimeter, and $\varepsilon_i = \frac{1}{2}$ to study finite boundaries.

The scaling behavior of $\mathbf{F}_s^\bullet(x)$ in the regime of large boundaries can be established using the asymptotics given in Appendix B and D, especially Lemma B.3 for $x(\varepsilon + \tau w)$ and Lemma D.1 for $\Upsilon_{b(s)}(\bar{\varepsilon} + \tau(\pm w \pm w_\infty))$.

Theorem 6.7. *Let (g, h) be a non-generic critical point at $u = 1$. When $u \rightarrow 1$, i.e., $q \rightarrow 0$, we have²:*

$$(6.1) \quad \mathbf{F}_s^\bullet(x)|_{\text{sing}} = \frac{q^{b(s)/2-1/2}}{1-q^{b(s)}} \Phi_{b(s)}\left(\frac{x-\gamma_+}{q^{1/2}}\right) + O(q^{b(s)/2}),$$

$$(6.2) \quad \mathbf{F}_s^\bullet(x)|_{\text{sing}} = \Psi_{b(s)}(x) - \frac{q^{b(s)}}{1-q^{b(s)}} \tilde{\Psi}_{b(s)}(x) + O(q).$$

The error in (6.1) is uniform for $\xi = q^{-\frac{1}{2}}(x - \gamma_+)$ in any fixed compact, and compatible³ with differentiation. The scaling function reads, in a parametric form:

$$(6.3) \quad \begin{cases} \Phi_{b(s)}(\xi(w)) &= \frac{2h(1-\alpha^2)}{2+ns} \frac{\cos(\pi b(s)w_\infty^*)}{\cos(\pi w_\infty^*)} \frac{\sin(\pi b(s)w)}{\sin(\pi w)}, \\ \xi(w) &= \frac{16 \cos(\pi w_\infty^*)}{(1-\alpha^2)h} \cos^2\left(\frac{\pi w}{2}\right) \end{cases}.$$

and in the case $\alpha = 1$ it simplifies to:

$$(6.4) \quad \begin{cases} \Phi_{b(s)}(\xi(w)) &= \frac{4h}{\rho\sqrt{2+ns}} \frac{\sin(\pi b(s)w)}{\sin(\pi w)}, \\ \xi(w) &= \frac{4\rho}{h} \cos^2(\pi w) \end{cases}.$$

The error in (6.2) is uniform for x away from γ_+ independently of u , and compatible with differentiation. The limit function reads:

$$\begin{cases} \Psi_{b(s)}(X(w)) &= \frac{-2}{2+ns} \frac{h(1-\alpha^2)}{\cos(\pi w_\infty^*)} \frac{(\cos(\pi w) - \cos(\pi w_\infty^*))^2}{\sin(\pi w)} \left(\frac{\cos[\pi(1-b(s))(w+w_\infty^*)]}{\sin[\pi(w+w_\infty^*)]} + \frac{\cos[\pi(1-b(s))(w-w_\infty^*)]}{\sin[\pi(w-w_\infty^*)]} \right), \\ X(w) - \gamma_+^* &= \frac{2 \cos(\pi w_\infty^*)}{h(1-\alpha^2)} \frac{1}{\cos(\pi w) - \cos(\pi w_\infty^*)} \end{cases}.$$

In the case of $\alpha = 1$, it simplifies to:

$$\begin{cases} \Psi_{b(s)}(X(w)) &= \frac{8h}{\rho\sqrt{2+ns}} \cot(\pi w) \sin[\pi(1-b(s))w], \\ X(w) - \gamma_+^* &= \frac{8\rho}{h \cos(\pi w)} \end{cases}.$$

The subleading order is given by $\tilde{\Psi}_{b(s)} = \Psi_{b(s)+2} - \Psi_{b(s)}$ which reads:

$$\tilde{\Psi}_{b(s)}(X(w)) = \frac{8u}{2+ns} \frac{h(1-\alpha^2) \cos(\pi b(s)w_\infty^*)}{\cos(\pi w_\infty^*)} [\cos(\pi w) - \cos(\pi w_\infty^*)]^2 \frac{\sin(\pi b(s)w)}{\sin(\pi w)}.$$

and for $\alpha = 1$:

$$\tilde{\Psi}_{b(s)}(X(w)) = \frac{16uh}{\rho\sqrt{2+ns}} \frac{\cos^2(\pi w) \sin(\pi b(s)w)}{\sin(\pi w)}.$$

²To be precise, we compute here the behavior of the singular part of $\mathbf{F}_s^\bullet(x)$, i.e., we did not include the shift in (5.26), as it will always give zero when performing a contour integral against x^L around the cut.

³I.e., it still yields a negligible term as compared to the previous ones.

6.3. Large deviations of the depth: main result.

Theorem 6.8. *Let (g, h) be a non-generic critical point at $u = 1$. Consider the random ensemble of refined disks of volume V , boundary perimeter L . When $V \rightarrow \infty$ and ℓ remains fixed positive, the probability that the origin is separated from the boundary by P loops behaves like:*

$$(6.5) \quad \mathbb{P}\left[P = \frac{c \ln V}{\pi} p \mid V, L = \ell\right] \sim \frac{A_1(p, \ell)}{\sqrt{\ln V} V^{\frac{c}{\pi} J(p)}},$$

$$(6.6) \quad \mathbb{P}\left[P = \frac{c \ln V}{2\pi} p \mid V, L = \ell V^{\frac{c}{2}}\right] \sim \frac{A_2(p, \ell)}{\sqrt{\ln V} V^{\frac{c}{2\pi} J(p)}}.$$

These asymptotics are uniform for $p \ll \ln V$. The large deviations function reads:

$$(6.7) \quad \begin{aligned} J(p) &= \sup_{s \in [0, 2/n]} \{p \ln(s) + \arccos(ns/2) - \arccos(n/2)\} \\ &= p \ln \left(\frac{2}{n} \frac{p}{\sqrt{1+p^2}} \right) + \operatorname{arccot}(p) - \arccos(n/2). \end{aligned}$$

The constant prefactor is non-universal:

$$A_j(p, \ell) = \frac{1}{\sqrt{2^{2-j} c p (p^2 + 1)}} \frac{\mathcal{I}_j(\ell, \pi^{-1} \operatorname{arccot}(p))}{\mathcal{I}_j(\ell, b)},$$

with:

$$\begin{aligned} \mathcal{I}_1(\ell, \beta) &= \oint \frac{dx x^\ell}{2i\pi} \frac{\tilde{\Psi}_\beta(x)}{[-\Gamma(-c\beta)] \Delta^{c\beta}}, \\ \mathcal{I}_2(\ell, \beta) &= \oint_{\tilde{c}} \oint_{\tilde{c}} \frac{d\tilde{u}}{2i\pi} \frac{d\tilde{x}}{2i\pi} \left(\frac{\tilde{u}}{\Delta} \right)^{\frac{c}{2}(\beta-1)} e^{\tilde{u} + \ell \tilde{x} / \gamma_+^*} \Phi_\beta \left(\frac{\tilde{x} \Delta^{\frac{c}{2}}}{\tilde{u}^{\frac{c}{2}}} \right), \end{aligned}$$

with $j = 1$ if we scale $L = \ell V^{\frac{c}{2}}$ for some finite positive ℓ , and $j = 2$ if L is kept finite.

From a macroscopic point of view, a pointed disk with a finite boundary looks like a sphere with two marked points, while a pointed disk with large boundary looks like a disk. We observe that in the regime $P \sim \ln V$:

$$\mathbb{P}[2P \mid V, L = \ell] \sim \mathbb{P}[P \mid V, L = \ell V^{\frac{c}{2}}]^2$$

Intuitively, this means that the nesting of loops in a sphere can be described by cutting the sphere in two independent halves (which are disks). In Section 9.4 and in particular Corollary 9.9, we will find an analog result for CLE.

The remaining of this section is devoted to the proof of these results. The probability that the origin of a pointed disk is separated from the boundary by P loops reads:

$$\mathbb{P}[P \mid V, L] = \frac{\mathcal{P}(V, L; P)}{\tilde{\mathcal{P}}(V, L)}$$

and we need to analyze, when $V \rightarrow \infty$, and L and P in various regimes, the behavior of the integrals:

$$(6.8) \quad \begin{aligned} \mathcal{P}(V, L; P) &= \oint \oint \oint \frac{du}{2i\pi u^{V+1}} \frac{x^L dx}{2i\pi} \frac{ds}{2i\pi s^{P+1}} \mathbf{F}_s^\bullet(x), \\ \tilde{\mathcal{P}}(V, L) &= \oint \oint \frac{du}{2i\pi u^{V+1}} \frac{x^L dx}{2i\pi} \mathbf{F}^\bullet(x). \end{aligned}$$

The contours for u and s are initially small circles around 0, and the contour for x surrounds the union of the cuts $[\gamma^-, \gamma^+]$ for the corresponding u 's.

6.4. Finite perimeters. When L is finite, we can keep the contour integral over x away from the cut. So, we need to use (6.2). The first term disappears when integrating over u , and remains:

$$(6.9) \quad \mathbf{F}_s^\bullet(x)|_{\text{sing}} = -\frac{q^{b(s)} \tilde{\Psi}_{b(s)}(x)}{1 - q^{b(s)}} + O(q),$$

where the error in (6.9) is uniform for x in any compact away from the cut. The first term does not depend on u , therefore it does not contribute to the contour integral. Since $q \sim \left(\frac{1-u}{\Delta}\right)^c$ when $u \rightarrow 1$, we find directly by transfer theorems:

$$(6.10) \quad \tilde{\mathcal{P}}(V, L) \sim \left\{ \oint_{[\gamma_-^*, \gamma_+^*]} \frac{x^L dx}{2i\pi} \tilde{\Psi}_b(x) \right\} \frac{1}{[-\Gamma(-bc)] \Delta^{bc}} \frac{1}{V^{1+bc}}.$$

To analyze $\mathcal{P}(V, L, P)$, we should study the critical points of:

$$(6.11) \quad \mathcal{S}_1(x, u, s) = -V \ln u - P \ln s + cb(s) \ln \left(\frac{1-u}{\Delta} \right) - \ln \left[1 - \left(\frac{1-u}{\Delta} \right)^{cb(s)} \right] + \ln \tilde{\Psi}_{b(s)}(x).$$

Let us denote (u^*, s^*) the coordinate of the critical point of \mathcal{S} , which is a function of x . Our strategy is to make assumptions on the location of s^* , which will imply several regimes as regards P . Then, we will reverse the point of view, and study the asymptotics of the integrals, by making the suitable change of variables guessed during the analysis of critical points, focusing on the regime $P \sim \ln V$ which is the most typical.

Let us assume that s^* has a limit away from $2/n$. This means that $b(s^*)$ has a non-zero limit when $V \rightarrow \infty$. Then, the third term in (6.11) is negligible and we have from $\partial_u \mathcal{S}_1 = 0$:

$$V \sim -\frac{cb(s^*)}{1 - u^*},$$

and from $\partial_s \mathcal{S}_1 = 0$:

$$\frac{P}{s^*} \sim \frac{nc \ln(1 - u^*)}{\pi \sqrt{4 - n^2(s^*)^2}}.$$

Therefore, let us define the functions:

$$(6.12) \quad \mathfrak{s}(p) = \frac{2}{n} \frac{p}{\sqrt{1 + p^2}}, \quad \mathfrak{b}(p) = \frac{\text{arccot}(p)}{\pi},$$

If we set $P = \frac{c \ln V}{\pi} p$, we obtain:

$$s^* = \mathfrak{s}(p), \quad b(s^*) = \mathfrak{b}(p),$$

and the condition that the third term was negligible imposes that p is such that $\mathfrak{b}(p) \ln V \rightarrow \infty$. This is of course valid if $p \in O(1)$. But, since $\mathfrak{b}(p) \sim \frac{1}{\pi p}$ when $p \rightarrow \infty$, this condition is actually checked as long as $p \ll \ln V$, *i.e.*, $P \ll (\ln V)^2$ using (6.4). Besides, we evaluate:

$$\partial_s^2 \mathcal{S}_1(x, u^*, \mathfrak{s}(p)) \sim \ln V.$$

Therefore, now assuming that:

$$P = \frac{c \ln V}{\pi} p \quad \text{with } p \ll \ln V,$$

we suggest the change of variable:

$$u = 1 - \frac{\tilde{u}}{V}, \quad s = \mathfrak{s}(p) + \frac{\tilde{s}}{\sqrt{\ln V}}.$$

We find that:

$$\frac{du}{u^{V+1}} \frac{ds}{s^{P+1}} \mathbf{F}_s^\bullet(x) \sim -\frac{d\tilde{u} d\tilde{s}}{V \sqrt{\ln V}} \frac{\tilde{\Psi}_{\mathfrak{b}(p)}(x)}{\mathfrak{s}(p)} e^{\tilde{u}} \left(\frac{\tilde{u}}{\Delta V} \right)^{c\mathfrak{b}(p)} V^{-\frac{cp}{\pi} \ln \mathfrak{s}(p)} \exp \left\{ \frac{cn^2(p^2 + 1)^2}{8\pi p} \tilde{s}^2 \right\},$$

where the convergence to the limit function in the right-hand side is uniform for \tilde{s} in any compact and x away from the cut. Let us deform the contour in (s, u) to a steepest descent contour passing through $(\mathfrak{s}(p), 1 + O(1/V))$ (see Figure 10). In particular, in (\tilde{s}, \tilde{u}) , this contour is $(\mathfrak{s}(p) + i\mathbb{R}) \times \mathcal{C}$ in the region $|\tilde{s}| \ll \sqrt{\ln V}$ and $|\tilde{u}| \ll V$, where \mathcal{C} is the imaginary axis, avoiding the point $\tilde{u} = 0$ by a small circle in the domain of $\text{Re } \tilde{u} > 0$. Since the integral along the steepest descent contour is convergent, and the module of the integrand is smaller than what it is in the region $|\tilde{s}| \ll \sqrt{\ln V}$ by definition of a steepest descent contour, we can apply dominated convergence and obtain:

$$\oint \oint \frac{du}{2i\pi u^{V+1}} \frac{ds}{s^{P+1}} \mathbf{F}_s^\bullet(x) \sim \frac{\tilde{\Psi}_{\mathfrak{b}(p)}(x)}{\mathfrak{s}(p) V^{1+c\mathfrak{b}(p)+\frac{cp}{\pi} \ln \mathfrak{s}(p)} \sqrt{\ln V}} \left\{ \oint_{\bar{\mathcal{C}}} \frac{-d\tilde{u} e^{\tilde{u}}}{2i\pi} \left(\frac{\tilde{u}}{\Delta} \right)^{c\mathfrak{b}(p)} \right\} \left\{ \int_{\mathbb{R}} \frac{d\tilde{s}}{2\pi} e^{-cn^2(p^2+1)^2 \tilde{s}^2 / 16\pi p} \right\},$$

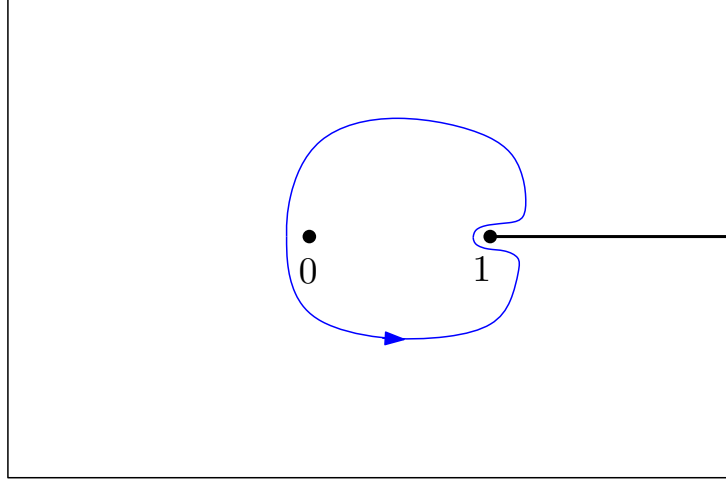
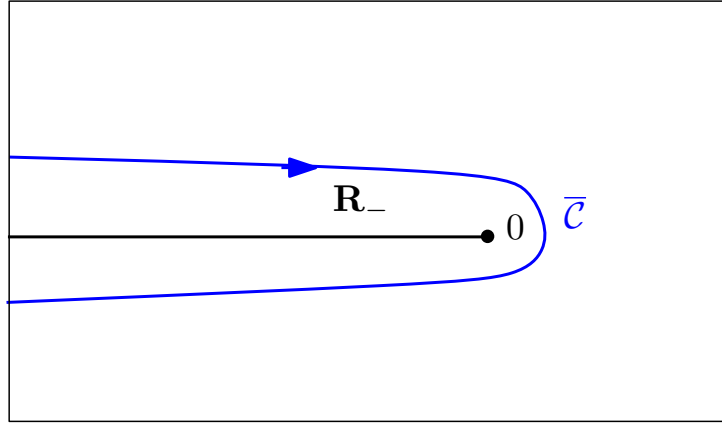
where $\bar{\mathcal{C}}$ is the continuation of \mathcal{C} to infinity making the integral convergent. This holds uniformly for x away from the cut. Both integrals can be performed explicitly, and we deduce:

$$(6.13) \quad \mathcal{P}\left(V, L, P = \frac{cp \ln V}{2\pi}\right) \sim \left\{ \oint_{[\gamma_-^*, \gamma_+^*]} \frac{x^L dx}{2i\pi} \frac{\tilde{\Psi}_{\mathfrak{b}(p)}(x)}{\Delta^{c\mathfrak{b}(p)}} \right\} \frac{V^{-1-c\mathfrak{b}(p)-\frac{c}{\pi} \ln \mathfrak{s}(p)} (\ln V)^{-1/2}}{\sqrt{2cp(p^2 + 1)} [-\Gamma(-c\mathfrak{b}(p))]}.$$

We remind that this result has been derived in the regime $p \ll \ln V$. In particular, it is valid for $p \ll 1$, p of order 1, and (not too) large p . Taking the ratio of (6.13) and (6.10) leads to the announced result (6.5).

6.5. Large perimeters. Now, we study the case where the (x^*, s^*) -coordinates of the critical point are such that $\xi^* = \frac{x^* - \gamma_+^*}{(q^*)^{1/2}}$ has a limit, and s^* has a limit away from $2/n$. We can then use (6.1):

$$(6.14) \quad \mathbf{F}_s^\bullet(x)|_{\text{sing}} \sim \frac{q^{b(s)/2-1/2}}{1 - q^{b(s)}} \Phi_{b(s)}\left(\frac{x - \gamma^+}{q^{1/2}}\right).$$

FIGURE 10. The contour of integration for \tilde{u} .FIGURE 11. The contour $\bar{\mathcal{C}}$.

We need to analyze the critical points of:

$$\mathcal{S}_2(u, x, s) = -V \ln u - P \ln s + L \ln x + \frac{c}{2}(b(s) - 1) \ln \left(\frac{1-u}{\Delta} \right) + \ln \Phi_{b(s)} \left(\frac{x - \gamma_+^*}{[(1-u)/\Delta]^{\frac{c}{2}}} \right).$$

Compared to (6.14), we have replaced γ_+ by γ_+^* , as it differs only by $O(q)$. The equation $\partial_u \mathcal{S}_2 = 0$ gives:

$$V \sim \frac{-\frac{c}{2}}{1-u^*} \left(b(s^*) - 1 + \xi^* (\ln \Phi_{b(s^*)})'(\xi^*) \right),$$

while the equation $\partial_x \mathcal{S}_2 = 0$ gives:

$$\frac{L}{\gamma_+^*} \sim - \left(\frac{\Delta}{1-u^*} \right)^{\frac{c}{2}} (\ln \Phi_{b(s^*)})'(\xi^*).$$

It is then necessary that $L \sim V^{\frac{c}{2}}$. The equation $\partial_s \mathcal{S}_2 = 0$ gives:

$$\frac{P}{s^*} \sim \frac{nc \ln(1 - u^*)}{2\pi \sqrt{4 - n^2(s^*)^2}}.$$

If we set $P = \frac{c \ln V}{2\pi} p$, we obtain $s^* \sim \mathfrak{s}(p)$ with the function introduced in (6.12). Notice the factor of $1/2$ compared to (6.4) in the previous section, due to the occurrence of $q^{b(s)/2}$ here and $q^{b(s)}$ there in the scaling limits of $\mathbf{F}_s^\bullet(x)$. We also evaluate:

$$\partial_s^2 \mathcal{S}_2(u^*, x^*, \mathfrak{s}(p)) \sim \ln V.$$

Therefore, let us now assume:

$$L = \ell V^{\frac{c}{2}}, \quad P = \frac{cp \ln V}{2\pi}$$

for a fixed positive ℓ , and for $p \ll (\ln V)$ – this asymptotic upper bound can be justified as in Section 6.4. The previous discussion suggests the change of variable to compute $\tilde{\mathcal{P}}(V, L)$:

$$u = 1 - \frac{\tilde{u}}{V}, \quad x = \gamma_+^* + \frac{\tilde{x}}{V^{\frac{c}{2}}}.$$

We then find:

$$\frac{du}{u^{V+1}} dx x^L \mathbf{F}_s^\bullet(x) \sim \frac{d\tilde{u} d\tilde{x}}{V^{1+\frac{cb}{2}}} \Phi_b\left(\frac{\tilde{x}}{(\tilde{u}/\Delta)^{\frac{c}{2}}}\right) e^{\tilde{u}+\ell\tilde{x}/\gamma_+^*} \left(\frac{u}{\Delta}\right)^{\frac{c}{2}(b-1)},$$

where the convergence to the limit function in the right-hand side is uniform for (\tilde{u}, \tilde{x}) in any compact away from \mathbb{R}_-^2 . The contours can be deformed to steepest descent contours \mathcal{C}^2 (see Figure 11), and we can conclude as before by dominated convergence:

$$(6.15) \quad \tilde{\mathcal{P}}(V, L) \sim \left\{ \oint_{\bar{\mathcal{C}}} \oint_{\bar{\mathcal{C}}} \frac{d\tilde{u} d\tilde{x}}{(2i\pi)^2} e^{\tilde{u}+\ell\tilde{x}/\gamma_+^*} \left(\frac{\tilde{u}}{\Delta}\right)^{\frac{c}{2}(b-1)} \Phi_b\left(\frac{\tilde{x}}{(\tilde{u}/\Delta)^{\frac{c}{2}}}\right) \right\} V^{-1-\frac{cb}{2}}.$$

Likewise, in order to compute $\mathcal{P}(V, L, P)$, we make the change of variable:

$$u = 1 - \frac{\tilde{u}}{V}, \quad s = \mathfrak{s}(p) + \frac{\tilde{s}}{\sqrt{\ln V}}, \quad x = \gamma_+^* + \frac{\tilde{x}}{V^{\frac{c}{2}}}.$$

We then find:

$$\begin{aligned} & \frac{du}{u^{V+1}} \frac{ds}{s^{P+1}} dx x^L \mathbf{F}_s^\bullet(x) \\ & \sim \frac{d\tilde{u} d\tilde{x} d\tilde{s} (\gamma_+^*)^L}{\mathfrak{s}(p) V^{1+\frac{c}{2}b(p)+\frac{cp}{2\pi}\ln \mathfrak{s}(p)} \sqrt{\ln V}} \Phi_{b(s)}\left(\frac{\tilde{x}}{(\tilde{u}/\Delta)^{\frac{c}{2}}}\right) e^{\tilde{u}+\ell\tilde{x}/\gamma_+^*} \left(\frac{\tilde{u}}{\Delta}\right)^{\frac{c}{2}(b(s)-1)} \exp\left\{\frac{cn^2(p^2+1)^2}{16\pi p} \tilde{s}^2\right\}, \end{aligned}$$

where the convergence to the limit function in the right-hand side is uniform for $\tilde{s}, \tilde{x}, \tilde{u}$ in any compact with \tilde{u} away from 0. We deform the contours to steepest descent contours \mathcal{C}^2 in the variables (x, u) , and $i\mathbb{R}$ in the variable $|\tilde{s}| \ll \sqrt{\ln V}$. By properties of steepest descent contours, we can apply dominated convergence and find:

$$(6.16) \quad \begin{aligned} \mathcal{P}(V, L, P) & \sim \left\{ \oint_{\bar{\mathcal{C}}} \oint_{\bar{\mathcal{C}}} \frac{d\tilde{x} d\tilde{u}}{(2i\pi)^2} e^{\tilde{u}+\ell\tilde{x}/\gamma_+^*} \left(\frac{\tilde{u}}{\Delta}\right)^{\frac{c}{2}(b(s)-1)} \Phi_{b(s)}\left(\frac{\tilde{x}}{(\tilde{u}/\Delta)^{\frac{c}{2}}}\right) \right\} \\ & \times \frac{(\ln V)^{-1/2} V^{-1-\frac{c}{2}b(p)-\frac{cp}{2\pi}\ln \mathfrak{s}(p)}}{\sqrt{cp(p^2+1)}}. \end{aligned}$$

Taking the ratio of (6.16) and (6.15) gives the desired distribution (6.6).

7. SEPARATING LOOPS IN CYLINDERS

Let us consider the probability that, in a random ensemble of planar maps of volume V , two boundaries of given perimeter L_1 and L_2 are separated by P loops:

$$\mathbb{P}[P \mid V, L_1, L_2] = \frac{\oint \oint \oint \oint \frac{du}{2i\pi u^{V+1}} \frac{x_1^{L_1} dx_1}{2i\pi} \frac{x_2^{L_2} dx_2}{2i\pi} \frac{ds}{2i\pi s^{P+1}} \mathbf{F}_s^{(2)}(x_1, x_2)}{\oint \oint \oint \frac{du}{2i\pi u^{V+1}} \frac{x_1^{L_1} dx_1}{2i\pi} \frac{x_2^{L_2} dx_2}{2i\pi} \mathbf{F}^{(2)}(x_1, x_2)}.$$

The analog of Theorem 6.7 for the behavior of $\mathbf{F}_s^{(2)}$ is derived in Appendix G, and it features singularities of the type $q^{b(s)/j}$ with $j = 1$ for x_1 and x_2 both close to or both away from γ_+^* , and $j = 2$ for x_1 close to γ_+^* and x_2 close to ∞ . In that regard, the origin in pointed disks behaves as a boundary face whose perimeter is kept finite in a cylinder. As the type of singularities encountered in the asymptotic analysis is identical, the result can be directly derived from Sections 6.4-6.5:

Theorem 7.1. *When $V \rightarrow \infty$, ℓ_1 and ℓ_2 are fixed positive parameters, and $p \ll \ln V$, we have:*

$$\begin{aligned} \mathbb{P}\left[P = \frac{c \ln V}{\pi} p \mid V, L_1 = \ell_1, L_2 = \ell_2\right] &\sim \frac{A_3(p, \ell_1, \ell_2)}{\sqrt{\ln V} V^{\frac{c}{\pi} J(p)}}, \\ \mathbb{P}\left[P = \frac{c \ln V}{2\pi} p \mid V, L_1 = \ell_1, L_2 = \ell_2 V^{\frac{c}{2}}\right] &\sim \frac{A_4(p, \ell_1, \ell_2)}{\sqrt{\ln V} V^{\frac{c}{2\pi} J(p)}}, \\ \mathbb{P}\left[P = \frac{c \ln V}{\pi} p \mid V, L_1 = \ell_1 V^{\frac{c}{2}}, L_2 = \ell_2 V^{\frac{c}{2}}\right] &\sim \frac{A_5(p, \ell_1, \ell_2)}{\sqrt{\ln V} V^{\frac{c}{\pi} J(p)}}. \end{aligned}$$

where the large deviations function $J(p)$ is the same as in (6.7). The constant prefactors are non-universal:

$$A_k(p, \ell_1, \ell_2) = \frac{1}{\sqrt{2^{\{k\}} c p (p^2 + 1)}} \frac{\mathcal{I}_k(\ell_1, \ell_2, \pi^{-1} \operatorname{arccot}(p))}{\mathcal{I}_k(\ell_1, \ell_2, b)},$$

where we declare $\{3\} = \{5\} = 2$ and $\{4\} = 1$, and:

$$\begin{aligned} \mathcal{I}_3(\ell_1, \ell_2, \beta) &= \oint \oint \frac{x_1^{\ell_1} dx_1}{2i\pi} \frac{x_2^{\ell_2} dx_2}{2i\pi} \frac{\Xi_{\beta,3}(x_1, x_2)}{[-\Gamma(-c\beta)] \Delta^{c\beta}}, \\ \mathcal{I}_4(\ell_1, \ell_2, \beta) &= \oint \oint \oint \frac{x_1^{\ell_1} dx_1}{2i\pi} \frac{d\tilde{x}_2}{2i\pi} \frac{d\tilde{u}}{2i\pi} e^{\tilde{u} + \ell_2 \tilde{x}_2 / \gamma_+^*} \left(\frac{\tilde{u}}{\Delta}\right)^{\frac{c}{2}(\beta-1)} \Xi_{\beta,4}\left(x_1, \frac{\tilde{x}_2}{(\tilde{u}/\Delta)^{\frac{c}{2}}}\right), \\ \mathcal{I}_5(\ell_1, \ell_2, \beta) &= \oint \oint \oint \frac{d\tilde{x}_1}{2i\pi} \frac{d\tilde{x}_2}{2i\pi} \frac{d\tilde{u}}{2i\pi} e^{\tilde{u} + (\ell_1 \tilde{x}_1 + \ell_2 \tilde{x}_2) / \gamma_+^*} \left(\frac{\tilde{u}}{\Delta}\right)^{\beta-1} \Xi_{\beta,5}\left(\frac{\tilde{x}_1}{(\tilde{u}/\Delta)^{\frac{c}{2}}}, \frac{\tilde{x}_2}{(\tilde{u}/\Delta)^{\frac{c}{2}}}\right). \end{aligned}$$

where $\Xi_{\beta,j}$ are defined in Appendix G. □

8. WEIGHTING LOOPS BY I.I.D. RANDOM VARIABLES

8.1. Definition and main result. Following [71], we introduce a model of random maps with weighted loop configurations ; we describe it for pointed disks, but it will be clear

that our reasoning extends to the cylinder topology. Let ξ be a random variable, with distribution μ , for which we assume that the cumulant function,

$$\Lambda_\mu(\lambda) := \ln \mathbb{E}[e^{\lambda\xi}],$$

exists for λ in a neighborhood of 0. Given a map with a self-avoiding loop configuration, let $(\xi_l)_{l \in \mathcal{L}}$ be a sequence of i.i.d. random variables distributed like ξ , indexed by the set \mathcal{L} of loops. Let $\mathcal{L}_{\text{sep}} \subseteq \mathcal{L}$ be the set of loops separating the boundary from the marked point. We would like to describe the joint distribution of the depth $P = |\mathcal{L}_{\text{sep}}|$ and of the sum $\Xi = \sum_{l \in \mathcal{L}_{\text{sep}}} \xi_l$.

Remind that $\mathbf{F}_{[P]}^\bullet(x)$ is the generating series of pointed disks with exactly P separating loops. Our problem is solved by introducing the generating series $\mathbf{F}_{s,\lambda}^\bullet(x)$, as the μ -expectation value of the generating series of pointed disks, whose usual weight in the loop model is multiplied by $\prod_{l \in \mathcal{L}_{\text{sep}}} s e^{\lambda \xi_l}$. By construction, we have:

$$\mathbf{F}_{s,\lambda}^\bullet(x) = \sum_{P \geq 0} (s e^{\Lambda_\mu(\lambda)})^P \mathbf{F}_{[P]}^\bullet(x) = \mathbf{F}_{s \exp(\Lambda_\mu(\lambda))}^\bullet(x).$$

In the ensemble of pointed disks with volume V and perimeter L , the joint distribution we look for reads:

$$\mathbb{P}(P, \Xi | V, L) = \frac{\mathcal{P}(V, L; P, \Xi)}{\tilde{\mathcal{P}}(V, L)}$$

with a new denominator – compare with (6.8):

$$\mathcal{P}(V, L; P, \Xi) = \oint \oint \oint \oint \frac{du}{2i\pi u^{V+1}} \frac{dx x^L}{2i\pi} \frac{ds}{2i\pi s^{P+1}} \frac{d\lambda e^{-\lambda\Xi}}{2i\pi} \mathbf{F}_{s,\lambda}^\bullet(x).$$

Theorem 8.1. *When $V \rightarrow \infty$, ℓ is a fixed positive parameter, and $p \ll \ln V$, $\phi \ll V$, we have:*

$$(8.1) \quad \mathbb{P}\left(P = \frac{c \ln V}{\pi} p \text{ and } \Xi = \frac{c \ln V}{\pi} q \mid V, L = \ell\right) \sim \frac{A_6(p, q, \ell)}{(\ln V) V^{\frac{c}{\pi} J(p, q)}},$$

$$(8.2) \quad \mathbb{P}\left(P = \frac{c \ln V}{2\pi} p \text{ and } \Xi = \frac{c \ln V}{2\pi} q \mid V, L = V^{\frac{c}{2}} \ell\right) \sim \frac{A_7(p, q, \ell)}{(\ln V) V^{\frac{c}{2\pi} J(p, q)}}.$$

The bivariate large deviations function reads:

$$J(p, q) = J(p) + q\lambda' - \Lambda_\mu(\lambda'),$$

in terms of $J(p)$ defined in (6.7), and λ' is the function of (p, q) which is the unique solution to

$$\frac{q}{p} = \frac{\partial \Lambda_\mu(\lambda')}{\partial \lambda'}.$$

The constant prefactors are non-universal:

$$A_j(p, q, \ell) = \frac{\pi n^2}{2^{j-6} c p \sqrt{(p^2 + 1)^{\frac{\partial^2 \Lambda_\mu}{\partial \lambda'^2}}}} \frac{\mathcal{I}_{j-5}(\ell, \pi^{-1} \operatorname{arccot}(p))}{\mathcal{I}_{j-5}(\ell, b)},$$

in terms of the functions already appearing in Theorem 6.8.

It is remarkable that the bivariate large deviations function is a sum of two terms, one being the usual n -dependent large deviations function for depth $J(p)$, the other being μ -dependent but n -independent.

8.1.1. *Bernoulli weights.* For instance, if μ is a signed Bernoulli random variable,

$$\mu[\xi = -1] = \mu[\xi = 1] = \frac{1}{2},$$

we have

$$\Lambda_\mu(\lambda) = \ln \cosh(\lambda), \quad \lambda' = \operatorname{arctanh}(q/p) = \frac{1}{2} \ln \left(\frac{p+q}{p-q} \right),$$

and

$$J(p, q) = J(p) + \frac{p+q}{2} \ln(p+q) + \frac{p-q}{2} \ln(p-q) - p \ln p.$$

Note that, as $\xi \leq 1$, we have $\Xi = \sum_{l \in \mathcal{L}_{\text{sep}}} \xi_l \leq P$, so we must have $q \leq p$.

8.1.2. *Gaussian weights.* If ξ is a Gaussian variable with variance σ^2 , we have:

$$\Lambda_\mu(\lambda) = \frac{\sigma^2 \lambda^2}{2}, \quad \lambda' = \frac{q}{p\sigma^2}$$

and therefore:

$$J(p, q) = J(p) + \frac{q^2}{2\sigma^2 p^2}.$$

8.2. **Proof of Theorem 8.1.** We give some details of the proof in the case of finite perimeters, as the modifications necessary in the case of large perimeters, $L = V^{\frac{5}{2}}\ell$, are parallel to the changes of Section 6.4 detailed in Section 6.5. As the strategy is similar to Section 6.4, we leave the details of the analysis to the reader. To analyze $\mathcal{P}(V, L; P, \Xi)$, we should study the critical points of:

$$\begin{aligned} \mathcal{S}_1(x, u, s, \lambda) &= \mathcal{S}_1(x, u, se^{\Lambda_\mu(\lambda)}) - \lambda \Xi \\ &= -V \ln u - P \ln s + cb(s) \ln \left(\frac{1-u}{\Delta} \right) - \ln \left[1 - \left(\frac{1-u}{\Delta} \right)^{cb(s \exp(\Lambda_\mu(\lambda)))} \right] \\ (8.3) \quad &+ \ln \tilde{\Psi}_{b(s \exp(\Lambda_\mu(\lambda)))}(x) - \lambda \Xi \end{aligned}$$

Let (s^*, λ^*) be the location of the critical point of $\tilde{\mathcal{S}}_1$, and assume that s^* has a limit away from $2/n$, and λ^* has a finite limit when $V \rightarrow \infty$. Using the scalings ⁴

$$P = \frac{c \ln V}{\pi} p, \quad \Xi = \frac{c \ln V}{\pi} q,$$

we find that the equation $\partial_s \tilde{\mathcal{S}}_1 = 0$ yields in the limit $V \rightarrow \infty$:

$$(8.4) \quad \frac{ne^{\Lambda_\mu(\lambda^*)}}{\sqrt{4 - (ns^* e^{\Lambda_\mu(\lambda^*)})^2}} = \frac{p}{s^*},$$

and the equation $\partial_\lambda \tilde{\mathcal{S}}_1 = 0$ yields likewise:

$$(8.5) \quad \frac{ne^{\Lambda_\mu(\lambda^*)} \Lambda'_\mu(\lambda^*)}{\sqrt{4 - (ns^* e^{\Lambda_\mu(\lambda^*)})^2}} = \frac{q}{s^*},$$

⁴This q is to be distinguished the variable of Theorem 6.3 controlling the distance to criticality.

while the equation $\partial_u \tilde{\mathcal{S}}_1 = 0$ yields:

$$V \sim -\frac{cb(s^* e^{\Lambda_\mu(\lambda^*)})}{1 - u^*}.$$

Let us define λ' as a function of (p, q) in such a way that:

$$(8.6) \quad \frac{\partial \Lambda_\mu}{\partial \lambda'} = \frac{q}{p}.$$

As $\frac{\partial \Lambda}{\partial \lambda'}(0) = \mathbb{E}[\xi]$ and $\frac{\partial^2 \Lambda_\mu}{\partial \lambda'^2}(0) = \text{Var}[\xi] > 0$, λ' is defined at least for q/p in the neighborhood of the value $\mathbb{E}[\xi]$, corresponding to λ' in a neighborhood of 0. We assume that q/p belongs to the (maximal) domain of definition of λ' . Combining (8.4) and (8.5), we find that the saddle λ^* is located at λ' , and:

$$s^* e^{\Lambda_\mu(\lambda')} = \mathfrak{s}(p), \quad b(s^* e^{\Lambda_\mu(\lambda')}) = \mathfrak{b}(p),$$

in terms of the functions \mathfrak{s} and \mathfrak{b} defined in (6.12).

We compute the Hessian matrix of $\tilde{\mathcal{S}}_1$ with respect to the variables (s, λ) , and evaluated at the saddle point (s^*, λ') . At leading order in V ,

$$\tilde{\mathcal{S}}_1 = \frac{c \ln V}{\pi} \Sigma(s, \lambda) + o(\ln V), \quad \text{with } \Sigma(s, \lambda) = \pi b(s e^{\Lambda_\mu(\lambda)}) - p \ln s,$$

where the error $o(\ln V)$ is stable under differentiation. After a tedious, but straightforward computation, we find:

$$\begin{aligned} \mathbf{H} &:= \left(\begin{array}{cc} \partial_s^2 \Sigma & \partial_\lambda \partial_s \Sigma \\ \star & \partial_\lambda^2 \Sigma \end{array} \right) \Big|_{\substack{s=s^* \\ \lambda=\lambda'}} \\ &= \left(\begin{array}{cc} \frac{n^2(p^2+1)^2}{4} \exp(2\Lambda_\mu(\lambda')) & \frac{n(1+p^2)^{3/2}}{2} \frac{\partial \Lambda_\mu}{\partial \lambda'} e^{\Lambda_\mu(\lambda')} \\ \star & p \left[\frac{\partial^2 \Lambda_\mu}{\partial \lambda'^2} + (p^2+1) \left(\frac{\partial \Lambda_\mu}{\partial \lambda'} \right)^2 \right] \end{array} \right) \end{aligned}$$

where the lower corner of the matrix is deduced by symmetry. We also need to compute

$$\det \mathbf{H} = \frac{n^2(p^2+1)^2}{4} \frac{\partial^2 \Lambda_\mu}{\partial \lambda'^2} e^{2\Lambda_\mu(\lambda')}.$$

Now, if we introduce the change of variables:

$$u = 1 - \frac{\tilde{u}}{V}, \quad s = e^{-\Lambda_\mu(\lambda')} \mathfrak{s}(p) + \frac{\tilde{s}}{\sqrt{\ln V}}, \quad \lambda = \lambda' + \frac{\tilde{\lambda}}{\sqrt{\ln V}},$$

we obtain

$$\begin{aligned} \frac{du}{u^{V+1}} \frac{ds}{s^{P+1}} d\lambda e^{-\lambda \Xi} &\sim -\frac{d\tilde{u} d\tilde{\lambda}}{V \ln V} \frac{\tilde{\Psi}_{\mathfrak{b}(s \exp(\Lambda_\mu(\lambda')))(x)}}{\mathfrak{s}(p) \exp(-\Lambda_\mu(\lambda'))} e^{\tilde{u}} \left(\frac{\tilde{u}}{\Delta V} \right)^{c\mathfrak{b}(p)} \\ &\quad \times V^{-\frac{c}{\pi} (p \ln \mathfrak{s}(p) - p \Lambda_\mu(\lambda') + q \lambda')} \exp \left\{ \frac{c}{\pi} (\tilde{s}, \tilde{\lambda}) \cdot \mathbf{H} \cdot (\tilde{s}, \tilde{\lambda})^T \right\}. \end{aligned}$$

We can perform the Gaussian integration in \tilde{s} and $\tilde{\lambda}$, while the remaining integration on \tilde{u} and x result in a prefactor already appearing in Section 6.4. The result is:

$$\mathcal{P}\left(V, L; P = \frac{cp \ln V}{\pi}; \Xi = \frac{cq \ln V}{\pi}\right) \sim \frac{\pi}{\Gamma(-cb(p))} \frac{n^2}{cp \sqrt{(p^2 + 1) \frac{\partial^2 \Lambda_\mu}{\partial \lambda'^2}}} \left\{ \oint_{\tilde{C}} \frac{x^L dx}{2i\pi} \frac{\tilde{\Psi}_{b(p)}(x)}{\Delta^{cb(p)}} \right\} \\ \times V^{-1 - cb(p) + \frac{c}{\pi}(-\ln s(p) + \Lambda_\mu(\lambda') - q\lambda')} (\ln V)^{-1}.$$

We obtain the final result (8.1) by dividing by $\tilde{\mathcal{P}}(V, L)$ given in (6.10). The proof of (8.2) is similar. \square

9. COMPARISON WITH NESTING IN CLE VIA KPZ

In this section, we compare the large deviations of loop nesting at criticality in the $O(n)$ model on a random planar map, as derived in the first sections of this work, with the large deviations of loop nesting in the so-called *conformal loop ensemble* in the plane.

9.1. Nesting in the conformal loop ensemble. The conformal loop ensemble CLE_κ for $\kappa \in (8/3, 8)$ is the canonical conformally invariant measure on countably infinite collections of non-crossing loops in a simply connected domain $D \subset \mathbb{C}$ [84, 86]. It is the analogue for loops of the celebrated *Schramm-Loewner Evolution* SLE_κ , the canonical conformally invariant measure on non-crossing paths [80] in the plane, depending on the real positive parameter κ , an invention which is on par with Wiener's 1923 mathematical construction of continuous Brownian motion. It gives the universal continuous scaling limit of 2d critical curves; of particular physical interest are the loop-erased random walk ($\kappa = 2$) [60], the self-avoiding walk ($\kappa = \frac{8}{3}$), the Ising model interface ($\kappa = 3$ or $\frac{16}{3}$) [88, 20], the GFF contour lines ($\kappa = 4$) [81], and the percolation interface ($\kappa = 6$) [87]. Critical phenomena in the plane were earlier well-known to be related to conformal field theory [6], a discovery anticipated in the so-called Coulomb gas approach to critical 2d statistical models (see, *e.g.*, [74]), and now including SLE [4, 45, 53].

In the same way as SLE_κ is proven or expected to be the scaling limit of a single interface in 2d critical discrete models, CLE_κ should be the limiting process of the collection of closed interfaces in such models. In particular, the critical $O(n)$ -model on a regular planar lattice is expected to converge in the continuum limit to the universality class of the $\text{SLE}_\kappa/\text{CLE}_\kappa$, for

$$(9.1) \quad n = 2 \cos [\pi(1 - 4/\kappa)] \quad n \in [0, 2], \quad \begin{cases} \kappa \in (\frac{8}{3}, 4] & \text{in dilute phase} \\ \kappa \in (4, 8) & \text{in dense phase.} \end{cases}$$

In [71] (see also [70]), Miller, Watson and Wilson were able to derive the almost sure multifractal dimension spectrum of *extreme nesting* in the conformal loop ensemble. Fix a simply connected proper domain $D \subset \mathbb{C}$ and let Γ be a configuration of CLE_κ . For each point $z \in D$, let $\mathcal{N}_z(\varepsilon)$ be the number of loops of Γ which surround the ball $B(z, \varepsilon)$ centered at z and of radius $\varepsilon > 0$. For $\nu > 0$, define the random set

$$(9.2) \quad \Phi_\nu = \Phi_\nu(\Gamma) := \left\{ z \in D : \lim_{\varepsilon \rightarrow 0} \frac{\mathcal{N}_z(\varepsilon)}{\ln(1/\varepsilon)} = \nu \right\}.$$

This Hausdorff dimension of this set is almost surely equal to a constant, which is expressed in terms of the distribution of the conformal radius of the gasket of the origin in

a CLE_κ in the unit disk \mathbb{D} . More precisely, the conformal radius $\text{CR}(z, \mathcal{U})$ of a simply connected proper domain $\mathcal{U} \subset \mathbb{C}$ is defined to be $|\varphi'(0)|$, where φ is the conformal map $\mathbb{D} \mapsto \mathcal{U}$ which sends 0 to z . For a configuration Γ of CLE_κ in \mathbb{D} , let then \mathcal{U}_Γ be the connected component containing the origin in the complement $\mathbb{D} \setminus \mathcal{L}$ of the largest loop \mathcal{L} of Γ surrounding the origin in \mathbb{D} , *i.e.* the interior of the outmost such loop. The cumulant generating function of $-\log(\text{CR}(0, \mathcal{U}_\Gamma))$ was computed in Ref. [82], and is given by

$$(9.3) \quad \Lambda_\kappa(\lambda) := \ln \mathbb{E} \left[(\text{CR}(0, \mathcal{U}_\Gamma))^{-\lambda} \right] = \ln \left(\frac{\cos \left[\pi \left(1 - \frac{4}{\kappa} \right) \right]}{\cos \left[\pi \sqrt{\left(1 - \frac{4}{\kappa} \right)^2 + \frac{8\lambda}{\kappa}} \right]} \right), \quad \lambda \in \left(-\infty, 1 - \frac{2}{\kappa} - \frac{3\kappa}{32} \right).$$

The Legendre-Fenchel symmetric transform, $\Lambda_\kappa^* : \mathbb{R} \rightarrow \mathbb{R}^+$ of Λ_κ is defined by

$$(9.4) \quad \Lambda_\kappa^*(x) := \sup_{\lambda \in \mathbb{R}} (\lambda x - \Lambda_\kappa(\lambda)).$$

The authors of Ref. [71] then define

$$(9.5) \quad \gamma_\kappa(\nu) := \begin{cases} \nu \Lambda_\kappa^*(1/\nu) & \text{if } \nu > 0 \\ 1 - \frac{2}{\kappa} - \frac{3\kappa}{32} & \text{if } \nu = 0, \end{cases}$$

which is right-continuous at 0. Then, for $\kappa \in (8/3, 8)$, the Hausdorff dimension of the set Φ_ν is almost surely [71, Theorem 1.1],

$$(9.6) \quad \dim_{\mathcal{H}} \Phi_\nu = \max(0, 2 - \gamma_\kappa(\nu)),$$

with Φ_ν being a.s. empty if $\gamma_\kappa(\nu) > 2$. Note that the Legendre-Fenchel transform equations above can be recast for $\gamma_\kappa(\nu)$, $\nu > 0$, as,

$$(9.7) \quad \frac{\gamma_\kappa(\nu)}{\nu} = \frac{\lambda}{\nu} - \Lambda_\kappa(\lambda), \quad \frac{1}{\nu} = \frac{\partial \Lambda_\kappa(\lambda)}{\partial \lambda},$$

from which we immediately get,

$$(9.8) \quad \lambda = \frac{\partial}{\partial(1/\nu)} \left(\frac{\gamma_\kappa(\nu)}{\nu} \right) = \gamma_\kappa(\nu) - \nu \frac{\partial}{\partial \nu} \gamma_\kappa(\nu).$$

9.2. Liouville quantum gravity. Polyakov [77] suggested in 1981 that the summation over random Riemannian metrics involved in a continuum theory of random surfaces could be represented canonically by the now celebrated *Liouville theory of quantum gravity* (see [47, 43, 72] and references therein). It is widely believed to provide, after a Riemann conformal map to a given planar domain, the proper conformal structure for the continuum limit of random planar maps weighted by the partition functions of various statistical models (see, *e.g.*, the reviews [30, 63]). In the case of usual random planar maps with faces of bounded degrees, the universal metric structure is that of the Brownian map [62, 66], and it has lately been identified with the one directly constructed from Liouville quantum gravity [67, 69, 68]. Here, we focus on the measure aspects associated with Liouville quantum gravity (LQG).

9.2.1. *Liouville quantum measure.* Consider a simply connected domain $D \subset \mathbb{C}$ as the parameter domain of the random surface, and h an instance of the massless *Gaussian free field* (GFF), a random distribution on D , associated with the Dirichlet energy,

$$(h, h)_\nabla := \frac{1}{2\pi} \int_D [\nabla h(z)]^2 d^2z,$$

and whose two point correlations are given by the Green's function on D with Dirichlet zero boundary conditions [83]. (Critical) Liouville quantum gravity consists in changing the Lebesgue area measure d^2z on D to the *quantum area measure*, formally written as $\mu_\gamma(d^2z) := e^{\gamma h(z)} d^2z$, where γ is a real parameter. The GFF h is a random distribution, not a function, but the random measure μ_γ can be constructed, for $\gamma \in [0, 2]$, as the limit of regularized quantities, as follows.

Given an instance h of the GFF on D , for each $z \in D$, let $h_\varepsilon(z)$ denote the mean value of h on the circle of radius ε centered at z – where $h(z)$ is defined to be zero for $z \in \mathbb{C} \setminus D$ [83]. One then has

$$\mathbb{E}[e^{\gamma h_\varepsilon(z)}] = e^{\gamma^2 \text{Var}[h_\varepsilon(z)]/2} = [\text{CR}(z, D)/\varepsilon]^{\gamma^2/2},$$

where $\text{CR}(z, D)$ the conformal radius of D viewed from z . This strongly suggests considering the limit,

$$(9.9) \quad \mu_\gamma(d^2z) := \lim_{\varepsilon \rightarrow 0} \varepsilon^{\gamma^2/2} e^{\gamma h_\varepsilon(z)} d^2z,$$

and one can indeed show that for $\gamma \in [0, 2]$ this (weak) limit exists and is non-degenerate, and is singular with respect to Lebesgue measure [37]. This mathematically defines Liouville quantum gravity, in a way reminiscent of so-called Wick normal ordering in quantum field theory – see also [49] for earlier work on the so-called Høegh-Krohn model, and Kahane's general study of the so-called Gaussian multiplicative chaos [52].

The critical case, $\gamma = 2$, requires additional care, and it is shown in [34, 35] that the weak limit,

$$(9.10) \quad \mu_{\gamma=2}(d^2z) := \lim_{\varepsilon \rightarrow 0} \sqrt{\ln(1/\varepsilon)} \varepsilon^2 e^{2h_\varepsilon(z)} d^2z,$$

exists and is almost surely non-atomic. $\mu_\gamma(D)$ will be called the *quantum area* of D .

Remark 9.1. The Liouville quantum action is usually written as $S(h) = \frac{1}{2}(h, h)_\nabla + \mathfrak{b} \mu_\gamma(D)$, where the “(bulk) cosmological constant”, $\mathfrak{b} \geq 0$, weights the partition function according to the quantum area of the random surface. The corresponding Boltzmann statistical weight, $\exp[-S(h)]$, should be integrated over with a “flat” uniform functional measure $\mathcal{D}h$ on h – which makes sense *a priori* for finite-dimensional approximations to h . The full Liouville quantum measure can then be constructed from the GFF one (see, *e.g.*, [24]), and for our purpose of studying the CLE_κ nesting properties, which are *local* ones, it will suffice to consider this measure for $\mathfrak{b} = 0$, *i.e.*, in the GFF case.

9.2.2. *Canonical coupling of LQG to SLE.* Various values of γ are expected to describe weighting the random map by the partition function of a critical statistical physical model defined on that map (*e.g.*, an Ising model, an $O(n)$ or a Potts model). The correspondence can be obtained by first considering *conformal welding* in Liouville quantum gravity [85, 38, 33] (see also [2]). It turns out that pieces of Liouville quantum gravity surfaces of

parameter $\gamma \in [0, 2)$ can be conformally welded together to produce as random seams SLE_κ curves, with the rigorous result,

$$(9.11) \quad \gamma = \begin{cases} \sqrt{\kappa} & \text{if } \kappa < 4 \\ 4/\sqrt{\kappa} & \text{if } \kappa > 4. \end{cases}$$

Together with (9.1), this provides us with the (γ, κ, n) correspondence that we sought after for the $O(n)$ model.

9.2.3. KPZ formula. By the usual conformal invariance *Ansatz* in physics, it is natural to expect that if one conditions on the random map to be infinite, maps it into the plane, and then samples the loops or clusters in critical models, their law, in the scaling limit, will be *independent* of the random measure. This independence in turn leads to the Knizhnik, Polyakov, and Zamolodchikov (KPZ) formula [57] – see also Refs. [23, 25] – which is a relationship between (half-)scaling dimensions (*i.e.*, conformal weights x) of fields defined using Euclidean geometry and analogous dimensions (Δ) defined via the Liouville quantum gravity measure μ_γ ,

$$(9.12) \quad x = U_\gamma(\Delta) := \frac{\gamma^2}{4} \Delta^2 + \left(1 - \frac{\gamma^2}{4}\right) \Delta.$$

The inverse to relation (9.12) that is positive is given by

$$(9.13) \quad \Delta = U_\gamma^{-1}(x) := \frac{1}{\gamma} \left(\sqrt{4x + a_\gamma^2} - a_\gamma \right), \quad a_\gamma := \left(\frac{2}{\gamma} - \frac{\gamma}{2} \right) \geq 0.$$

A mathematical proof of the KPZ relation, based on the stochastic properties of the GFF, first appeared in [37]; it was then also proved for multiplicative cascades [7] and in the framework of Gaussian multiplicative chaos [78, 35]. The KPZ formula holds for any fractal structure sampled *independently* of the GFF, and measured with the random measure μ_γ , and for any $0 \leq \gamma \leq 2$.

9.2.4. Quantum and Lebesgue measures. Define the (random) Liouville quantum measure of the Euclidean ball $B(z, \varepsilon)$,

$$(9.14) \quad \delta := \int_{B(z, \varepsilon)} \mu_\gamma(d^2z),$$

and the logarithmic coordinates,

$$(9.15) \quad t := \ln(1/\varepsilon), \quad A := \gamma^{-1} \ln(1/\delta).$$

For z fixed, a given quantum area δ , hence a given logarithmic coordinate A , corresponds through (9.14) to a random Euclidean radius ε , and the corresponding random value T_A of t in (9.15) can be seen as a stopping time of some Brownian process [36, 37]. The probability density of T_A , such that $\mathcal{P}(t|A)dt := \mathbb{P}(T_A \in [t, t+dt])$, is obtained as a by-product of the KPZ analysis in [36, 37]:

$$(9.16) \quad \mathcal{P}(t|A) = \frac{A}{\sqrt{2\pi t^3}} \exp\left(-\frac{(A - a_\gamma t)^2}{2t}\right);$$

it characterizes, in logarithmic coordinates, the distribution of the Euclidean radius ε of a ball of given quantum area δ .

Note that we can rewrite it as

$$(9.17) \quad \mathcal{P}(t'A | A) = \frac{A^{-1/2}}{\sqrt{2\pi t'^3}} \exp\left(-\frac{A}{2t'}(1 - a_\gamma t')^2\right).$$

In the regime $\delta \rightarrow 0$, we have $A \rightarrow +\infty$, so the distribution (9.17) becomes localized at $a_\gamma t' = 1$, thus $t = A/a_\gamma$. This gives the typical scaling of the quantum area of balls in γ -Liouville quantum gravity, $\delta \asymp \varepsilon^{\gamma a_\gamma} = \varepsilon^{2-\gamma^2/2}$ [50]. The large deviations from this typical value, associated with (9.17), will be the key in comparing the extreme nesting of CLE_κ in the plane, as seen with the Euclidean (Lebesgue) measure, or with the Liouville quantum measure μ_γ .

9.3. Nesting of CLE_κ in Liouville quantum gravity.

9.3.1. *Definition.* One ingredient in the proof of (9.6) in Ref. [71] is the following one-point estimate [71, Lemma 3.2]. For $z \in D$, define

$$\tilde{\mathcal{N}}_z(\varepsilon) := \frac{\mathcal{N}_z(\varepsilon)}{\ln(1/\varepsilon)}.$$

Then

$$(9.18) \quad \lim_{\varepsilon \rightarrow 0} \frac{\ln \mathbb{P}(\tilde{\mathcal{N}}_z(\varepsilon) \in [\nu - \omega_-(\varepsilon), \nu + \omega_+(\varepsilon)])}{\ln \varepsilon} = \gamma_\kappa(\nu) \quad \text{for } \nu > 0,$$

uniformly in D and for all $\omega_\pm(\varepsilon)$ decreasing to 0 sufficiently slowly. A similar result holds for $\nu = 0$. We shall rewrite the above result, for $\varepsilon \rightarrow 0$, in the more compact way,

$$(9.19) \quad \mathbb{P}(\mathcal{N}_z \approx \nu \ln(1/\varepsilon) \mid \varepsilon) \asymp \varepsilon^{\gamma_\kappa(\nu)},$$

where the sign \approx stands for a scaling of the form $(\nu + o(1)) \ln(1/\varepsilon)$. We also recall that the \asymp sign means an asymptotic equivalence of logarithms, *i.e.*, a form $\varepsilon^{\gamma_\kappa(\nu) + o(1)}$ on the r.h.s. Recalling definition (9.15), this is also for $t \rightarrow +\infty$,

$$(9.20) \quad \mathbb{P}(\mathcal{N}_z \approx \nu t \mid t) \asymp e^{-\gamma_\kappa(\nu)t}.$$

To define an analog of this nesting probability in Liouville quantum gravity instead of conditioning on the Euclidean radius ε – hence on t – we condition on the quantum area δ (9.14) of the ball $B(z, \varepsilon)$ – hence on A (9.15). The number of loops \mathcal{N}_z surrounding the ball $B(z, \varepsilon)$ stays the same. This conditional probability is then given by the convolution,

$$(9.21) \quad \mathbb{P}_\mathcal{Q}(\mathcal{N}_z \mid A) := \int_0^\infty dt \mathbb{P}(\mathcal{N}_z \mid t) \mathcal{P}(t \mid A),$$

where $\mathcal{P}(t \mid A)$ is as in (9.16)-(9.17). We call it the *quantum nesting probability*.

9.3.2. *Saddle-point computation.* For large A , if we let \mathcal{N}_z scale as $\mathcal{N}_z \approx \gamma p A$, with $p \in \mathbb{R}_+$, we may also set $\mathcal{N}_z \approx \nu t$, where ν is now *defined* as

$$(9.22) \quad \nu = \nu(t) = \gamma p A / t,$$

where p and A are considered as parameters. The asymptotic result (9.20) then yields, for $A \rightarrow +\infty$,

$$(9.23) \quad \mathbb{P}_\mathcal{Q}(\mathcal{N}_z \approx \gamma p A \mid A) \asymp \int_0^\infty \frac{dt A}{\sqrt{2\pi t^3}} \exp\left(-\frac{(A - a_\gamma t)^2}{2t} - \gamma_\kappa(\nu)t\right).$$

Consistently, the above integral is evaluated by a saddle-point method, by looking for the extremum of

$$(9.24) \quad \mathcal{E}(t) := \frac{1}{2t} (A - a_\gamma t)^2 + \gamma_\kappa(\nu)t,$$

along trajectories at *constant* value of $\nu t = \gamma p A$, and for *fixed* p and A . We then have

$$t \frac{\partial \gamma_\kappa}{\partial t}(\nu) = -\nu \frac{\partial \gamma_\kappa}{\partial \nu}(\nu),$$

and using (9.8),

$$\frac{\partial}{\partial t}(\gamma_\kappa(\nu)t) = \gamma_\kappa(\nu) - \nu \frac{\partial \gamma_\kappa}{\partial \nu}(\nu) = \lambda.$$

This in turn gives

$$(9.25) \quad \frac{\partial \mathcal{E}}{\partial t} = \lambda - \frac{1}{2} \left[\left(\frac{A}{t} \right)^2 - a_\gamma^2 \right],$$

and a saddle-point value t^* of t at

$$(9.26) \quad \frac{A}{t^*} := u = u(\lambda) := \sqrt{2\lambda + a_\gamma^2}.$$

which is implicitly a function of p .

Note that from (9.8) again,

$$\frac{\partial \lambda}{\partial t} = -\nu \frac{\partial}{\partial \nu} \left(\gamma_\kappa(\nu) - \nu \frac{\partial \gamma_\kappa}{\partial \nu} \right) = \nu^2 \frac{\partial^2 \gamma_\kappa}{\partial \nu^2} > 0$$

so that

$$\frac{\partial^2 \mathcal{E}}{\partial t^2} = \frac{\partial \lambda}{\partial t} + \frac{A^2}{t^3} > 0.$$

And the saddle-point lies, as expected, at the minimum \mathcal{E}^* of $\mathcal{E}(t)$,

$$(9.27) \quad \mathcal{E}^* := \mathcal{E}(t^*) = A \left(\frac{(u - a_\gamma)^2}{2u} + \frac{\gamma_\kappa(\nu)}{u} \right),$$

where, owing to definition (9.22) and to (9.26), ν is hereafter understood as the *saddle-point value*,

$$(9.28) \quad \nu = \nu(t^*) = \gamma p \frac{A}{t^*} = \gamma p u(\lambda).$$

Owing to (9.7)-(9.26) and (9.28), we have

$$(9.29) \quad \frac{\gamma_\kappa(\nu)}{u} = \frac{\lambda - \nu \Lambda_\kappa(\lambda)}{u} = \frac{u^2 - a_\gamma^2}{2u} - \gamma p \Lambda_\kappa(\lambda),$$

so that we finally get the simple form,

$$(9.30) \quad \frac{\mathcal{E}^*}{A} = u(\lambda) - a_\gamma - \gamma p \Lambda_\kappa(\lambda).$$

Notice that (9.7), (9.26) and (9.28) also imply

$$(9.31) \quad \frac{1}{\gamma p} = \frac{u}{\nu} = u(\lambda) \frac{\partial \Lambda_\kappa(\lambda)}{\partial \lambda} = \frac{\partial \Lambda_\kappa(\lambda)}{\partial u(\lambda)}.$$

9.3.3. *Role of the KPZ relation.* Let us define:

$$\Theta(p) := \frac{\mathcal{E}^*}{\gamma A}.$$

We have just computed:

$$(9.32) \quad \Theta(p) = U_\gamma^{-1}\left(\frac{\lambda}{2}\right) - p \Lambda_\kappa(\lambda),$$

where λ is the function of p determined by (9.31), and where the inverse KPZ relation (9.13) precisely yields,

$$(9.33) \quad U_\gamma^{-1}\left(\frac{\lambda}{2}\right) = \frac{u(\lambda) - a_\gamma}{\gamma}.$$

Note also that $1/p$ as in (9.31) is the derivative of Λ_κ with respect to (9.33). Thus, setting $\lambda' := U_\gamma^{-1}(\frac{\lambda}{2})$, we get the Legendre-Fenchel transform equations:

$$(9.34) \quad \Theta(p) = \lambda' - p (\Lambda_\kappa \circ 2U_\gamma)(\lambda'), \quad \frac{1}{p} = \frac{\partial(\Lambda_\kappa \circ 2U_\gamma)(\lambda')}{\partial \lambda'}.$$

Comparing this result to the Legendre-Fenchel equations (9.7) in the Euclidean case, we get

Theorem 9.2. *In presence of γ -Liouville quantum gravity, the generating function Λ_κ (9.3) is transformed into*

$$(9.35) \quad \Lambda_\kappa^\mathcal{Q} := \Lambda_\kappa \circ 2U_\gamma,$$

where U_γ is the KPZ function (9.12), with γ given by (9.11). The nesting distribution around a ball of given quantum area δ (9.23) is then given asymptotically for $A = \gamma^{-1} \ln(1/\delta) \rightarrow +\infty$, by

$$\begin{aligned} \mathbb{P}_\mathcal{Q}(\mathcal{N}_z \approx \gamma p A \mid A) &\asymp e^{-\gamma \Theta(p) A} = \delta^{\Theta(p)}, \\ \Theta(p) &= \lambda - p \Lambda_\kappa^\mathcal{Q}(\lambda), \end{aligned}$$

where λ is determined as a function of p by:

$$\frac{1}{p} = \frac{\partial \Lambda_\kappa^\mathcal{Q}(\lambda)}{\partial \lambda}.$$

Remark 9.3. The occurrence of a factor 2 in the composition law (9.35) is simply due to a different choice of scale when measuring large deviations, *i.e.*, that of a *quantum area* δ in the quantum case, as opposed to that of a *radius* ε in the Euclidean one. This is seen in particular in the $\kappa \rightarrow 0$ limit, where U_γ simply becomes the identity function.

Remark 9.4. Theorem 9.2 shows that the KPZ relation, or its inverse as in (9.32), can directly act on an arbitrary continuum variable, here the conjugate variable in the cumulant generating function (9.3) for the CLE_κ log-conformal radius. To our knowledge, this is the first occurrence of such a role for the KPZ relation, which usually concerns scaling dimensions.

Remark 9.5. The derivation above is clearly independent on the precise form of the large deviations function. Moreover, as shown in Refs. [36, 37], the KPZ relation holds in full generality for any (fractal) random system in the plane and in Liouville quantum gravity, provided that the sampling of the random system is *independent* of that of the Gaussian free field defining LQG. Therefore, the map $\Lambda \mapsto \Lambda^\mathcal{Q} = \Lambda \circ 2U_\gamma$, from Euclidean geometry to Liouville quantum gravity, holds for any large deviations problem, where the large deviations function is the Legendre-Fenchel transform of a certain generating function Λ .

9.3.4. *Comparison to Theorem 2.2.* Let us finally compute explicitly the Liouville large deviations function Θ , in order compare with the main results above regarding extreme nesting in the $O(n)$ model on a random planar map. The easiest way is to rewrite (9.3) as

$$(9.36) \quad \Lambda_\kappa(\lambda) = \ln \left(\frac{\cos \left[\pi \left(1 - \frac{4}{\kappa} \right) \right]}{\cos v} \right), \quad v = v(\lambda) := \frac{2\pi}{\sqrt{\kappa}} \sqrt{\left(\frac{\sqrt{\kappa}}{2} - \frac{2}{\sqrt{\kappa}} \right)^2 + 2\lambda}$$

for $\lambda \in (-\infty, 1 - \frac{2}{\kappa} - \frac{3\kappa}{32})$, and to notice that (9.26) and (9.11) give

$$u(\lambda) = \frac{\sqrt{\kappa}}{2\pi} v(\lambda).$$

Equations (9.31) and (9.32) then take the compact form,

$$(9.37) \quad \Theta(p) = \Theta = \frac{c}{2\pi} (v - a' - p' \Lambda_\kappa), \quad \frac{1}{p'} = \frac{\partial \Lambda_\kappa(v)}{\partial v},$$

where we used the notations

$$c := \frac{\sqrt{\kappa}}{\gamma}, \quad p := \frac{c}{2\pi} p', \quad a_\gamma = \left(\frac{2}{\gamma} - \frac{\gamma}{2} \right) := \frac{\sqrt{\kappa}}{2\pi} a'.$$

Because of (9.11), we find as parameters,

$$(9.38) \quad c = \min(1, \kappa/4), \quad a' = \pi b = \pi |1 - 4/\kappa| = \arccos(n/2),$$

where b and c are the exponents defined in (2.4) and Section 2.3. The explicit form (9.36) immediately yields the parametric solution to Legendre-Fenchel equations (9.37),

$$(9.39) \quad p' = \cot v, \quad \Theta = \frac{c}{2\pi} \left[v - (\cot v) \ln \left(\frac{n}{2 \cos v} \right) - \arccos(n/2) \right].$$

One has $p' \in \mathbb{R}_+$ for $v \in [0, \pi/2)$, so that

$$\cos v = \frac{p'}{\sqrt{p'^2 + 1}} \geq 0,$$

which finally yields

$$(9.40) \quad \Theta(p) = \frac{c}{2\pi} J(p'), \quad J(p') := \operatorname{arccot}(p') + p' \ln \left(\frac{2}{n} \frac{p'}{\sqrt{1 + p'^2}} \right) - \arccos(n/2).$$

Note that the $p = \frac{c}{2\pi} p'$ substitution above simply gives $\gamma p A = \frac{c}{2\pi} p' \ln(1/\delta)$. Theorem 9.2 then yields

Theorem 9.6. *The quantum nesting probability for CLE_κ loops, with $\kappa \in (8/3, 8)$ in a simply connected proper domain $D \subsetneq \mathbb{C}$, surrounding a ball centered at z with given quantum area δ , behaves as*

$$\mathbb{P}_{\mathcal{Q}}(\mathcal{N}_z \approx \frac{c}{2\pi} p \ln(1/\delta) \mid \delta) \asymp \delta^{\frac{c}{2\pi} J(p)}, \quad \delta \rightarrow 0,$$

where the large deviations function J is as in (9.40) and Theorem 2.2, and where c and n are given in (9.38) as functions of κ .

Remark 9.7. We see that this result perfectly matches the second large deviations result in Theorem 2.2 for nesting in the $O(n)$ loop model on a random map with the topology of a pointed disk: one simply replaces $1/\delta$ here with the large volume V of the map there. Indeed, one may assign elementary area $1/V$ to each face in the dual map, so that the dual map has in total unit area; then, the marked point corresponds in the dual to a face of elementary area $1/V$, and its depth $P = \frac{c}{2\pi} p \ln V$ is the number of loops separating this face from the boundary of the disk.

It is interesting to compare the classical and quantum cases for nesting in CLE_κ . In the classical case [71], the parametric equations of the Legendre-Fenchel transform (9.7) are

$$\begin{aligned} \nu &= \frac{\kappa}{(2\pi)^2} v \cot v \\ \gamma_\kappa(\nu) &= \frac{\kappa}{(2\pi)^2} \left[\frac{v^2}{2} - (v \cot v) \ln \left(\frac{n}{2 \cos v} \right) - \frac{1}{2} (\arccos(n/2))^2 \right] \end{aligned}$$

for $v \in [0, \pi/2)$, and

$$\begin{aligned} \nu &= \frac{\kappa}{(2\pi)^2} w \coth w \\ \gamma_\kappa(\nu) &= \frac{\kappa}{(2\pi)^2} \left[-\frac{w^2}{2} - (w \coth w) \ln \left(\frac{n}{2 \cosh w} \right) - \frac{1}{2} (\arccos(n/2))^2 \right] \end{aligned}$$

for $v = iw$ with $w \in \mathbb{R}_+$. These parametric equations cannot be easily solved, whereas the quantum parametric equations (9.39), though similar, are simpler and explicitly solvable. Note also that in the classical case, the parameter λ is in the range $\lambda \in (-\infty, \lambda_{\max}]$, with the values $\lambda_{\max} = 1 - \frac{2}{\kappa} - \frac{3\kappa}{32}$ corresponding to $\nu \rightarrow 0$ or equivalently $v \rightarrow \pi/2$, while $\lambda \rightarrow -\infty$ corresponds to $\nu \rightarrow +\infty$ or $v = iw$ with $w \rightarrow \infty$. We observe more precisely that

$$(9.41) \quad \gamma_\kappa(\nu) \sim \frac{(2\pi)^2}{\kappa} \frac{\nu^2}{2}, \quad \nu \rightarrow +\infty.$$

In the quantum case (9.39), v is restricted to $v \in [0, \pi/2)$, and λ spans a finite interval only, $\lambda \in [\lambda_{\min}, \lambda_{\max}]$, where $\lambda_{\min} = 1 - \frac{2}{\kappa} - \frac{\kappa}{8}$ is the point at which the square root $v(\lambda)$ vanishes, corresponding to $p' \rightarrow +\infty$. And this results in $\lambda' = U_\gamma^{-1}(\lambda/2)$ spanning $[\frac{1}{2} - \frac{2}{\kappa}, \frac{3}{4} - \frac{2}{\kappa}]$ if $\frac{8}{3} < \kappa \leq 4$, and $[\frac{1}{2} - \frac{\kappa}{8}, \frac{1}{2} - \frac{\kappa}{16}]$ if $4 \leq \kappa < 8$.

9.4. Sphere topology. Conformal loop ensembles can also be defined on the Riemann sphere $\hat{\mathbb{C}}$ [70, 56]. In particular, for any $\kappa \in (8/3, 4]$, the law of the simple nested CLE_κ in the full plane has been shown to be invariant under the inversion $z \mapsto 1/z$ (and therefore under any Möbius transformation of the Riemann sphere) [56, Theorem 1]. In this section,

we connect the nesting statistics of CLE_κ in $\hat{\mathbb{C}}$ with the nesting statistics in the $O(n)$ loop model on large random planar maps with the topology of the doubly punctured sphere.

We first discuss the properties of $\text{CLE}_\kappa(\hat{\mathbb{C}})$. Let us pick two points (punctures), z_1, z_2 , on the sphere, which we may take to be $(z_1, z_2) = (0, \infty)$ using a suitable Möbius transformation. Consider the two balls $B(z_i, \varepsilon_i)$, $i = 1, 2$, centered at these points. In stereographic projection, the connected domain $\hat{\mathbb{C}} \setminus (\overline{B(z_1, \varepsilon_1)} \cup \overline{B(z_2, \varepsilon_2)})$ corresponds to the annulus $\mathbb{A}(\varepsilon_2^{-1}, \varepsilon_1) := \varepsilon_2^{-1}\mathbb{D} \setminus \overline{B(z_1, \varepsilon_1)}$.

Consider then in the whole $\text{CLE}_\kappa(\hat{\mathbb{C}})$ on the Riemann sphere, the loops which can be contracted to each one of the two punctures on $\hat{\mathbb{C}}$, *i.e.*, those loops which in projection belong to the above annulus. By scale invariance, their number can depend only the *product* $\varepsilon_1 \varepsilon_2$, and we write it as $\mathcal{N}(\varepsilon_1 \varepsilon_2)$. The nesting probability on the Riemann sphere is then defined as,

$$\mathbb{P}^{\hat{\mathbb{C}}}[\mathcal{N}(\varepsilon_1 \varepsilon_2) \approx \nu \ln(\varepsilon_1 \varepsilon_2)^{-1} \mid \varepsilon_1, \varepsilon_2],$$

where we recall that \approx is a short-hand notation for the event $\mathcal{N}(\varepsilon_1 \varepsilon_2) / \ln(\varepsilon_1 \varepsilon_2)^{-1} \in [\nu - \omega_-, \nu + \omega_+]$, for $\omega_\pm = \omega_\pm(\varepsilon_1 \varepsilon_2)$ decreasing to 0 sufficiently slowly with the ε_i 's— see (9.18).

9.4.1. Approximation to full-plane CLE and nesting estimates. Following Ref. [70, Appendix A], about the rapid convergence of CLE on a large disk to full-plane CLE, we can take as a large disk, $(\varepsilon \varepsilon_2)^{-1}\mathbb{D}$, with $0 < \varepsilon < 1$, which contains the annulus $\mathbb{A}(\varepsilon_2^{-1}, \varepsilon_1)$ above. Using scale invariance, we may simply consider events in \mathbb{D} and in the annulus $\mathbb{A}(\varepsilon, \varepsilon \varepsilon_1 \varepsilon_2)$ (see Figure 12), and by choosing ε small enough, approximate to any desired precision the probability of any event concerning a ball of radius ε in the ensemble $\text{CLE}_\kappa(\hat{\mathbb{C}})$ (with probability law denoted by $\mathbb{P}^{\hat{\mathbb{C}}}$) by the probability of the same event in the ensemble CLE_κ on the unit disk (with probability law simply denoted by \mathbb{P}).

As before, let $\mathcal{N}_0(\varepsilon)$ be the number of loops surrounding the ball $B(0, \varepsilon)$ in \mathbb{D} , and let $\mathcal{N}_\cap(\varepsilon)$ be the number of loops surrounding the origin and intersecting $\partial B(0, \varepsilon)$. We seek for an estimation of the law of the number of loops in the annulus $B(0, \varepsilon) \setminus \overline{B(0, \varepsilon \rho)}$,

$$(9.42) \quad \hat{\mathcal{N}}(\varepsilon \rho) := \mathcal{N}_0(\varepsilon \rho) - \mathcal{N}_0(\varepsilon) - \mathcal{N}_\cap(\varepsilon), \quad \rho := \varepsilon_1 \varepsilon_2,$$

as illustrated in Figure 12.

From Ref. [71, Lemma 3.5], we know that $\mathcal{N}_\cap(\varepsilon) < c_0 \ln(1/\varepsilon)$ for some constant $c_0 > 0$, except with probability exponentially small in $\ln(1/\varepsilon)$.

From Ref. [71, Lemma 3.2], and the convexity of $\gamma_\kappa(\nu)$, we know that there exists $\eta(\varepsilon) \rightarrow 0$, such that,

$$(9.43) \quad \mathbb{P}(\mathcal{N}_0(\varepsilon) > \nu \ln(1/\varepsilon)) \leq \varepsilon^{\gamma_\kappa(\nu) - \eta(\varepsilon)},$$

uniformly in $\nu \geq \nu_0$, with ν_0 fixed but strictly larger than the point at which $\gamma_\kappa(\nu)$ reaches its minimum 0. We thus have in particular,

$$(9.44) \quad \mathbb{P}(\mathcal{N}_0(\varepsilon) \leq \nu_0 \ln(1/\varepsilon)) \geq \frac{1}{2}.$$

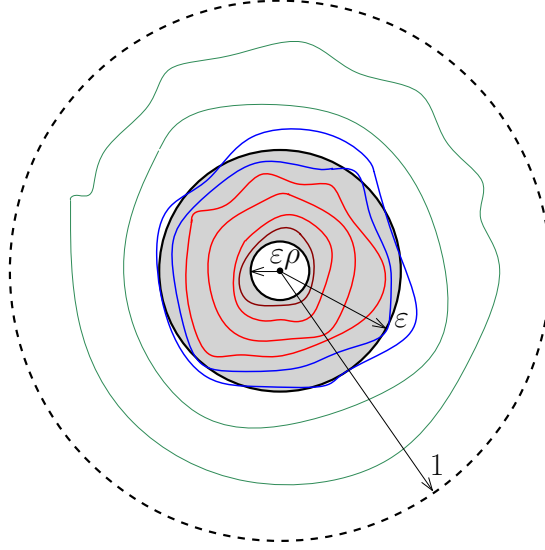


FIGURE 12. The whole set of loops in the unit disk \mathbb{D} is counted by $\mathcal{N}_0(\varepsilon\rho)$, with $\rho = \varepsilon_1\varepsilon_2$. The set of loops contained in the inner annulus, as counted by $\widehat{\mathcal{N}}(\varepsilon\rho)$ (resp. the set of intersecting loops, as counted by $\mathcal{N}_\cap(\varepsilon)$) appears in red (resp. blue).

Besides, we also know from [71, Lemma 3.2] that there exists $\omega(\varepsilon)$, with $\omega(\varepsilon) \rightarrow 0$ as $\varepsilon \rightarrow 0$, such that,

$$(9.45) \quad (\varepsilon\rho)^{\gamma_\kappa(\nu)+\eta(\varepsilon\rho)} \leq \mathbb{P}\left(|\mathcal{N}_0(\varepsilon\rho) - \nu \ln(\varepsilon\rho)^{-1}| \leq \omega(\varepsilon\rho) \ln(\varepsilon\rho)^{-1}\right) \leq (\varepsilon\rho)^{\gamma_\kappa(\nu)-\eta(\varepsilon\rho)}.$$

Using these estimates will allow us shortly to show the existence of functions ω_\pm and η of ε and ρ , with $\omega_\pm(\varepsilon, \rho), \eta(\varepsilon, \rho) \rightarrow 0$ when $\rho \rightarrow 0$, such that,

$$(9.46) \quad (\varepsilon\rho)^{\gamma_\kappa(\nu)+\eta(\varepsilon, \rho)} \leq \mathbb{P}\left(\frac{\widehat{\mathcal{N}}(\varepsilon\rho)}{\ln(1/\varepsilon\rho)} \in [\nu - \omega_-, \nu + \omega_+]\right) \leq (\varepsilon\rho)^{\gamma_\kappa(\nu)-\eta(\varepsilon, \rho)}.$$

Proof. Let us denote by $\widehat{A}_\nu(\varepsilon, \rho)$ the event of interest in (9.46), by $A_\nu(\varepsilon)$ the event $\{\mathcal{N}_0(\varepsilon) \leq \nu \ln(1/\varepsilon)\}$, and by $\bar{A}_\nu(\varepsilon)$ the latter's complement. Define also the logarithmic ratio,

$$r = r(\varepsilon, \rho) := \frac{\ln(1/\varepsilon)}{\ln(1/\varepsilon\rho)}; \quad r(\varepsilon, \rho) \rightarrow 0 \text{ as } \rho \rightarrow 0.$$

For a lower bound, we write

$$\mathbb{P}(\widehat{A}_\nu(\varepsilon, \rho)) \geq \mathbb{P}(\widehat{A}_\nu(\varepsilon, \rho) \cap A_{\nu_0}(\varepsilon)) = \mathbb{P}(A_{\nu_0}(\varepsilon)) \mathbb{P}(\widehat{A}_\nu(\varepsilon, \rho) \mid A_{\nu_0}(\varepsilon)).$$

Choosing ν_0 as in (9.44), the first factor is bounded from below by $\frac{1}{2}$, and using the lower bound (9.45) for the second factor, we get the desired lower bound in (9.46), up to replacing $\omega(\varepsilon\rho)$ of (9.45) by $\omega_\pm(\varepsilon, \rho) := \omega(\varepsilon\rho) \mp (\nu_0 + c_0) r(\varepsilon, \rho)$.

For the upper bound, we write

$$(9.47) \quad \mathbb{P}(\widehat{A}_\nu(\varepsilon, \rho)) \leq \mathbb{P}(\widehat{A}_\nu(\varepsilon, \rho) \cap A_{\nu_1}(\varepsilon)) + \mathbb{P}(\bar{A}_{\nu_1}(\varepsilon)),$$

where, by using the estimate (9.43) for ν_1 large enough, $\mathbb{P}(\bar{A}_{\nu_1}(\varepsilon)) \leq \varepsilon^{\gamma_\kappa(\nu_1) - \eta(\varepsilon)}$. We will choose $\nu_1 = \nu_1(\varepsilon, \rho)$, such that $\nu_1(\varepsilon, \rho) \rightarrow \infty$ when $\rho \rightarrow 0$, as allowed by uniformity of (9.43). As $\gamma_\kappa(\nu)$ grows quadratically in ν – see (9.41) – the latter estimate can be bounded, for large enough ν_1 , as

$$(9.48) \quad \varepsilon^{\gamma_\kappa(\nu_1) - \eta(\varepsilon)} \leq \varepsilon^C \nu_1^2 = (\varepsilon \rho)^{C \nu_1^2 r(\varepsilon, \rho)},$$

for some constant $C > 0$. On the other hand, the first term in (9.47) can be estimated via the upper bound in (9.45) to yield an upper bound as in (9.46), provided that

$$(9.49) \quad \nu_1(\varepsilon, \rho) r(\varepsilon, \rho) \rightarrow 0, \quad \rho \rightarrow 0,$$

as this is the error term to be subtracted, together with $c_0 r(\varepsilon, \rho)$, from $\omega(\varepsilon \rho)$ as the result of the restriction to event $A_{\nu_1}(\varepsilon)$. If we would like (9.48) to be negligible in front of the first term in (9.47), we would have to choose ν_1 in such a way that

$$(9.50) \quad \nu_1^2(\varepsilon, \rho) r(\varepsilon, \rho) \rightarrow \infty, \quad \rho \rightarrow 0.$$

To satisfy both (9.49) and (9.50), choose for instance, $\nu_1(\varepsilon, \rho) = r(\varepsilon, \rho)^{-3/4}$. Then, the second term in (9.47) is bounded by $(\varepsilon \rho)^{C r^{-1/2}}$, which, since $r \rightarrow 0$ as $\rho \rightarrow 0$, is negligible as compared to the first term of order $(\varepsilon \rho)^{\gamma_\kappa(\nu)}$. This completes the proof of (9.46). \square

Invoking then the exponentially fast convergence in $\ln(1/\varepsilon)$ when $\varepsilon \rightarrow 0$ (see [70, Theorem A.1]), of the approximation of $\text{CLE}_\kappa(\widehat{\mathbb{C}})$ by the restriction of $\text{CLE}_\kappa(\mathbb{D})$ to the ball $B(0, \varepsilon)$, we may summarize the result above by

Theorem 9.8. *The nesting probability in $\text{CLE}_\kappa(\widehat{\mathbb{C}})$ between two balls of radius ε_1 and ε_2 and centered at two distinct punctures, has the large deviations form,*

$$\mathbb{P}^{\widehat{\mathbb{C}}}(\mathcal{N}(\varepsilon_1 \varepsilon_2) \approx \nu \ln(1/\varepsilon_1 \varepsilon_2)) \asymp (\varepsilon_1 \varepsilon_2)^{\gamma_\kappa(\nu)}, \quad \nu \geq 0, \quad \varepsilon_1, \varepsilon_2 \rightarrow 0,$$

where $\gamma_\kappa(\nu)$ is the same large deviations function (9.5) as in the case of the disk topology, and where notations are as in (9.18)-(9.19).

Even though the sphere and disk large deviations involve the same function γ_κ , the scalings involved actually differ by powers of 2. Indeed, if we take the two balls on the Riemann sphere to have same radius ε , and measure nesting in $\ln(1/\varepsilon)$ units, we have from Theorem 9.8,

Corollary 9.9. *The nesting probability in $\text{CLE}_\kappa(\widehat{\mathbb{C}})$ between two balls of same radius ε and centered at two distinct punctures, has the large deviations form,*

$$\mathbb{P}^{\widehat{\mathbb{C}}}(\mathcal{N}(\varepsilon^2) \approx \nu \ln(1/\varepsilon)) \asymp \varepsilon^{\widehat{\gamma}_\kappa(\nu)}, \quad \nu \geq 0, \quad \varepsilon \rightarrow 0,$$

where $\widehat{\gamma}_\kappa(\nu)$ is related to the disk large deviations function (9.5) by

$$\widehat{\gamma}_\kappa(2\nu) = 2\gamma_\kappa(\nu).$$

Using hereafter the variables $t_i := \ln(1/\varepsilon_i)$, $i = 1, 2$, we have from Theorem 9.8

$$(9.51) \quad \mathbb{P}^{\widehat{\mathbb{C}}}(\mathcal{N}(\varepsilon_1 \varepsilon_2) \approx \nu(t_1 + t_2)) \asymp e^{-\gamma_\kappa(\nu)(t_1 + t_2)}, \quad t_1, t_2 \rightarrow +\infty.$$

9.4.2. *Nesting on the quantum sphere.* In Liouville quantum gravity, following the same steps as in Section 9.3, let us condition on each ball being of same quantum area $\delta = e^{-\gamma A}$. The sought-for distribution should be given by the convolution

$$(9.52) \quad \mathbb{P}_{\mathbb{Q}}^{\widehat{\mathbb{C}}}(\mathcal{N} | A) := \int_0^\infty \int_0^\infty dt_1 dt_2 \mathbb{P}^{\widehat{\mathbb{C}}}(\mathcal{N} | t_1, t_2) \mathcal{P}(t_1 | A) \mathcal{P}(t_2 | A),$$

where $\mathcal{P}(t | A)$ is as in (9.16)-(9.17). For large A , we let \mathcal{N} scale as $\mathcal{N} \approx \gamma p A$, with $p \in \mathbb{R}_+$, and also set $\mathcal{N} \approx \nu(t_1 + t_2)$, where ν is now defined such that,

$$(9.53) \quad \nu = \nu(t_1, t_2) := \gamma p A / (t_1 + t_2),$$

where p and A are thought of as parameters. The asymptotic result (9.51) then yields when $A \rightarrow +\infty$

$$\begin{aligned} \mathbb{P}_{\mathbb{Q}}^{\widehat{\mathbb{C}}}(\mathcal{N}_z \approx \gamma p A | A) &\asymp \int_0^\infty \int_0^\infty \frac{A^2 dt_1 dt_2}{2\pi \sqrt{t_1^3 t_2^3}} \exp[-\mathcal{E}(t_1) - \mathcal{E}(t_2)] \\ \mathcal{E}(t_1) + \mathcal{E}(t_2) &= \frac{1}{2t_1} (A - a_\gamma t_1)^2 + \frac{1}{2t_2} (A - a_\gamma t_2)^2 + \gamma_\kappa(\nu)(t_1 + t_2). \end{aligned}$$

The above integral is evaluated by a saddle-point method, by looking for the minimum of $\mathcal{E}(t_1) + \mathcal{E}(t_2)$ at *fixed* $\nu(t_1 + t_2) = \gamma p A$. We then have for each $i = 1, 2$,

$$(t_1 + t_2) \partial_{t_i} \gamma_\kappa(\nu) = -\nu \frac{\partial \gamma_\kappa}{\partial \nu},$$

and using (9.8),

$$\frac{\partial}{\partial t_i} ((t_1 + t_2) \gamma_\kappa(\nu)) = \gamma_\kappa(\nu) - \nu \frac{\partial \gamma_\kappa}{\partial \nu} = \lambda.$$

This in turn gives for each $i = 1, 2$,

$$\frac{\partial}{\partial t_i} (\mathcal{E}(t_1) + \mathcal{E}(t_2)) = \lambda - \frac{1}{2} \left[\left(\frac{A}{t_i} \right)^2 - a_\gamma^2 \right],$$

so that both saddle-points t_1^* and t_2^* for t_1 and t_2 are located at the same point t^* as in (9.26) in the case of the disk topology. We thus have at this double saddle point

$$\begin{cases} 2\nu t^* = \gamma p A \\ \mathcal{E}(t_1^*) + \mathcal{E}(t_2^*) = 2\mathcal{E}(t^*). \end{cases}$$

Setting:

$$\widehat{\Theta}(p) := \frac{2\mathcal{E}(t^*)}{\gamma A}$$

we deduce

Theorem 9.10. *The large deviations function $\widehat{\Theta}(p)$ which governs the quantum nesting probability of CLE_κ on $\widehat{\mathbb{C}}$,*

$$\mathbb{P}_{\mathbb{Q}}^{\widehat{\mathbb{C}}}(\mathcal{N} \approx p \ln(1/\delta) | \delta) \asymp \delta^{\widehat{\Theta}(p)}, \quad \delta \rightarrow 0,$$

is related to the large deviations function $\Theta(p)$ for the disk topology (Theorem 9.2) by

$$\widehat{\Theta}(2p) = 2\Theta(p).$$

Using alternatively the explicit formulation, as in Theorem 9.6, we get

Corollary 9.11. *In the same setting as in Theorem 9.10,*

$$\mathbb{P}_Q^{\widehat{\mathbb{C}}} \left(\mathcal{N} \approx \frac{cp}{\pi} \ln(1/\delta) \mid \delta \right) \asymp \delta^{\frac{c}{\pi} J(p)}, \quad \delta \rightarrow 0,$$

where $J(p)$ is as in (9.40).

This is in complete agreement with:

- The first result in Theorem 2.2, which describes the large deviations of the number of separating loops between a marked point and a microscopic boundary in a critical $O(n)$ model on a random map with a disk topology;
- The first result in Theorem 7.1, which describes the large deviations of the number of separating loops between two microscopic boundaries in a critical $O(n)$ model on a random map with a cylinder topology.

These are indeed the sort of topologies considered in Section 9.4.1 above. We also remark that it agrees with:

- The third result of Theorem 7.1, which describes the large deviations of the number of separating loops between two macroscopic boundaries in a critical $O(n)$ model on a random map with cylinder topology.

This should also in principle be deduced from the nesting of a CLE_κ process on a cylinder.

9.5. Weighted loops.

9.5.1. *Weighting CLE_κ .* Our argument can be refined to include a model where loops receive independent random weights, in parallel to the results in Ref. [71, Section 5]. A motivation to introduce this model, beyond the fact it offers a natural generalization of the counting of loops, is that loops weighted with a Bernoulli random variable for $\kappa = 4$ are related to the extremes of the GFF [50].

Conditionally on a configuration Γ of a CLE_κ in a proper simply connected domain D , let $(\xi_l)_{l \in \Gamma}$ be a collection of independent, identically distributed real random variables indexed by Γ . We denote by μ the law of each ξ_l . For $z \in D$ and $\varepsilon > 0$, let $\Gamma_z(\varepsilon)$ be the set of loops which surround $B(z, \varepsilon)$, and define

$$\Xi_z(\varepsilon) = \sum_{l \in \Gamma_z(\varepsilon)} \xi_l, \quad \widetilde{\Xi}_z(\varepsilon) = \frac{\Xi_z(\varepsilon)}{\ln(1/\varepsilon)}.$$

For a realization of the CLE_κ and of the $(\xi_l)_l$, and any fixed $(\nu, \alpha) \in \mathbb{R}_+ \times \mathbb{R}$, let

$$\Phi_{\nu, \alpha}^\mu = \left\{ z \in D : \lim_{\varepsilon \rightarrow 0} \widetilde{\mathcal{N}}_z(\varepsilon) = \nu \quad \text{and} \quad \lim_{\varepsilon \rightarrow 0} \widetilde{\Xi}_z(\varepsilon) = \alpha \right\}.$$

The cumulant generating function associated with the moments of μ is

$$(9.54) \quad \Lambda_\mu(\lambda) := \ln \mathbb{E}[e^{\lambda \xi}],$$

and its symmetric Legendre-Fenchel transform, $\Lambda_\mu^* : \mathbb{R} \rightarrow \mathbb{R}^+$, is defined as

$$(9.55) \quad \Lambda_\mu^*(x) := \sup_{\lambda \in \mathbb{R}} (\lambda x - \Lambda_\mu(\lambda)).$$

The Hausdorff dimension of the set $\Phi_{\nu, \alpha}^\mu$ is then almost surely constant, with value found in [71, Theorem 5.1]

$$\dim_{\mathcal{H}} \Phi_{\nu, \alpha}^\mu = \max\{0, 2 - \gamma_\kappa(\nu, \alpha)\},$$

as long as $\gamma_\kappa(\alpha, \nu) \leq 2$, with $\Phi_{\alpha, \nu}^\mu = \emptyset$ otherwise, and with the definition

$$(9.56) \quad \gamma_\kappa(\nu, \alpha) := \begin{cases} \nu \Lambda_\mu^*(\alpha/\nu) + \nu \Lambda_\kappa^*(1/\nu) & \text{if } \nu > 0 \\ \lim_{\nu' \rightarrow 0^+} \gamma_\kappa(\nu', \alpha) & \text{if } \nu = 0 \text{ and } \alpha \neq 0 \\ \lim_{\nu' \rightarrow 0^+} \gamma_\kappa(\nu') = 1 - \frac{2}{\kappa} - \frac{3\kappa}{32} & \text{if } (\nu, \alpha) = (0, 0), \end{cases}$$

where the limits exist by convexity of Λ_κ^* and Λ_μ^* . When $\nu \neq 0$, we thus have

$$(9.57) \quad \begin{aligned} \gamma_\kappa(\nu, \alpha) &= \gamma_\kappa(\nu) + \gamma_\mu(\nu, \alpha), \\ \gamma_\mu(\nu, \alpha) &:= \nu \Lambda_\mu^*(\alpha/\nu) = \lambda' \alpha - \nu \Lambda_\mu(\lambda'), \end{aligned}$$

where λ' is a function of (ν, α) determined by:

$$\frac{\alpha}{\nu} = \frac{\partial \Lambda_\mu(\lambda')}{\partial \lambda'}.$$

By homogeneity, we find the useful identity

$$(9.58) \quad \left(\nu \frac{\partial}{\partial \nu} + \alpha \frac{\partial}{\partial \alpha} \right) \gamma_\mu(\nu, \alpha) = \gamma_\mu(\nu, \alpha).$$

Uniformly for a point $z \in D$, we have the following joint probability scaling [71]

$$(9.59) \quad \mathbb{P}(\mathcal{N}_z \approx \nu t \text{ and } \Xi_z \approx \alpha t \mid t) \asymp e^{-\gamma_\kappa(\nu, \alpha)t}.$$

9.5.2. Weighted CLE_κ in Liouville Quantum Gravity. One follows exactly the same procedure as in Section 9.3. We study the nesting around small balls $B(z, \varepsilon)$ conditionally to a given quantum area δ (9.14), hence conditionally on A (9.15), while the counts \mathcal{N}_z and Ξ_z are unchanged,

$$(9.60) \quad \mathbb{P}_Q(\mathcal{N}_z, \Xi_z \mid A) := \int_0^\infty dt \mathbb{P}(\mathcal{N}_z, \Xi_z \mid t) \mathcal{P}(t \mid A),$$

where $\mathcal{P}(t \mid A)$ is as in (9.16)-(9.17).

For large A , we let $\mathcal{N}_z \approx \gamma p A$ and $\Xi_z \approx \gamma q A$, with $(p, q) \in \mathbb{R}_+ \times \mathbb{R}$, and also have $\mathcal{N}_z \approx \nu t$, $\Xi_z \approx \alpha t$, where ν and α are defined by:

$$(9.61) \quad \gamma p A = \nu t, \quad \gamma q A = \alpha t,$$

and p, q, A are considered as parameters. The asymptotic result (9.59) then yields, for $A \rightarrow +\infty$,

$$(9.62) \quad \begin{aligned} \mathbb{P}_Q(\mathcal{N}_z \approx \gamma p A \text{ and } \Xi_z \approx \gamma q A \mid A) &\asymp \int_0^\infty \frac{A e^{-\mathcal{E}(t)} dt}{\sqrt{2\pi t^3}}, \\ \mathcal{E}(t) &= \frac{1}{2t} (A - a_\gamma t)^2 + \gamma_\kappa(\nu, \alpha)t. \end{aligned}$$

The above integral is evaluated by the saddle-point method, looking for the minimum of $\mathcal{E}(t)$ along trajectories at constant values of νt and αt according to (9.61). We then have

$$t \frac{\partial}{\partial t} \gamma_\mu(\nu, \alpha) = - \left(\nu \frac{\partial}{\partial \nu} + \alpha \frac{\partial}{\partial \alpha} \right) \gamma_\mu(\nu, \alpha),$$

and using (9.58),

$$\frac{\partial}{\partial t} (t \gamma_\mu(\nu, \alpha)) = 0,$$

so that,

$$\frac{\partial}{\partial t}(t \gamma_\kappa(\nu, \alpha)) = \frac{\partial}{\partial t}(t \gamma_\kappa(\nu)) = \lambda,$$

as in (9.7). This shows that $\frac{\partial \mathcal{E}}{\partial t}$ is the same as in (9.25),

$$\frac{\partial \mathcal{E}}{\partial t} = \lambda - \frac{1}{2} \left[\left(\frac{A}{t} \right)^2 - a_\gamma^2 \right],$$

with the same saddle-point as in (9.26),

$$\frac{A}{t^*} = u = u(\lambda) := \sqrt{2\lambda + a_\gamma^2}.$$

The saddle-point value resides at the minimum \mathcal{E}^* of $\mathcal{E}(t)$,

$$(9.63) \quad \mathcal{E}^* := \mathcal{E}(t^*) = A \left[\frac{(u - a_\gamma)^2}{2u} + \frac{\gamma_\kappa(\nu, \alpha)}{u} \right],$$

where, because of condition (9.61), ν and α are now functions of (p, q) determined by

$$(9.64) \quad \nu = \gamma p \frac{A}{t^*} = \gamma p u(\lambda), \quad \alpha = \gamma q \frac{A}{t^*} = \gamma q u(\lambda).$$

It yields

$$\frac{\gamma_\mu(\nu, \alpha)}{u} = \frac{\alpha \lambda' - \nu \Lambda_\mu(\lambda')}{u} = \gamma q \lambda' - \gamma p \Lambda_\mu(\lambda'), \quad \text{with} \quad \frac{\alpha}{\nu} = \frac{q}{p} = \frac{\partial \Lambda_\mu(\lambda')}{\partial \lambda'}.$$

Recalling (9.29) and (9.30), we get the simple form,

$$\Theta(p, q) := \frac{\mathcal{E}^*}{\gamma A} = \frac{u(\lambda) - a_\gamma}{\gamma} + q \lambda' - p(\Lambda_\kappa(\lambda) + \Lambda_\mu(\lambda')).$$

Comparing to (9.32)-(9.33), we get

Theorem 9.12. *The joint distribution of the number of loops \mathcal{N}_z surrounding a ball of given quantum area δ centered at z in a simply connected domain $D \subsetneq \mathbb{C}$, and of the sum of weights Ξ_z on these loops in the ensemble of μ -weighted loops in a CLE_κ , satisfies the large deviations estimate,*

$$\mathbb{P}_\mathcal{Q}(\mathcal{N}_z \approx p \ln(1/\delta) \text{ and } \Xi_z \approx q \ln(1/\delta) \mid \delta) \asymp \delta^{\Theta(p, q)}, \quad \delta \rightarrow 0,$$

with

$$\Theta(p, q) = \Theta(p) + q \lambda' - p \Lambda_\mu(\lambda'),$$

where $\Theta(p)$ is as in Theorem 9.2, and where the conjugate variable λ' is the function of (p, q) uniquely determined by

$$(9.65) \quad \frac{q}{p} = \frac{\partial \Lambda_\mu(\lambda')}{\partial \lambda'}.$$

We can also switch to parameters (p', q') such that

$$(9.66) \quad p = \frac{c}{2\pi} p', \quad q = \frac{c}{2\pi} q',$$

where c is the exponent defined in 9.38. Then, after writing $\Theta(p, q) = \frac{c}{2\pi} J(p', q')$, we get

Corollary 9.13. *In the same setting as in Theorem 9.12, we have*

$$\mathbb{P}_{\mathcal{Q}}\left(\mathcal{N}_z \approx \frac{c}{2\pi} p \ln(1/\delta) \text{ and } \Xi_z \approx \frac{c}{2\pi} q \ln(1/\delta) \mid \delta\right) \asymp \delta^{\frac{c}{2\pi} J(p,q)}, \quad \delta \rightarrow 0,$$

with the bivariate large deviations function

$$J(p, q) = J(p) + q\lambda' - p\Lambda_{\mu}(\lambda'),$$

where $J(p)$ is given by (9.40) and where λ' is uniquely determined as a function of (p, q) by

$$\frac{q}{p} = \frac{\partial \Lambda_{\mu}(\lambda')}{\partial \lambda'}.$$

Corollary 9.13 in LQG matches with the bivariate large deviations of nesting and sum of loop weights for critical $O(n)$ models on random maps with the topology of a pointed disk (first result of Theorem 8.1). The case of the bivariate distribution on the Riemann sphere can be analyzed in exactly the same way as in Section 9.4, and we skip the details here.

Theorem 9.14. *On the Riemann sphere $\widehat{\mathbb{C}}$, the joint distribution of the nesting between two balls of given quantum area δ and the weight carried by the separating loops, behaves as*

$$\mathbb{P}_{\widehat{\mathcal{Q}}}(\mathcal{N} \approx p \ln(1/\delta) \text{ and } \Xi \approx q \ln(1/\delta) \mid \delta) \asymp \delta^{\widehat{\Theta}(p,q)}, \quad \delta \rightarrow 0,$$

where the large deviations function $\widehat{\Theta}(p, q)$ is given in terms of the large deviations function $\Theta(p, q)$ for the quantum disk, as obtained in Theorem 9.12, by

$$\widehat{\Theta}(p, q) = 2 \Theta(p/2, q/2).$$

Switching to variables (9.66), we get

Corollary 9.15. *In the same setting as in Theorem 9.14, we have*

$$\mathbb{P}_{\widehat{\mathcal{Q}}}(\mathcal{N} \approx \frac{cp}{\pi} \ln(1/\delta) \text{ and } \Xi \approx \frac{cq}{\pi} \ln(1/\delta) \mid \delta) \asymp \delta^{\frac{c}{\pi} J(p,q)}, \quad \delta \rightarrow 0,$$

where $J(p, q)$ is the function as defined in Corollary 9.13.

This last result is the exact analog, in Liouville quantum gravity, of the first large deviations result of Theorem 8.1 in the critical $O(n)$ model on random disks with μ -weighted loops, for the topology of a pointed disk with a microscopic boundary.

APPENDIX A. THETA FUNCTION

The properties and conventions we use for elliptic functions can be found in [48].

Let τ be a complex number in the upper-half plane. The Jacobi theta function is the entire function of $v \in \mathbb{C}$ defined by:

$$(A.1) \quad \vartheta_1(v|\tau) = - \sum_{m \in \mathbb{Z}} e^{i\pi\tau(m+1/2)^2 + i\pi(w+1/2)(2m+1)}.$$

Its main properties are:

$$(A.2) \quad \vartheta_1(-v|\tau) = \vartheta_1(v+1|\tau) = -\vartheta_1(v|\tau), \quad \vartheta_1(v+\tau|\tau) = -e^{-2i\pi(v+\tau/2)} \vartheta_1(v|\tau),$$

and the effect of the modular transformation:

$$(A.3) \quad \vartheta_1(v|\tau) = \frac{e^{-i\pi v^2/\tau}}{\sqrt{-i\tau}} \vartheta_1(v/\tau | -1/\tau)$$

APPENDIX B. THE PARAMETRIZATION $x \leftrightarrow v$

Consider given values of γ_{\pm} and $\varsigma(\gamma_{\pm})$ such that:

$$(B.1) \quad \gamma_- < \gamma_+ < \varsigma(\gamma_+) < \varsigma(\gamma_-).$$

We set:

$$(B.2) \quad v = iC \int_{\varsigma(\gamma_+)}^x \frac{dy}{\sqrt{(y - \varsigma(\gamma_-))(y - \varsigma(\gamma_+))(y - \gamma_+)(y - \gamma_-)}}.$$

The normalizing constant is chosen such that, for x moving from the origin $\varsigma(\gamma_+)$ to $\varsigma(\gamma_-)$ with a small negative imaginary part, v is moving from 0 to $1/2$. When x moves on the real axis from $\varsigma(\gamma_+)$ to γ_+ , v moves from 0 to a purely imaginary value denoted $\tau = iT$. Then, the function $v \mapsto x(v)$ has the properties:

$$x(v + 2\tau) = x(v + 1) = x(-v) = x(v), \quad \varsigma(x(v)) = x(v - \tau),$$

and is depicted in Figure 9. $x'(v)$ has zeroes when $v \in \mathbb{Z}/2 + \tau\mathbb{Z}$, and double poles at $v = v_{\infty} + \mathbb{Z} + 2\tau\mathbb{Z}$. From (B.2), paying attention to the determination of the squareroot at infinity obtained by analytic continuation, we can read in particular:

$$(B.3) \quad x'(v) \sim \frac{iC}{(v - v_{\infty})^2}, \quad v \rightarrow v_{\infty}.$$

From (B.1), we know that $v_{\infty} = \frac{1}{2} + \tau w_{\infty}$, where $w_{\infty} \in (0, 1)$ is determined as a function of γ_{\pm} and $\varsigma(\gamma_{\pm})$.

There is an alternative expression for (B.2) in terms of Jacobi functions:

$$(B.4) \quad v = \frac{2iC \operatorname{arcsn}^{-1} \left[\sqrt{\frac{\varsigma(\gamma_+) - \gamma_-}{\varsigma(\gamma_-) - \gamma_-} \frac{x - \varsigma(\gamma_+)}{x - \varsigma(\gamma_-)}}; k \right]}{\sqrt{(\varsigma(\gamma_+) - \gamma_-)(\varsigma(\gamma_-) - \gamma_+)}} ,$$

with:

$$k = \sqrt{\frac{(\varsigma(\gamma_-) - \gamma_-)(\varsigma(\gamma_+) - \gamma_+)}{(\varsigma(\gamma_-) - \gamma_+)(\varsigma(\gamma_+) - \gamma_-)}}.$$

By specialization at $x = \gamma_-$ and $x = \varsigma(\gamma_-)$, we deduce the expressions:

$$(B.5) \quad C = \frac{\sqrt{(\varsigma(\gamma_+) - \gamma_-)(\varsigma(\gamma_-) - \gamma_+)}}{4K'(k)},$$

$$(B.6) \quad T = \frac{K(k)}{2K'(k)}.$$

in terms of the complete elliptic integrals. By matching poles and zeroes, we can infer an expression for $x(v) - \gamma_+$ in terms of Jacobi theta functions:

$$(B.7) \quad x(v) - \gamma_+ = -iC \frac{\vartheta_1'(0|2\tau)\vartheta_1(2v_{\infty}|2\tau)}{\vartheta_1(v_{\infty} - \tau|2\tau)\vartheta_1(v_{\infty} + \tau|2\tau)} \frac{\vartheta_1(v - \tau|2\tau)\vartheta_1(v + \tau|2\tau)}{\vartheta_1(v - v_{\infty}|2\tau)\vartheta_1(v + v_{\infty}|2\tau)}.$$

From (B.2), one can derive the expansion of $x(v)$ when $v \rightarrow v_{\infty}$.

Lemma B.1. *When $v \rightarrow v_\infty$, we have the expansion:*

$$x(v) = \frac{-iC}{v - v_\infty} + \frac{E_1}{4} + \frac{i}{C} \frac{3E_1^2 - 8E_2}{48} (v - v_\infty) + \frac{-E_1^3 + 4E_1E_2 - 8E_3}{64C^2} (v - v_\infty)^2 + O(v - v_\infty)^3,$$

where we introduced the symmetric polynomials in the endpoints:

$$(B.8) \quad E_1 = \gamma_- + \gamma_+ + \varsigma(\gamma_+) + \varsigma(\gamma_-),$$

$$(B.9) \quad E_2 = \gamma_- \{ \gamma_+ + \varsigma(\gamma_+) + \varsigma(\gamma_-) \} + \gamma_+ \{ \varsigma(\gamma_+) + \varsigma(\gamma_-) \} + \varsigma(\gamma_+) \varsigma(\gamma_-),$$

$$(B.10) \quad E_3 = \gamma_- \gamma_+ \varsigma(\gamma_+) + \gamma_- \gamma_+ \varsigma(\gamma_-) + \gamma_- \varsigma(\gamma_-) \varsigma(\gamma_+) + \gamma_+ \varsigma(\gamma_+) \varsigma(\gamma_-).$$

More generally, the coefficient of $(v - v_\infty)^k$ in this expansion is a homogeneous symmetric polynomial of degree $(k + 1)$ in the endpoints, with rational coefficients up to an overall factor $(iC)^{-k}$. \square

In the study of non-generic critical points, we want to take the limit where γ_+ and $\varsigma(\gamma_+)$ collide to the fixed point of the involution:

$$\gamma_+^* = \frac{1}{(\alpha + 1)h},$$

while $\gamma_- \rightarrow \gamma_-^*$ remains distinct from $\varsigma(\gamma_-^*)$. This implies $T \rightarrow 0$, or equivalently $k \rightarrow 0$. This limit is easily studied using the modular transformation (A.3) in (B.7), or the properties of the elliptic integrals. If we set:

$$q = e^{-\frac{\pi}{T}},$$

we arrive to:

Lemma B.2.

$$\begin{aligned} q &= \left(\frac{k}{4}\right)^4 \{1 + O(k^2)\}, \\ w_\infty &= w_\infty^* \{1 + O(q^{\frac{1}{2}})\}. \end{aligned}$$

\square

We shall need the asymptotic behavior of $x(v)$ near the vertical lines $\text{Im } v = 0$ and $\text{Im } v = \frac{1}{2}$.

Lemma B.3. *Let $v = \varepsilon + \tau w$ for $\varepsilon \in \{0, \frac{1}{2}\}$. We have:*

$$x(v) - \gamma_+ = q^{\frac{1-2\varepsilon}{2}} \{x_\varepsilon^*(w) + O(q^{\frac{1}{2}})\}.$$

The error is uniform for w in any compact independent of $\tau \rightarrow 0$, and this is stable under differentiation with respect to v . It is actually an asymptotic series in $q^{\frac{1}{2}}$. The limit functions are:

$$\begin{aligned} x_0^*(w) &= 8\sqrt{(\varsigma(\gamma_-^*) - \gamma_+^*)(\gamma_+^* - \gamma_-^*)} \sin(\pi w_\infty^*) \cos^2\left(\frac{\pi w}{2}\right), \\ x_{\frac{1}{2}}^*(w) &= \sqrt{(\varsigma(\gamma_-^*) - \gamma_+^*)(\gamma_+^* - \gamma_-^*)} \frac{\sin(\pi w_\infty^*)}{\cos(\pi w) - \cos(\pi w_\infty^*)}. \end{aligned}$$

\square

If we specialize the second equation to $v = \frac{1}{2} + \tau$, use the expression (5.2) of $\varsigma(x)$ and perform elementary trigonometric manipulations, we find:

Corollary B.4.

$$\cos(\pi w_\infty^*) = \frac{1 - \alpha}{1 + \alpha} \cdot \frac{1 - h(1 + \alpha)\gamma_-^*}{1 + h(1 - \alpha)\gamma_-^*}.$$

□

We may consider w_∞^* as a parameter for the non-generic critical line. Specializing again Lemma B.3 to $v = \varepsilon + \tau$ and using Corollary B.4 yields:

Corollary B.5. *There exists a constant ρ_1 such that:*

$$\begin{aligned} 2h(\gamma_+^* - \gamma_+) &= \frac{16 \cos(\pi w_\infty^*)}{(1 - \alpha^2)} q^{\frac{1}{2}} + O(q), \\ 2h(\gamma_-^* - \gamma_-) &= \rho_1 q^{\frac{1}{2}} + O(q), \\ E_1 &= \frac{1 - \alpha \sin^2(\pi w_\infty^*)}{(1 - \alpha^2)h \sin^2(\pi w_\infty^*)} + \frac{2\rho_1 \cos(\pi w_\infty^*)}{h(1 - \cos(\pi w_\infty^*))^2} q^{\frac{1}{2}} + O(q), \\ E_2 &= \frac{2((3\alpha^2 - 1) \sin^2(\pi w_\infty^*) - 2(3\alpha - 2))}{(\alpha^2 - 1)^2 h^2 \sin^2(\pi w_\infty^*)} + \frac{2\rho_1(3\alpha - 2)}{h^2(1 - \alpha^2)(1 - \cos(\pi w_\infty^*))^2} q^{\frac{1}{2}} + O(q), \\ E_3 &= \frac{4(\alpha^2 \sin^2(\pi w_\infty^*) - \alpha(2 + \cos^2(\pi w_\infty^*) + 1))}{(1 - \alpha)^2(1 + \alpha)^3 \sin^2(\pi w_\infty^*) h^3} + O(q^{\frac{1}{2}}). \end{aligned}$$

The first four lines are used in Appendix E to describe the phase diagram and the critical exponents of the model. The expression for E_3 is only used to leading order in Appendix F, to get the constant prefactor in the asymptotic number of planar maps of large volume.

Straightforward computations with (B.5)-(B.6) yield:

Corollary B.6.

$$\begin{aligned} \frac{\pi C}{T} &= \sqrt{(\varsigma(\gamma_-) - \gamma_+^*)(\gamma_+^* - \gamma_-) + O(q)}, \\ &= \frac{2 \cot(\pi w_\infty^*)}{(1 - \alpha^2)h} + \frac{(1 + \cos(\pi w_\infty^*))\rho_1}{2(1 - \cos(\pi w_\infty^*)) \sin(\pi w_\infty^*)} q^{\frac{1}{2}} + O(q). \end{aligned}$$

□

There are some simplifications in absence of bending energy, *i.e.*, $\alpha = 1$. We then have $w_\infty^* = \frac{1}{2}$ which is in agreement with Corollary B.4. The non-generic critical line is then parametrized by $\rho = 1 - 2h\gamma_-^*$, which is related to the former parametrization by letting $\alpha \rightarrow 1$ and $w_\infty^* \rightarrow \frac{1}{2}$ in such a way that:

$$(B.11) \quad \left(\frac{1}{2} - w_\infty^*\right) \sim \frac{(1 - \alpha)}{2\pi} \rho.$$

Corollary B.5 specializes to:

Corollary B.7. *For $\alpha = 1$, we have:*

$$\begin{aligned} 2h(\gamma_+^* - \gamma_+) &= O(q), \\ E_1 &= \frac{2}{h} + O(q), \\ E_2 &= \frac{6 - \rho^2}{4h^2} - \frac{\rho\rho_1}{2h^2} q^{\frac{1}{2}} + O(q), \\ E_3 &= \frac{2 - \rho^2}{4h^3} + O(q^{\frac{1}{2}}), \\ \frac{\pi C}{T} &= \frac{\rho}{2h} + \frac{\rho_1}{2h} q^{\frac{1}{2}} + O(q). \end{aligned}$$

□

The fact that $\varsigma(x) = \frac{1}{h} - x$ and $\gamma_+^* = \frac{1}{2h}$ gives the exact relation $E_1 = \frac{2}{h}$, in agreement with the second line.

APPENDIX C. COEFFICIENTS $(\tilde{g}_k)_{k \geq 0}$

In the loop model with bending energy where all faces are triangles, the parameters are: g (resp. h) the weight per face not visited (resp. visited) by a loop, α the bending energy, and n the weight per loop. We can compute \tilde{g}_k from their definition (5.14) if we insert the expansion of Lemma B.1. We remind that C is the constant in (B.2), and E 's are symmetric polynomials in the endpoints defined in Lemma (B.1). If we introduce:

$$\tilde{g}_k = (iC)^k \hat{g}_k,$$

we find:

$$\begin{aligned} \hat{g}_3 &= \frac{2g}{4 - n^2}, \\ \hat{g}_2 &= \frac{2 - gE_1}{4 - n^2}, \\ \hat{g}_1 &= \frac{g(3E_1^2 - 4E_2) - 6E_1}{12(4 - n^2)}, \\ \hat{g}_0 &= -\frac{2u}{2 + n}. \end{aligned}$$

We remark that \hat{g}_3 and \hat{g}_0 depend on the parameters of the model in a very simple way, whereas \hat{g}_1 and \hat{g}_2 have a non-trivial behavior in the non-generic critical regime, which can be deduced up to $O(q)$ from Corollary B.5, either in terms of the parameter w_∞^* , or the parameter ρ if $\alpha = 1$.

Corollary C.1. *We have:*

$$\begin{aligned} \hat{g}_2 &= \frac{1}{4 - n^2} \left[1 + \frac{2g}{h} \left(\alpha - \frac{1}{\sin^2(\pi w_\infty^*)} \right) \right] - \frac{g}{h} \frac{\rho_1 \cos(\pi w_\infty^*)}{(1 - \cos(\pi w_\infty^*))^2 (4 - n^2)} q^{\frac{1}{2}} + O(q), \\ \hat{g}_1 &= \frac{2g[(3\alpha^2 + 1)\sin^4(\pi w_\infty^*) + 2(3\alpha - 2)\sin^2(\pi w_\infty^*) + 6] + 3h\sin^2(\pi w_\infty^*)(1 - \alpha^2)(\alpha\sin^2(\pi w_\infty^*) + 1)}{3(1 - \alpha^2)^2 h^2 (4 - n^2) \sin^4(\pi w_\infty^*)} \\ &\quad + \frac{\cos(w)\rho_1 \{ 2g[-3\alpha\sin^2(\pi w_\infty^*) + 2\cos^2(\pi w_\infty^*) + 4] - 3h\sin^2(\pi w_\infty^*)(1 - \alpha^2) \}}{(1 - \cos(\pi w_\infty^*))^2 \sin^2(\pi w_\infty^*)(1 - \alpha^2) h^2 (4 - n^2)} q^{\frac{1}{2}} + O(q). \end{aligned}$$

□

There are some simplifications for $\alpha = 1$. Owing to the exact relation $E_1 = \frac{2}{h}$, only \widehat{g}_1 has a non-trivial dependence in the non-critical regime:

Corollary C.2. *For $\alpha = 1$, we have:*

$$\begin{aligned}\widehat{g}_2 &= \frac{2}{4-n^2} \left(1 - \frac{g}{h}\right), \\ \widehat{g}_1 &= \frac{1}{h(4-n^2)} \left(-1 + \frac{g}{h}(\rho^2 + 6)\right) + \frac{g\rho\rho_1}{h^2(4-n^2)} q^{\frac{1}{2}} + O(q).\end{aligned}$$

□

APPENDIX D. THE SPECIAL FUNCTION $\Upsilon_b(v)$

$\Upsilon_b(v)$ is the unique meromorphic function with a simple pole at $v = 0$ with residue 1, and the pseudo-periodicity properties:

$$\Upsilon_b(v+1) = \Upsilon_b(v), \quad \Upsilon_b(v+\tau) = e^{i\pi b} \Upsilon_b(v).$$

We have several expressions:

$$\begin{aligned}\Upsilon_b(v) &= \sum_{m \in \mathbb{Z}} e^{-i\pi b m} \cot \pi(v + m\tau) \\ &= \frac{\vartheta'_1(0|\tau)}{\vartheta_1(-\frac{b}{2}|\tau)} \frac{\vartheta_1(v - \frac{b}{2}|\tau)}{\vartheta_1(v|\tau)} \\ (D.1) \quad &= \frac{e^{\frac{i\pi b v}{\tau}}}{iT} \frac{\vartheta'_1(0|\frac{1}{\tau})}{\vartheta_1(-\frac{b}{2\tau}|\frac{1}{\tau})} \frac{\vartheta_1(\frac{v-b/2}{\tau}|\frac{1}{\tau})}{\vartheta_1(\frac{v}{\tau}|\frac{1}{\tau})}.\end{aligned}$$

Curiously, this function also appears in the dynamical R -matrix of an integrable elliptic Calogero system [3]. The last expression is convenient to study the regime $T \rightarrow 0$. We set:

$$q = e^{-\frac{\pi}{T}} \rightarrow 0$$

Lemma D.1. *Let $v = \varepsilon + \tau w$. We have, for $b \in (0, 1)$:*

$$\Upsilon_b(v) = \frac{2\pi q^{\varepsilon \frac{b}{2}}}{T(1-q^b)} \cdot \begin{cases} \Upsilon_{b,0}^*(w) - q^b \Upsilon_{b+2,0}^*(w) + O(q^{2-b}) & \text{if } \varepsilon = 0 \\ \Upsilon_{b,\frac{1}{2}}^*(w) - (q^{1-b} - q) \Upsilon_{b-2,\frac{1}{2}}^*(w) + q \Upsilon_{b+2,\frac{1}{2}}^*(w) + O(q^{1+b}) & \text{if } \varepsilon = 1/2 \end{cases}.$$

The errors are uniform for w in any compact independent of $\tau \rightarrow 0$, and the expressions for the limit functions are:

$$(D.2) \quad \Upsilon_{b,0}^*(w) = \frac{e^{i\pi(b-1)w}}{2i \sin(\pi w)},$$

$$(D.3) \quad \Upsilon_{b,\frac{1}{2}}^*(w) = -e^{i\pi b w}.$$

□

APPENDIX E. PROOF OF THE PHASE DIAGRAM AND VOLUME EXPONENT

The equations $\mathbf{G}^\bullet(\varepsilon + \tau) = 0$ for $\varepsilon \in \{0, \frac{1}{2}\}$ determine γ_\pm in terms of the weights of the model. Since $v_\infty = \frac{1}{2} + \tau w_\infty$ and $\tilde{g}_k = (iC)^k \hat{g}_k$, they take the form:

$$\sum_{k \geq 0} \frac{(-1)^k \hat{g}_k}{k!} \left(\frac{\pi C}{T} \right)^k \partial_{\pi w_\infty}^k \left[\Upsilon_b(\bar{\varepsilon} + \tau(w_\infty + 1)) + \Upsilon_b(\bar{\varepsilon} + \tau(1 - w_\infty)) \right. \\ \left. - \Upsilon_b(\bar{\varepsilon} + \tau(w_\infty - 1)) - \Upsilon_b(\bar{\varepsilon} - \tau(1 + w_\infty)) \right] = 0.$$

where we have denoted $\bar{\varepsilon} = \frac{1}{2} - \varepsilon$. In the non-generic critical regime, we have $\tau = iT \rightarrow 0$ and inserting the asymptotic expansions from Corollary D.1 yields:

$$(E.1) \quad \sum_{k=0}^3 \frac{(-1)^k \hat{g}_k}{k!} \left(\frac{\pi C}{T} \right)^k \left[Y_{b,0}^{(k)}(\pi w_\infty) - q^{1-b} Y_{b-2,0}^{(k)}(\pi w_\infty) + O(q) \right] = 0,$$

$$(E.2) \quad \sum_{k=0}^3 \frac{(-1)^k \hat{g}_k}{k!} \left(\frac{\pi C}{T} \right)^k \left[Y_{b,\frac{1}{2}}^{(k)}(\pi w_\infty) - q^b Y_{b+2,\frac{1}{2}}^{(k)}(\pi w_\infty) + O(q) \right] = 0.$$

with coefficients:

$$Y_{b,0}(w) = \cos(bw), \quad Y_{b,\frac{1}{2}}(w) = \frac{\sin[(1-b)w]}{\sin w}.$$

E.1. The non-generic critical line. At a non-generic critical point, we must have $u = 1$ and $q = 0$, thus:

$$-\frac{2}{2+n} + \sum_{k=1}^3 \frac{(-1)^k \hat{g}_k^*}{k!} \left(\frac{2 \cot(\pi w_\infty^*)}{(1-\alpha^2)h} \right)^k \frac{Y_{b,\varepsilon}^{(k)}(\pi w_\infty^*)}{Y_{b,\varepsilon}(\pi w_\infty^*)} = 0 \quad \varepsilon \in \{0, \frac{1}{2}\}.$$

We note that the critical values \hat{g}_k^* obtained in Section C are such that (E.1)-(E.2) give a system of two linear equations determining $\frac{g}{h}$ and h^2 , in terms of the parameter w_∞^* , or in the case of $\alpha = 1$, in terms of the parameter ρ .

For $\alpha = 1$, the solution is:

$$(E.3) \quad \frac{g}{h} = \frac{4(\rho b \sqrt{2+n} - \sqrt{2-n})}{\rho^2(b^2 - 1)\sqrt{2-n} + 4\rho b \sqrt{2+n} - 2\sqrt{2-n}},$$

$$(E.4) \quad h^2 = \frac{\rho^2 b}{24\sqrt{4-n^2}} \frac{\rho^2 b(1-b^2)\sqrt{2+n} - 4\rho\sqrt{2-n} + 6b\sqrt{2+n}}{-\rho^2(1-b^2)\sqrt{2-n} + 4\rho b \sqrt{2+n} - 2\sqrt{2-n}},$$

as claimed in Theorem 6.1. Since g/h and h^2 must be non-negative, we must have $\rho \in [\rho'_{\min}, \rho_{\max}]$, with:

$$(E.5) \quad \rho'_{\min} = \frac{2\sqrt{1-b^2}\sqrt{2-n} - \sqrt{2}\sqrt{(10+n)b^2 - 4 + 2n}}{b\sqrt{1-b^2}\sqrt{2-n}},$$

$$(E.6) \quad \rho_{\max} = \frac{1}{b} \sqrt{\frac{2-n}{2+n}}.$$

However, we will see later that the non-generic critical line only exists until some value $\rho_{\min} > \rho'_{\min}$, so (E.5) will become irrelevant.

In the general case $\alpha \neq 1$:

$$(E.7) \quad \frac{g}{h} = 6(1 - \alpha^2) \sin^2(\pi w_\infty^*) \frac{\sum_{k=0}^1 b^k \tilde{P}_k(\alpha, \pi w_\infty^*)}{b^2 P_2(b, \pi w_\infty^*) + \sum_{k=0}^1 b^k P_k(\alpha, \pi w_\infty^*)},$$

$$(E.8) \quad h^2 = \frac{2b \cos^2(\pi w_\infty^*)}{(1 - \alpha^2)^2 (2 - n) \sin^3(\pi w_\infty^*)} \frac{b^3 \tilde{Q}_3(b, \pi w_\infty^*) + \sum_{k=0}^2 b^k \tilde{Q}_k(\alpha, \pi w_\infty^*)}{b^2 P_2(b, \pi w_\infty^*) + \sum_{k=0}^1 b^k P_k(\alpha, \pi w_\infty^*)},$$

with:

$$\begin{aligned} \tilde{P}_1(\alpha, w) &= \sin(2w) [\alpha \sin^2(w) - 1 - 2 \cos^2(bw)], \\ \tilde{P}_0(\alpha, w) &= \sin(2bw) [-\alpha \sin^2(w) + 1 + 2 \cos^2 w], \\ P_2(b, w) &= \sin^2(2w) [b \sin(2w) - 3 \sin(2bw)], \\ P_1(\alpha, w) &= -2 \sin(2w) [3\alpha^2 \sin^4(w) - 6\alpha \sin^2(w)(2 \cos^2(bw) + 1) \\ &\quad + \cos^4(w) + 2 \cos^2(w) + 3 + 12 \cos^2(bw)(\cos^2(w) + 1)], \\ P_0(\alpha, w) &= 6 \sin(2bw) [\alpha^2 \sin^4(w) - 2\alpha \sin^2(w)(2 \cos^2(w) + 1) + 3 \cos^4(w) + 6 \cos^2(w) + 1], \\ \tilde{Q}_3(b, w) &= \sin(w) \sin(2w) [-b \sin(2w) + \sin(2bw)], \\ \tilde{Q}_2(\alpha, w) &= -2 \sin(w) \sin(2w) [3\alpha^2 \sin^4(w) + 2\alpha \sin^2(w)(2 \cos^2(bw) - 5) \\ &\quad - \cos^4(w) - 6 \cos^2(w) + 7 - 4 \cos^2(bw)(2 \cos^2(w) + 1)], \\ \tilde{Q}_1(\alpha, w) &= -2 \sin(w) \sin(2bw) [3\alpha^2 \sin^4(w) - 6\alpha \sin^2(w)(2 \cos^2(w) + 1) \\ &\quad + 7 \cos^4(w) + 14 \cos^2(w) + 3], \\ \tilde{Q}_0(\alpha, w) &= 2 \cos(w) \sin^2(bw) [3\alpha^2 \sin^4(w) - 4\alpha \sin^2(w)(\cos^2(w) + 2) \\ &\quad - \cos^4(w) + 2 \cos^2(w) + 5]. \end{aligned}$$

We have checked that, in the limit $\alpha \rightarrow 1$ such that $(\frac{1}{2} - w_\infty^*) \sim \frac{1-\alpha}{2} \rho$, these expressions retrieve (E.3)-(E.4).

E.2. Near criticality. Let us fix (g, h) on the non-generic critical line for $u = 1$. We now study the behavior when $u \neq 1$ but $u \rightarrow 1$ of the endpoints γ_\pm . In particular, since the behavior of the elliptic functions is conveniently expressed in this regime in terms of $q = e^{-\frac{\pi}{T}}$, our first task is to relate $(1 - u)$ to $q \rightarrow 0$. For this purpose, we look at (E.1), and note that u only appears in \hat{g}_0 . There could be a term of order $q^{\frac{1}{2}}$ stemming from near-criticality corrections to w_∞ , \hat{g}_k and $\frac{\pi C}{T}$, but computation reveals that it is absent. Therefore, we obtain:

$$1 - u = \frac{n+2}{2} \left(\sum_{k=0}^3 \frac{(-1)^k \hat{g}_k^*}{k!} \left(\frac{2 \cot(\pi w_\infty^*)}{(1 - \alpha^2)h} \right)^k \frac{Y_{b-2,0}^{(k)}(\pi w_\infty^*)}{Y_{b,0}(\pi w_\infty^*)} \right) q^{1-b} + O(q),$$

where $\hat{g}_0^* = -\frac{2}{2+n}$ and $(\hat{g}_k^*)_{k \geq 1}$ should be replaced by their values in terms of (g, h, w_∞^*) from Section C, and (g, h) by their parametrization (E.7)-(E.8) on the critical line.

E.2.1. *Case $\alpha = 1$.* Here, we rather use the parametrization (E.3)-(E.4), and the resulting formula is relatively simple:

$$(E.9) \quad 1 - u = \Delta q^{1-b} + (\Delta_1 + c' \rho_1)q + o(q).$$

with:

$$\begin{aligned} \Delta &= \frac{12}{b} \frac{\rho^2(1-b)^2\sqrt{2+n} + 2\rho(1-b)\sqrt{2-n} - 2\sqrt{2+n}}{-\rho^2b(1-b^2)\sqrt{2+n} + 4\rho(1-b^2)\sqrt{2-n} - 6b\sqrt{2+n}}, \\ \Delta_1 &= \frac{24}{b} \frac{-\rho^2(b^2+1)\sqrt{2+n} + 2\rho b\sqrt{2-n} + 2\sqrt{2+n}}{-\rho^2b(1-b^2)\sqrt{2+n} + 4\rho(1-b^2)\sqrt{2-n} - 6b\sqrt{2+n}}. \end{aligned}$$

The value of c' is irrelevant because we will soon show that $\rho_1 = 0$. This quantity is non-negative iff $\Delta \geq 0$, which demands $\rho \in [0, \rho_{\max}]$ with:

$$(E.10) \quad \rho_{\min} = \frac{\sqrt{6+n} - \sqrt{2-n}}{(1-b)\sqrt{2+n}}.$$

We observe that this lower bound is larger than ρ'_{\min} for any $n \in [0, 2]$, therefore the non-generic critical line can only exist in the range $\rho \in [\rho_{\min}, \rho_{\max}]$ provided by (E.10)-(E.6). These necessary conditions were also obtained in [11] – where the lower bound arose from the constraint of positivity of the spectral density associated with the generating series of disks $\mathbf{F}(x)$ – and it was checked that these conditions are sufficient.

We now turn to the second equation (E.2). We have checked that the term in q^b vanishes, as we expect by consistency with (E.9). Then, the term of order $q^{\frac{1}{2}}$ is proportional to ρ_1 , therefore we must have, in both dense and dilute phase:

$$\rho_1 = 0,$$

which means that $\gamma_- - \gamma_-^* \in O(q)$.

We see that for $\rho \in (\rho_{\min}, \rho_{\max}]$:

$$q \sim (1-u)^{\frac{1}{1-b}}.$$

which corresponds, by definition, to the "dense phase". For $\rho = \rho_{\min}$, we have $\Delta = 0$, and (E.9) specializes to:

$$1 - u = \frac{24}{b(1-b)(2-b)} q + o(q).$$

Hence

$$q \sim (1-u),$$

which corresponds to the dilute phase.

E.2.2. *General α .* We find (E.9) with a constant:

$$\Delta_0^* = \frac{4(2-b)}{b \cos(bw) \sin(w)} \frac{b^3 R_3(b, \pi w_\infty^*) + \sum_{k,j=0}^2 \alpha^j b^k R_{j,k}(\pi w_\infty^*)}{b^3 \tilde{Q}_3(b, \pi w_\infty^*) + \sum_{k=0}^2 b^k \tilde{Q}_k(\alpha, \pi w_\infty^*)},$$

with:

$$R_3(b, w) = b^3 \sin^2(w) \sin^2(2w) \left[\left(\frac{1}{2} - b \right) \sin(2w) \cos[(b-2)w] \right. \\ \left. + \sin(2w) \cos(bw) + \frac{1}{4} \sin(2bw) \cos[(b-2)w] \right],$$

and more complicated expressions for $R_{j,k}$.

APPENDIX F. PLANAR MAPS WITH LARGE VOLUME AND γ_{str}

Planar pointed rooted maps are pointed disks whose boundary face is a triangle. Therefore, their generating series with vertex weight u is:

$$(F.1) \quad [x^{-4}] \mathbf{F}^\bullet = - \operatorname{Res}_{x \rightarrow \infty} dx x^3 \mathbf{F}^\bullet(x) = - \operatorname{Res}_{v \rightarrow v_\infty} dv (x(v))^3 \mathbf{G}^\bullet(v).$$

We shall prove:

Lemma F.1. *When $u \rightarrow 1$, the singular part of (F.1) with respect to u behaves like:*

$$[x^{-4}] \mathbf{F}^\bullet|_{\text{sing}} \sim A \left(\frac{1-u}{\Delta} \right)^{bc}.$$

By transfer theorems [41], this implies that the generating series of planar pointed rooted maps with fixed volume $V \rightarrow \infty$ behaves like:

$$[u^V \cdot x^{-4}] \mathbf{F}^\bullet \sim \frac{A}{\Gamma(-bc) \Delta^{bc} V^{1+bc}}.$$

as claimed in Corollary 6.5.

Proof. We remind the expression from Proposition (5.2) of $\mathbf{G}^\bullet(v)$, specialized to $v = \frac{1}{2} + \tau w$:

$$\mathbf{G}^\bullet\left(\frac{1}{2} + \tau w\right) = \frac{2u}{2+n} \left[-\Upsilon_b(w + w_\infty) - \Upsilon_b(w - w_\infty) + \Upsilon_b(-w + w_\infty) + \Upsilon_b(-w - w_\infty) \right],$$

and it has a simple pole when $w \rightarrow w_\infty$. To compute the residue (F.1), we insert the Laurent expansion of $x(v)$ given in Lemma B.1. Then, in the regime $u \rightarrow 1$, we insert the behavior of $\Upsilon_b(\varepsilon + \tau \tilde{w})$ with $\varepsilon = 0$ from Lemma D.1. The leading term is of order 1 and does not contain a singularity in u , so we must include the subleading term which is of order:

$$q^b \sim \left(\frac{1-u}{\Delta} \right)^{bc},$$

and which also receives a contribution from the prefactor $\frac{1}{1-q^b}$. Paying attention to the change of variable $v = iTw$ in the residue (F.1), we get a polynomial of degree 3 in the combination $\frac{\pi C}{T}$, which we then replace by its critical value given in Corollary B.4. The outcome is:

$$[x^{-4}] \mathbf{F}^\bullet|_{\text{sing}} = A \left(\frac{1-u}{\Delta} \right)^{bc} + o(1-u)^{bc},$$

with constant:

$$(F.2) \quad A = \frac{16 \cos(\pi b w_\infty^*) \cos(\pi w_\infty^*) \left(\sum_{k=0}^2 b^k A_k(\alpha, \pi w_\infty^*) \right)}{(1 - \alpha^2)^3 h^3 (2+n) \sin^5(\pi w_\infty^*)},$$

and:

$$\begin{aligned} A_2(\alpha, w) &= \sin^2(2w) \sin(bw), \\ A_1(\alpha, w) &= 6 \sin(2w) \cos(bw) (1 - \alpha \sin^2(w)), \\ A_0(\alpha, w) &= 2 \sin(bw) [-3(1 - \alpha \sin^2 w)^2 + \cos^2(w)(\cos^2(w) - 2)]. \end{aligned}$$

For $\alpha \rightarrow 1$ according to (B.11), it simplifies to:

$$(F.3) \quad A = \frac{\rho(-\rho^2(1-b^2)\sqrt{2-n} + 6\rho b\sqrt{2+n} - 6\sqrt{2-n})}{2h^3}.$$

The value of h appearing (F.2) or (F.3) is itself parametrized in terms of w_∞^* via (E.8), or ρ via (E.4). \square

APPENDIX G. SCALING LIMITS FOR CYLINDER GENERATING SERIES

We distinguish whether the variable x_i coupled to the perimeter of the i -th boundary is away from γ_+^* – in which case the perimeter remains typically finite – or close to γ_+^* at scale $O(q^{\frac{1}{2}})$ – in which case the perimeter typically diverges.

G.1. Refined cylinders: finite/finite. This is governed by the regime $x_i = x(\frac{1}{2} + \tau w_i)$, and leads to:

$$\begin{aligned} \mathbf{F}_s^{(2)}(x_1, x_2) &= \frac{(1-\alpha^2)^2 h^2}{4\pi \cos^2(\pi w_\infty^*)} \left[\prod_{i=1}^2 \frac{(\cos(\pi w_i) - \cos(\pi w_\infty^*))^2}{\sin(\pi w_i)} \right] \\ &\quad \times \left\{ \frac{R_{b(s)}(w_1, w_2) - q^{b(s)} R_{b(s)+2}(w_1, w_2)}{(4 - n^2 s^2)(1 - q^{b(s)})} + O(q) \right\} \\ &= \frac{(1-\alpha^2)^2 h^2}{4\pi(4 - n^2 s^2) \cos^2(\pi w_\infty^*)} \left[\prod_{i=1}^2 \frac{(\cos(\pi w_i) - \cos(\pi w_\infty^*))^2}{\sin(\pi w_i)^2} \right] \\ &\quad \times \left\{ R_{b(s)}(w_1, w_2) + \frac{q^{b(s)}}{1 - q^{b(s)}} (R_{b(s)}(w_1, w_2) - R_{b(s)+2}(w_1, w_2)) + O(q) \right\}, \end{aligned}$$

where:

$$R_b(w_1, w_2) = 2i\partial_{w_1} [\Upsilon_{b,0}^*(w_1 + w_2) - \Upsilon_{b,0}^*(w_1 - w_2) + \Upsilon_{b,0}^*(-w_1 + w_2) - \Upsilon_{b,0}^*(-w_1 - w_2)].$$

The first term $R_{b(s)}$ does not feature a singularity when $u \rightarrow 1$, and thus will not contribute to large volume asymptotics. We compute using the expression of $\Upsilon_{b,0}^*$ in (D.2):

$$(G.1) \quad R_{b(s)}(w_1, w_2) - R_{b(s)+2}(w_1, w_2) = -8\pi b(s) \sin(\pi b(s)w_1) \sin(\pi b(s)w_2).$$

Therefore:

$$\mathbf{F}_s^{(2)}(x_1, x_2)|_{\text{sing}} = -\frac{b(s) q^{b(s)}}{1 - q^{b(s)}} \Xi_{b(s),3}(x_{\frac{1}{2}}^*(w_1), x_{\frac{1}{2}}^*(w_2)) + O(q),$$

with:

$$\Xi_{b(s),3} = \frac{2h^2(1-\alpha^2)^2}{4 - n^2 s^2} \left[\prod_{i=1}^2 \frac{(\cos(\pi w_i) - \cos(\pi w_\infty^*))^2 \sin(\pi b(s)w_i)}{\cos(\pi w_\infty^*) \sin(\pi w_i)} \right].$$

For $\alpha = 1$, it specializes to:

$$\Xi_{b(s),3} = \frac{-32h^2}{\rho^2(4 - n^2s^2)} \left[\prod_{i=1}^2 \frac{\cos^2(\pi w_i) \sin(\pi b(s)w_i)}{\sin(\pi w_i)} \right].$$

G.2. Refined cylinders: finite/large. This is governed by $x_1 = x(\frac{1}{2} + \tau w_1)$ and $x_2 = x(\tau w_2)$, and leads to:

$$\begin{aligned} \mathbf{F}_s^{(2)}(x_1, x_2)|_{\text{sing}} &= \frac{q^{(b(s)-1)/2}}{1 - q^{b(s)}} \frac{(1 - \alpha^2)^2 h^2 (\cos(\pi w_1) - \cos(\pi w_\infty^*))^2}{16\pi(4 - n^2s^2) \cos^2(\pi w_\infty^*) \sin(\pi w_1) \sin(\pi w_2)} \\ &\quad \times \{ \tilde{R}_{b(s)}(w_1, w_2) + O(q^{(1-b(s))/2}) \}, \end{aligned}$$

with:

$$\begin{aligned} \tilde{R}_{b(s)}(w_1, w_2) &= -2i \{ (\Upsilon_{b(s), \frac{1}{2}}^*)'(w_1 + w_2) - (\Upsilon_{b(s), \frac{1}{2}}^*)'(w_1 - w_2) \\ &\quad - (\Upsilon_{b(s), \frac{1}{2}}^*)'(w_2 - w_1) + (\Upsilon_{b(s), \frac{1}{2}}^*)'(-w_1 - w_2) \} \\ &= 8\pi b(s) \sin(\pi b(s)w_1) \sin(\pi b(s)w_2). \end{aligned}$$

Therefore:

$$\mathbf{F}_s^{(2)}(x_1, x_2)|_{\text{sing}} = \frac{b(s) q^{(b(s)-1)/2}}{1 - q^{b(s)}} \Xi_{b(s),4}(x_{\frac{1}{2}}^*(w_1), x_0^*(w_2)) + O(q^{(1-b(s))/2}),$$

with:

$$\Xi_{b(s),4} = \frac{(1 - \alpha^2)^2 h^2 [\cos(\pi w_1) - \cos(\pi w_\infty^*)]^2}{2(4 - n^2s^2) \cos^2(\pi w_\infty^*)} \left[\prod_{i=1}^2 \frac{\sin(\pi b(s)w_i)}{\sin(\pi w_i)} \right].$$

In particular for $\alpha = 1$, we find:

$$\Xi_{b(s),4} = \frac{8h^2}{\rho^2(4 - n^2s^2)} \cos^2(\pi w_1) \left[\prod_{i=1}^2 \frac{\sin(\pi b(s)w_i)}{\sin(\pi w_i)} \right].$$

G.3. Refined cylinders: large/large. This is governed by $x_i = x(\tau w_i)$, and leads to:

$$\begin{aligned} \mathbf{F}_s^{(2)}(x_1, x_2)|_{\text{sing}} &= \frac{(1 - \alpha^2)^2 h^2}{32\pi(4 - n^2s^2) \cos^2(\pi w_\infty^*) \sin(\pi w_1) \sin(\pi w_2)} \\ &\quad \times \left\{ q^{-1} R_{b(s)}(w_1, w_2) + \frac{q^{b(s)-1}}{1 - q^{b(s)}} (R_{b(s)}(w_1, w_2) - R_{b(s)+2}(w_1, w_2) + O(1)) \right\}. \end{aligned}$$

The first term does not carry a dominant singularity in s , therefore, using (G.1):

$$\mathbf{F}_s^{(2)}(x_1, x_2)|_{\text{sing}} = \frac{b(s) q^{b(s)-1}}{1 - q^{b(s)}} \Xi_{b(s),5}(x_0^*(w_1), x_0^*(w_2)) + O(1).$$

with:

$$\Xi_{b(s),5} = \frac{(1 - \alpha^2)^2 h^2}{4(4 - n^2s^2) \cos^2(\pi w_\infty^*)} \left[\prod_{i=1}^2 \frac{\sin(\pi b(s)w_i)}{\sin(\pi w_i)} \right].$$

In particular for $\alpha = 1$, we find:

$$\Xi_{b(s),5} = \frac{4h^2}{\rho^2(4 - n^2s^2)} \left[\prod_{i=1}^2 \frac{\sin(\pi b(s)w_i)}{\sin(\pi w_i)} \right].$$

REFERENCES

- [1] J. Ambjørn and T. Budd. Geodesic distances in Liouville quantum gravity. *Nucl. Phys. B*, 889:676–691, 2014. arXiv:1405.3424.
- [2] K. Astala, A. Kupiainen, E. Saksman, and P. Jones. Random conformal weldings. *Acta Math.*, 207(2):203–254, 2011. arXiv:0909.1003.
- [3] O. Babelon, D. Bernard, and M. Talon. *Introduction to classical integrable systems*. Cambridge Monographs on Mathematical Physics. Cambridge University Press, Cambridge, 2002.
- [4] M. Bauer and D. Bernard. Conformal field theories of stochastic Loewner evolutions. *Commun. Math. Phys.*, 239:493–521, 2003. arXiv:hep-th/0210015.
- [5] R. Baxter, S. Kelland, and F. Wu. Equivalence of the Potts model or Whitney polynomial with an ice-type model. *J. Phys. A*, 9:397–411, 1976.
- [6] A. Belavin, A. Polyakov, and A. Zamolodchikov. Infinite conformal symmetry in two-dimensional quantum field theory. *Nucl. Phys. B*, 241:333–380, 1984.
- [7] I. Benjamini and O. Schramm. KPZ in One Dimensional Random Geometry of Multiplicative Cascades. *Commun. Math. Phys.*, 289:46–56, 2009. arXiv:0806.1347.
- [8] G. Bonnet and B. Eynard. The Potts- q random matrix model: loop equations, critical exponents, and rational case. *Phys. Lett. B*, 463:273–279, 1999. arXiv:hep-th/9906130.
- [9] G. Borot. Formal multidimensional integrals, stuffed maps, and topological recursion. *Annales Institut Poincaré - D*, 1(2):225–264, 2014. arXiv:math-ph/1307.4957.
- [10] G. Borot, J. Bouttier, and E. Guitter. Loop models on random maps via nested loops: case of domain symmetry breaking and application to the Potts model. *J. Phys. A: Math. Theor.*, 2012. Special issue: Lattice models and integrability: in honour of F.Y. Wu, arXiv:math-ph/1207.4878.
- [11] G. Borot, J. Bouttier, and E. Guitter. More on the $O(n)$ model on random maps via nested loops: loops with bending energy. *J. Phys. A: Math. Theor.*, 45(275206), 2012. arXiv:math-ph/1202.5521.
- [12] G. Borot, J. Bouttier, and E. Guitter. A recursive approach to the $O(n)$ model on random maps via nested loops. *J. Phys. A: Math. Theor.*, 45(045002), 2012. arXiv:math-ph/1106.0153.
- [13] G. Borot and B. Eynard. Enumeration of maps with self avoiding loops and the $O(n)$ model on random lattices of all topologies. *J. Stat. Mech.*, (P01010), 2011. arXiv:math-ph/0910.5896.
- [14] G. Borot, B. Eynard, and N. Orantin. Abstract loop equations, topological recursion, and applications. *Commun. Number Theory and Physics*, 2015. arXiv:math-ph/1303.5808.
- [15] G. Borot and E. Failde. Nesting statistics in the $O(n)$ loop model on random maps of arbitrary topologies. In preparation.
- [16] D. Boulatov and V. Kazakov. The Ising model on a random planar lattice: the structure of the phase transition and the exact critical exponents. *Phys. Lett. B*, 186:379–384, 1987.
- [17] J. Bouttier and E. Guitter. Planar maps and continued fractions. *Commun. Math. Phys.*, 309(3):623–662, 2010. arXiv:math.CO/1007.0419.
- [18] M. Bowick, V. John, and G. Thorleifsson. The Hausdorff dimension of surfaces in two-dimensional gravity coupled to Ising minimal matter. arXiv:hep-th/9608030.
- [19] E. Brézin, C. Itzykson, G. Parisi, and J.-B. Zuber. Planar diagrams. *Commun. Math. Phys.*, 59:35–51, 1978.
- [20] D. Chelkak and S. Smirnov. Universality in the 2D Ising model and conformal invariance of fermionic observables. *Invent. Math.*, 189(3):515–580, 2012. <http://www.unige.ch/~smirnov/papers/universality-j.pdf>.
- [21] R. Cori and B. Vauquelin. Planar maps are well-labeled trees. *Can. J. Math.*, 33(5):1023–1042, 1981.
- [22] J. Daul. Q -states Potts model on a random planar lattice. arXiv:hep-th/9502014.
- [23] F. David. Conformal field theories coupled to 2-D gravity in the conformal gauge. *Mod. Phys. Lett. A*, 3(17):1651–1656, 1988.
- [24] F. David, A. Kupiainen, R. Rhodes, and V. Vargas. Liouville quantum gravity on the Riemann sphere. *Commun. Math. Phys.*, 342(3):869–907, 2016. arXiv:1410.7318.
- [25] J. Distler and H. Kawai. Conformal field theory and 2D quantum gravity. *Nucl. Phys. B*, 321(2):509–527, 1989.

- [26] E. Domany, D. Mukamel, B. Nienhuis, and A. Schwimmer. Duality relations and equivalences for models with $O(n)$ and cubic symmetry. *Nucl. Phys. B [FS3]*, 190:279–287, 1981.
- [27] B. Duplantier. Geodesic duality and the Hausdorff dimension of two-dimensional quantum gravity. arXiv:math-ph/1108.3327.
- [28] B. Duplantier. Higher conformal multifractality. *J. Stat. Phys.*, 110:691–738, 2003. Special issue in honor of Michael E. Fisher’s 70th birthday (Piscataway, NJ, 2001). arXiv:cond-mat/0207743.
- [29] B. Duplantier. Conformal fractal geometry & boundary quantum gravity. In *Fractal geometry and applications: a jubilee of Benoît Mandelbrot, Part 2*, volume 72 of *Proc. Sympos. Pure Math.*, pages 365–482. Amer. Math. Soc., Providence, RI, 2004. arXiv:math-ph/0303034.
- [30] B. Duplantier. Liouville quantum gravity, KPZ and Schramm-Loewner evolution. In S. Y. Jang, Y. R. Kim, D.-W. Lee, and I. Yie, editors, *Proceedings of the International Congress of Mathematicians, Seoul 2014*, volume 3, pages 1035–1061, Seoul, Korea, August 13–21, 2014. Kyung Moon SA Co. Ltd., Seoul, Korea. Open access at <http://www.icm2014.org/en/vod/proceedings>.
- [31] B. Duplantier and I. Kostov. Conformal spectra of polymers on a random surface. *Phys. Rev. Lett.*, 61:1433–1437, 1988.
- [32] B. Duplantier and I. K. Kostov. Geometrical critical phenomena on a random surface of arbitrary genus. *Nucl. Phys. B*, 340:491–541, 1990.
- [33] B. Duplantier, J. Miller, and S. Sheffield. Liouville quantum gravity as a mating of trees. 2014. arXiv:1409.7055.
- [34] B. Duplantier, R. Rhodes, S. Sheffield, and V. Vargas. Critical Gaussian multiplicative chaos: Convergence of the derivative martingale. *Ann. Probab.*, 42(5):1769–1808, 2014. arXiv:1206.1671.
- [35] B. Duplantier, R. Rhodes, S. Sheffield, and V. Vargas. Renormalization of Critical Gaussian Multiplicative Chaos and KPZ Relation. *Commun. Math. Phys.*, 330(1):283–330, 2014. arXiv:1212.0529.
- [36] B. Duplantier and S. Sheffield. Duality and KPZ in Liouville quantum gravity. *Phys. Rev. Lett.*, 102:150603, 2009. arXiv:0901.0277.
- [37] B. Duplantier and S. Sheffield. Liouville quantum gravity and KPZ. *Invent. Math.*, 185:333–393, 2011. arXiv:0808.1560.
- [38] B. Duplantier and S. Sheffield. Schramm-Loewner evolution and Liouville quantum gravity. *Phys. Rev. Lett.*, 107(13):131305, 2011. arXiv:1012.4800.
- [39] B. Eynard. *Counting surfaces*. Progress in Mathematical Physics. Birkhäuser Science, Basel, 2016.
- [40] B. Eynard and C. Kristjansen. Exact solution of the $O(n)$ model on a random lattice. *Nucl. Phys. B*, 455:577–618, 1995. arXiv:hep-th/9506193.
- [41] P. Flajolet and R. Sedgewick. *Analytic combinatorics*. Cambridge University Press, 2009. <http://algo.inria.fr/flajolet/Publications/books.html>.
- [42] C. Fortuin and P. Kasteleyn. On the random-cluster model. I- introduction and relation to other models. *Physica*, 57:536–564, 1972.
- [43] P. D. Francesco, P. Ginsparg, and J. Zinn-Justin. 2d gravity and random matrices. *Phys. Rep.*, 254(1), 1994. arXiv:hep-th/9306153v2.
- [44] P. D. Francesco, P. Mathieu, and D. Sénéchal. *Conformal field theory*, chapter The $O(n)$ model, pages 229–231. Springer, Berlin, corrected edition, 1999.
- [45] R. Friedrich and W. Werner. Conformal restriction, highest weight representations and SLE. *Commun. Math. Phys.*, 243:105–122, 2003. arXiv:math-ph/0301018.
- [46] M. Gaudin and I. Kostov. $O(n)$ on a fluctuating lattice. Some exact results. *Phys. Lett. B*, 220(1–2):200–206, 1989.
- [47] P. Ginsparg and G. Moore. Lectures on 2d gravity and 2d string theory (TASI 1992). In J. Harvey and J. Polchinski, editors, *Recent direction in particle theory, Proceedings of the 1992 TASI*. World Scientific, Singapore, 1993. arXiv:hep-th/9304011.
- [48] D. R. Guo and Z. X. Wang. *Special functions*. World Scientific, Singapore, 1989.
- [49] R. Høegh-Krohn. A general class of quantum fields without cut-offs in two space-time dimensions. *Commun. Math. Phys.*, 21:244–255, 1971.
- [50] X. Hu, J. Miller, and Y. Peres. Thick points of the Gaussian free field. *Ann. Probab.*, 38(2):896–926, 2010. arXiv:0902.3842.

- [51] W. Kager and B. Nienhuis. A guide to stochastic Löwner evolution and its applications. *J. Statist. Phys.*, 115(5-6):1149–1229, 2004. arXiv:math-ph/0312056.
- [52] J.-P. Kahane. Sur le chaos multiplicatif. *Ann. Sci. Math. Québec*, 9(2):105–150, 1985.
- [53] N. Kang and N. G. Makarov. *Gaussian free field and conformal field theory*. Astérisque 353. Paris: Société Mathématique de France (SMF), 2013. arXiv:1101.1024.
- [54] V. A. Kazakov. Ising model on a dynamical planar random lattice: Exact solution. *Phys. Lett. A*, 119:140–144, 1986.
- [55] V. A. Kazakov. Exactly solvable Potts models, bond- and tree-like percolation on dynamical (random) planar lattice. *Nucl. Phys. B (Proc. Suppl.)*, 4:93–97, 1988.
- [56] A. Kemppainen and W. Werner. The nested simple conformal loop ensembles in the Riemann sphere. *Probab. Theory Relat. Fields*, pages 1–32, 2015. Published online: 07 Aug. 2015. arXiv:1402.2433.
- [57] V. G. Knizhnik, A. M. Polyakov, and A. B. Zamolodchikov. Fractal structure of 2D-quantum gravity. *Mod. Phys. Lett. A*, 3(8):819–826, 1988.
- [58] I. Kostov. $O(n)$ vector model on a planar random lattice: spectrum of anomalous dimensions. *Mod. Phys. Lett. A*, 4:217, 1989.
- [59] I. Kostov and M. Staudacher. Multicritical phases of the $O(n)$ model on a random lattice. *Nucl. Phys. B*, 384:459–483, 1992. arXiv:hep-th/9203030.
- [60] G. F. Lawler, O. Schramm, and W. Werner. Conformal invariance of planar loop-erased random walks and uniform spanning trees. *Ann. Probab.*, 32(1B):939–995, 2004. arXiv:math/0112234.
- [61] J.-F. Le Gall. The topological structure of scaling limits of large planar maps. *Invent. Math.*, 169(3):621–670, 2007. math.PR/0607567.
- [62] J.-F. Le Gall. Uniqueness and universality of the Brownian map. *Ann. Probab.*, 41(4):2880–2960, 2013. arXiv:math.PR/1105.4842.
- [63] J.-F. Le Gall. Random Geometry on the Sphere. In S. Y. Jang, Y. R. Kim, D.-W. Lee, and I. Yie, editors, *Proceedings of the International Congress of Mathematicians, Seoul 2014*, volume 1, pages 421–442, Seoul, Korea, August 13-21, 2014. Kyung Moon SA Co. Ltd., Seoul, Korea. Open access at <http://www.icm2014.org/en/vod/proceedings>.
- [64] J.-F. Le Gall and G. Miermont. Scaling limits of random planar maps with large faces. *Ann. Probab.*, 39(1):1–69, 2011. arXiv:math.PR/0907.3262.
- [65] J. Marckert and A. Mokkadem. Limit of normalized random quadrangulations: the Brownian map. *Ann. Probab.*, 34(6):2144–2202, 2006. arXiv:math.PR/0403398.
- [66] G. Miermont. The Brownian map is the scaling limit of uniform random plane quadrangulations. *Acta Math.*, 210(2):319–401, 2013. arXiv:math.PR/1104.1606.
- [67] J. Miller and S. Sheffield. An axiomatic characterization of the Brownian map. arXiv:1506.03806.
- [68] J. Miller and S. Sheffield. Liouville quantum gravity and the Brownian map I: The QLE(8/3,0) metric. arXiv:1507.00719.
- [69] J. Miller and S. Sheffield. Liouville quantum gravity spheres as matings of finite-diameter trees. arXiv:1506.03804.
- [70] J. Miller, S. S. Watson, and D. B. Wilson. The conformal loop ensemble nesting field. *Probab. Theory Relat. Fields*, 163(3):769–801, 2015. arXiv:math.PR/1401.0218.
- [71] J. Miller, S. S. Watson, and D. B. Wilson. Extreme nesting in the conformal loop ensemble. *Ann. Probab.*, 44(2):1013–1052, 2016. arXiv:math.PR/1401.0217.
- [72] Y. Nakayama. Liouville field theory: a decade after the revolution. *Internat. J. Modern Phys. A*, 19(17-18):2771–2930, 2004. arXiv:hep-th/0402009.
- [73] B. Nienhuis. Exact critical point and critical exponents of $O(n)$ models in two dimensions. *Phys. Rev. Lett.*, 49:1062–1065, 1982.
- [74] B. Nienhuis. Critical behavior of two-dimensional spin models and charge asymmetry in the Coulomb gas. *J. Stat. Phys.*, 34:731–761, 1984.
- [75] B. Nienhuis. Coulomb gas formulation of two-dimensional phase transitions. In C. Domb and J. Lebowitz, editors, *Phase transition and critical phenomena*, volume 11. Academic Press, London, 1987.

- [76] J. Perk and F. Wu. Nonintersecting string model and graphical approach: equivalence with a Potts model. *J. Stat. Phys.*, 42:727–742, 1986.
- [77] A. M. Polyakov. Quantum geometry of bosonic strings. *Phys. Lett. B*, 103(3):207–210, 1981.
- [78] R. Rhodes and V. Vargas. KPZ formula for log-infinitely divisible multifractal random measures. *ESAIM Probab. Stat.*, 15:358–371, 2011. arXiv:0807.1036.
- [79] G. Schaeffer. Conjugaison d’arbres et cartes combinatoires aléatoires. 1999. Thèse de doctorat, Université de Bordeaux I.
- [80] O. Schramm. Scaling limits of loop-erased random walks and uniform spanning trees. *Israel J. Math.*, 118:221–288, 2000. arXiv:math/9904022.
- [81] O. Schramm and S. Sheffield. Contour lines of the two-dimensional discrete Gaussian free field. *Acta Math.*, 202(1):21–137, 2009. arXiv:math/0605337.
- [82] O. Schramm, S. Sheffield, and D. B. Wilson. Conformal radii for conformal loop ensembles. *Commun. Math. Phys.*, 288:43–53, 2009. arXiv:math.PR/0611687.
- [83] S. Sheffield. Gaussian free fields for mathematicians. *Probab. Theory Relat. Fields*, 139(3-4):521–541, 2007. arXiv:math/0312099.
- [84] S. Sheffield. Exploration trees and conformal loop ensembles. *Duke Math. J.*, 147(1):79–129, 03 2009. arXiv:math/0609167.
- [85] S. Sheffield. Conformal weldings of random surfaces: SLE and the quantum gravity zipper. 2010. arXiv:1012.4797, to appear in Annals of Probability.
- [86] S. Sheffield and W. Werner. Conformal loop ensembles: the Markovian characterization and the loop-soup construction. *Ann. Math. (2)*, 176(3):1827–1917, 2012. arXiv:1006.2374.
- [87] S. Smirnov. Critical percolation in the plane: conformal invariance, Cardy’s formula, scaling limits. *C. R. Acad. Sci. Paris Sér. I Math.*, 333(3):239–244, 2001. arXiv:0909.4499. <http://www.unige.ch/~smirnov/papers/percras-j.pdf>.
- [88] S. Smirnov. Conformal invariance in random cluster models. I. Holomorphic fermions in the Ising model. *Ann. Math. (2)*, 172(2):1435–1467, 2010. arXiv:0708.0039.
- [89] T. Truong. Structural properties of a $Z(N^2)$ -spin model and its equivalent $Z(N)$ -vertex model. *J. Stat. Phys.*, 42:349–379, 1986.
- [90] W. Tutte. A census of planar triangulations. *Can. J. Math.*, 14:21, 1962.
- [91] W. Tutte. A census of planar maps. *Can. J. Math.*, 15:249, 1963.
- [92] W. Tutte. On the enumeration of planar maps. *Bull. Amer. Math. Soc.*, 74(1):64–74, 1968.
- [93] P. Zinn-Justin. The dilute Potts model on random surfaces. *J. Stat. Phys.*, 98:245–264, 2000. arXiv:cond-mat/9903385.

MAX PLANCK INSTITUT FÜR MATHEMATIK, VIVATSGASSE 7, 53111 BONN, GERMANY AND MIT
 MATHS DEPARTMENT, 77 MASSACHUSETTS AVENUE, CAMBRIDGE MA 02139, USA.

E-mail address: gborot@mpim-bonn.mpg.de

INSTITUT DE PHYSIQUE THÉORIQUE, UNIVERSITÉ PARIS-SACLAY, DIRECTION DE LA RECHERCHE
 FONDAMENTALE CEA/SACLAY, UMR 3681 INP-CNRS, F-91191 GIF-SUR-YVETTE CEDEX, FRANCE
 AND DÉPARTEMENT DE MATHÉMATIQUES ET APPLICATIONS, ÉCOLE NORMALE SUPÉRIEURE, 45 RUE
 D’ULM, 75231 PARIS CEDEX 05, FRANCE

E-mail address: jeremie.bouttier@cea.fr

INSTITUT DE PHYSIQUE THÉORIQUE, UNIVERSITÉ PARIS-SACLAY, DIRECTION DE LA RECHERCHE
 FONDAMENTALE CEA/SACLAY, UMR 3681 INP-CNRS, F-91191 GIF-SUR-YVETTE CEDEX, FRANCE

E-mail address: bertrand.duplantier@cea.fr